

---

Institute of Plant Nutrition  
University of Hohenheim  
Prof. Dr. Nicolaus von Wirén

**Iron and ammonium sensing differentially modulate  
root plasticity in *Arabidopsis thaliana***

Dissertation

Submitted in fulfillment of the requirements for the degree

“Doktor der Agrarwissenschaften”

(Dr. Sc. agr. / Ph.D in Agricultural Sciences)

to the  
Faculty of Agricultural Sciences

presented by

**Joni Esrom Lima**

from Brazil

2010

---

---

---

---

---

---

This thesis was accepted as a doctoral dissertation in fulfillment of the requirements for the degree “Doktor der Agrarwissenschaften” by the Faculty of Agricultural Sciences at the University of Hohenheim.

Date of the oral examination: 24<sup>th</sup> September 2010

**Examination Committee**

Supervisor and reviewer	Prof. Dr. Nicolaus von Wirén
Co-reviewer	Prof. Dr. Gerd Weber
Additional examiner	Prof. Dr. Andreas Schaller
Dean and head of the committee	Prof. Dr. Andreas Fangmeier

---

---

---

## Table of contents

<b>1. Summary- Zusammenfassung</b>	<b>1</b>
1.1. Summary .....	1
1.2. Zusammenfassung.....	2
<b>2. General introduction</b>	<b>4</b>
2.1. The root system.....	4
2.1.1. <i>Lateral root development</i> .....	5
2.2. Root plasticity .....	13
2.2.1. <i>Nitrate signaling and nitrate-induced root plasticity</i> .....	13
2.2.2. <i>Ammonium transport and signaling in yeast and plants</i> .....	15
2.2.3. <i>Phosphorus-regulated root plasticity</i> .....	18
2.2.4. <i>Sulfur-regulated root plasticity</i> .....	19
2.2.5. <i>Potassium-regulated root plasticity</i> .....	20
2.2.6. <i>Iron signaling and iron acquisition</i> .....	21
2.3. Objectives of the thesis .....	25
<b>3. Local Supply of Iron Distinctly Defines Lateral Root Number and Elongation in Arabidopsis thaliana</b>	<b>26</b>
3.1. Introduction.....	26
3.2. Material and methods.....	28
3.2.1. <i>Plant material and growth conditions</i> .....	28
3.2.2. <i>Root growth measurements</i> .....	28
3.2.3. <i>Histochemical analysis</i> .....	29
3.2.4. <i>Histochemical localization of iron</i> .....	29
3.2.5. <i>Expression analysis</i> .....	30
3.2.6. <i>Mineral element and chlorophyll analysis</i> .....	30
3.3. Results .....	31

---

3.3.1.	<i>Localized supply of iron stimulates lateral root development in Arabidopsis</i>	31
3.3.2.	<i>Influence of the mode of iron supply on the nutritional status of the shoot</i>	35
3.3.3.	<i>Effect of localized Fe supply on early lateral root development</i>	39
3.3.4.	<i>Involvement of IRT1 in the differential response of the number and length of lateral roots to localized iron supply</i>	41
3.3.5.	<i>Influence of FIT on lateral root development under localized iron supply</i>	43
3.3.6.	<i>Influence of FRD3 on lateral root development and the expression of Fe-responsive genes</i>	44
3.4.	Discussion	49
3.4.1.	<i>Localized Fe supply differentially regulates lateral root number and lateral root length</i>	49
3.4.2.	<i>The local regulation of lateral root development by iron</i>	50
<b>4.</b>	<b>Ammonium triggers lateral root branching in Arabidopsis in an AMT1;3-dependent manner</b>	<b>53</b>
4.1.	Introduction	53
4.2.	Material and methods	55
4.2.1.	<i>Plant Material</i>	55
4.2.2.	<i>Plant in vitro culture</i>	56
4.2.3.	<i>Heterologous expression of AMT1;3 mutants in yeast</i>	56
4.2.4.	<i>Root growth measurements</i>	57
4.2.5.	<i>Histochemical analysis and microscopy</i>	57
4.2.6.	<i>Gene expression analysis</i>	58
4.2.7.	<i>Accession Numbers</i>	58
4.3.	Results	59
4.3.1.	<i>Lateral root formation is stimulated by local ammonium supply</i>	59
4.3.2.	<i>Ammonium-induced lateral root branching is subject to systemic repression</i>	64
4.3.3.	<i>Ammonium and nitrate regulate lateral root development in a complementary way</i>	71
4.3.4.	<i>The ammonium transporter-defective mutant qko shows decreased ammonium-triggered lateral root branching</i>	72
4.3.5.	<i>The role of AMT1;3 in lateral root branching</i>	74

---

---

4.3.6.	<i>Ammonium promotes lateral root initiation to local auxin signalling</i> .....	84
4.4.	Discussion .....	88
4.4.1.	<i>A complementary role for ammonium and nitrate in lateral root development</i> .....	88
4.4.2.	<i>The possible function of AMT1;3 in ammonium-triggered lateral root development</i> .....	90
<b>5.</b>	<b>General discussion</b>	<b>93</b>
5.1.	Environmental factors and responses in the root system.....	93
5.2.	Systemic versus local nutrient signaling-responses controlling root morphology .....	103
5.3.	The nutrient transceptor model for coordinating changes in root morphology .....	106
<b>6.</b>	<b>References</b>	<b>109</b>
<b>7.</b>	<b>Acknowledgments</b>	<b>124</b>
<b>8.</b>	<b>Curriculum vitae</b>	<b>127</b>

---

# 1. Summary- Zusammenfassung

## 1.1. Summary

Plant growth depends on a continuous nutrient uptake by roots. In natural or agricultural ecosystems nutrients are often sparingly available and subject to a non-homogenous or patchy distribution in the rooted soil volume. Plants may then alter their root system architecture to better exploit nutrient patches in the soil. Directed root growth towards a nutrient source may be seen as an indication for nutrient sensing. So far, changes in root system architecture have been systematically investigated only for nitrate, sulphate and phosphate. It was therefore the aim of this thesis to investigate changes in root morphology to other nutrients which are restricted in their mobility in soils, namely iron and ammonium.

The first part of the present thesis describes how the root system architecture is altered by localized iron (Fe) supply. In the low concentration range, increasing Fe concentrations in a homogenous or localized supply enhanced lateral root number in a similar manner. Lateral root length, however, was twofold higher under localized relative to homogenous Fe supply. With further increasing Fe concentrations lateral root length was repressed even though shoot growth was unaffected. Using *Arabidopsis* mutants which are defective in Fe acquisition or Fe translocation within the plant, it was possible to show that lateral root elongation is under control of a local rather than a systemic regulatory loop involving the high-affinity Fe transporter IRT1.

The second part of the thesis describes and investigates a novel phenotype in root system architecture that depends on localized ammonium supply. Under these conditions, *Arabidopsis* plants increased lateral root initiation and higher-order lateral root branching, whereas localized nitrate supply favored lateral root elongation. Since ammonium-stimulated lateral root number or density decreased after ammonium or glutamine supply to a separate root fraction and did not correlate with cumulative uptake of <sup>15</sup>N-labeled ammonium, lateral root branching was not purely due to a nutritional effect but most likely reflected a sensing event. Thus, ammonium and nitrate coordinate root morphology in an additive and complementary way. Using *AMMONIUM TRANSPORTER (AMT)* mutants, ammonium-induced lateral root branching was demonstrated to involve in particular AMT1;3. With the identification of

---

---

a stimulated lateral root initiation in response to localized ammonium and a tightly regulated lateral root elongation in response to localized Fe supply, this thesis contributed to a better understanding of how roots adapt to localized nutrient supplies which is an important issue for an efficient utilization of placed fertilization in crops.

## **1.2. Zusammenfassung**

Pflanzliches Wachstum ist abhängig von einer kontinuierlichen Aufnahme von Nährstoffen durch die Wurzel. Diese Nährstoffe sind im durchwurzelten Boden in natürlichen als auch in Agrarökosystemen oft nur spärlich verfügbar und inhomogen bzw. uneinheitlich verteilt. Durch Veränderung ihrer Wurzelsystemarchitektur passen sich Pflanzen an diese ungleiche Verteilung der Nährstoffe an und können sie dadurch besser ausschöpfen. Das gezielte Wachstum von Wurzeln in Richtung einer Nährstoffquelle kann als Hinweis für ein Nährstoff –„Sensing“ betrachtet werden. Bisher wurden nur Nitrat, Sulfat und Phosphat systematisch auf ihre Wirkung auf das Wurzelsystem überprüft. Das Ziel der vorliegenden Arbeit war daher die Untersuchung von Veränderungen in der Wurzelmorphologie durch die Nährstoffe Eisen (Fe) und Ammonium ( $\text{NH}_4^+$ ), deren Mobilität im Boden begrenzt ist.

Der erste Teil dieser Arbeit befasst sich mit der Wirkung eines lokal begrenzten Eisenangebotes auf die Architektur des Wurzelsystems. Bei niedrigen Konzentrationen führte eine ansteigende Eisenkonzentration sowohl bei platzierter, als auch bei homogener Verteilung des Nährstoffes zu einer erhöhten Seitenwurzelanzahl. Die Seitenwurzellänge war jedoch doppelt so hoch unter lokalisiertem gegenüber homogenem Eisenangebot. Mit steigender Eisenkonzentration zeigte sich jedoch eine Hemmung der Seitenwurzellänge obwohl das Sprosswachstum unbeeinflusst blieb. Unter Verwendung von Arabidopsislinien, die in ihrer Eisenaufnahme oder –verlagerung innerhalb der Pflanze gestört sind, konnte gezeigt werden, dass die Seitenwurzelstreckung eher unter der Kontrolle eines lokalen als eines systematischen Regelkreises steht, in den auch der hochaffine Eisentransporter IRT1 involviert ist.

Im zweiten Teil der Arbeit wird ein neuer, Phänotyp der Wurzelsystemarchitektur beschrieben und untersucht, welcher von lokalisiertem Ammoniumangebot abhängig ist. Dabei zeigten Arabidopsispflanzen eine erhöhte Seitenwurzelinitiation und eine stärkere Verzweigung von Seitenwurzeln höherer Ordnung, während ein lokales Angebot von Nitrat die Seitenwurzelstreckung begünstigte. Da der von Ammonium

---

induzierte Effekt auf die Seitenwurzelanzahl oder –dichte durch eine Gabe von Ammonium oder Glutamin zu einer separaten Wurzelfraktion abnahm und nicht mit der kumulativen Aufnahme von <sup>15</sup>N-markiertem Ammonium korrelierte, ist die Verzweigung der Seitenwurzeln nicht allein durch einen Ernährungseffekt zu erklären. Eher spiegelt dies einen Sensing-Vorgang wieder. Folglich koordinieren Ammonium und Nitrat die Wurzelmorphologie in einer additiven und sich komplementierenden Weise. Mit Hilfe von Ammoniumtransporter(AMT)-Mutanten konnte gezeigt werden, dass die durch Ammonium induzierte Seitenwurzelverzweigung vorwiegend mit AMT1;3 verknüpft ist.

Mit der Identifizierung einer stimulierten Seitenwurzelinduktion durch eine lokale Ammoniumgabe und einer streng regulierten Seitenwurzelelongation als Antwort auf ein lokales Eisenangebot trägt diese Arbeit zu einem besseren Verständnis der Adaption von Wurzeln auf eine lokale Nährstoffzufuhr bei, welches vor allem ein wichtiges Thema für eine effiziente Nutzung platzierter Düngermittel in der landwirtschaftlichen Produktion ist.

## 2. General introduction

During their development, plants need to continuously coordinate the formation and growth rate of organs in response to environmental cues. This developmental plasticity is part of a strategy to overcome their sessile fate and allow plants improving the acquisition of limiting resources. In this context, plant roots are responsible for nutrient and water uptake, and to provide an anchor in the soil (Marschner, 1995). Therefore, a root system is the primary site that perceives inadequate nutrient supply. Investigating the factors that determine root architecture is of outstanding importance not only for studying adaptive responses to varying nutrient availabilities but also for improving nutrient use efficiency in agricultural production systems.

### 2.1. The root system

The root system of higher plants consists of an embryonic primary root and post-embryonic lateral and adventitious root. Roots of the model plant *Arabidopsis thaliana* have a simple anatomy composed of single layers of epidermal, cortical and endodermal cells which surround the vascular tissue. A pivotal issue in post-embryonic development is to continuously maintain pools of totipotent stem cells in their apical meristems, which allow an ongoing development of root and shoot organs (Weigel and Jürgens, 2002; Laux, 2003; Dinneny and Benfey, 2008).

In many dicotyledonous species, a significant part of the root system originates after the establishment of the primary root through the formation of lateral roots. The root system of cereal crop species differs in its architecture and anatomy, by developing adventitious roots (Hochholdinger et al., 2004). Although, root patterning genes are essentially common (e.g. *SHORTROOT* and *SCARECROW*) among most root types, the identification of root-defective mutants in cereals suggests that primary, lateral and adventitious roots are at least in part regulated by different pathways (Hochholdinger et al., 2004). A deeper understanding of these pathways might also facilitate breeding approaches for a better adaptation of the root system architecture to varying nutrient supplies (Malamy, 2005).

### **2.1.1. Lateral root development**

Recent advances in the study of lateral root formation have led to the identification of important regulatory processes. In *Arabidopsis*, lateral roots originate from pericycle founder cell layer located opposite to xylem poles and follow a chronological development (Malamy and Benfey, 1997). In principle, lateral root formation can be divided in three major steps defined as pre-initiation, initiation and post-initiation (Péret et al., 2009).

#### **2.1.1.1. Pre-initiation of a lateral root**

To form lateral roots, pericycle cells in the primary root apex dedifferentiate and re-enter mitotic cell division. Although, most of the pericycle cells, for example, the phloem poles remain in the G1 phase, the xylem pole cell advance to the G2 phase (Casimiro et al., 2003). Thereby, xylem-pole pericycle cells maintain their ability to divide after leaving the root apical meristem (Dubrovsky et al., 2000). Using a reverse genetic approach, a mutant with altered lateral root initiation was identified in *Arabidopsis* (Celenza et al., 1995). The mutant *aberrant lateral root formation4* (*alf4*) prevents lateral root initiation due to a defect in completing mitosis (Celenza et al., 1995). The nuclear protein ALF4 is required to maintain xylem pole pericycle cells in a mitotically competent state and its function is independent of auxin signaling (DiDonato et al., 2004). In the basal meristem, which is right behind the root apical meristem, the xylem pore pericycle cells get primed to further induce asymmetrical cell divisions and generate pairs of founder cells in an auxin-dependent signaling process (De Smet et al., 2007). The existence of an auxin signal in the basal meristem supports the importance of the root tip for the regulation of root branching and supports the idea that the auxin pool in the root tip drives the initial stages of lateral root primordia formation (De Smet et al., 2007).

#### **2.1.1.2. Auxin regulates lateral root initiation**

With the classical work from Skoog and Miller (1957), the plant hormone auxin has been related to root development. Exogenous application of auxin or mutants that accumulate high levels of auxin, like *superroot1* (*sur1*), stimulate lateral root formation (Boerjan et al., 1995; Hobbie, 1998). In contrast, auxin-resistant or auxin-

depleted mutants have a reduced number of lateral roots (Casimiro et al., 2003). The mechanisms underlying auxin-mediated differentiation of xylem pole pericycle cells into founder cells still remain elusive, although, auxin is likely to be the plant hormone responsible for competence acquisition of dedifferentiated cells (Sena et al., 2009). Under normal growth conditions, lateral root initiation occurs at a regular rhythm during primary root growth. This rhythm is governed by an auxin oscillation in the pericycle founder cell, which expresses in intervals of approximately 15 hours (De Smet et al., 2007). Interestingly, each peak of the observed auxin-reporter gene expression correlated with the initiation of a new lateral root primordium along the primary root (De Smet et al., 2007). Thus, auxin pulses close to the adjacent xylem pole regulate the spacing of lateral root initiation. This process is dependent on an auxin transport carrier, *AUX1* (*AUXIN RESISTANT1*), which is essential for root gravitropic responses (De Smet et al., 2007; Bennett et al., 1996). *AUX1* significantly contributes to lateral root formation by controlling overall auxin levels in the root tip, unloading the auxin transported via the phloem, and controlling its availability at the site of lateral root initiation; this is governed by basipetal auxin transport from the root tip (Marchant et al., 2002). Recently, another mechanism was implied in the regulation of the spacing of founder cells that give rise to lateral primordia development. Under mechanical stimuli by either gravitropic curvature or by forced bending of the root, auxin accumulates at the site of lateral root induction (Ditengou et al., 2008). The transient bending process is dependent on a redistribution of auxin by *PIN1* (*PIN-FORMED1*) re-localizing to pericycle cells on the outside of the bending. The enhanced auxin flow triggers the expression of *AUX1* generating an auxin maximum that precedes lateral root initiation. On the other hand, the auxin efflux to adjacent protoxylem cells under mechanical induction is independent of *AUX1* (Ditengou et al., 2008). Thus, mechanical signaling mechanism programming the “priming” of pericycle founder cells to turn into lateral root initial appears to be independent of auxin (Ditengou et al., 2008). In summary, the positioning of lateral root initials along the primary root is under influence of endogenous auxin signals, in particular oscillatory auxin pulses, and environmental signals, such as mechanical stimuli.

Several components of the auxin signaling pathway leading to lateral root initiation have recently been identified (Fukaki et al., 2007). The mutant *solitary root1* (*slr1*) is blocked in lateral initiation and external auxin applications cannot rescue the phenotype (Fukaki et al., 2002). *SLR1* encodes IAA14, a member of a large family of

Aux/IAA proteins that act as transcriptional repressors of auxin-regulated genes (Fukaki et al., 2002). Mutant phenotypes expressing stabilized forms of IAA1, IAA3, IAA18, IAA19 or IAA28 exhibit reduced numbers of laterals, but still allow lateral root initiation (Yang et al., 2004; Tian and Reed, 1999; Rogg et al., 2001; Tatematsu et al., 2004). Thus, Aux/IAA proteins control lateral root development and growth at different developmental stages (Péret et al., 2009).

In roots, auxin is perceived through a *TIR1* (*TRANSPORTER INHIBITOR RESPONSE 1*) or *AFB1-3* (*AUXIN RECEPTOR F-BOX PROTEIN1-3*) dependent receptor mechanism, which is a component of a cellular protein complex known as the SCF<sup>TIR1/AFB</sup> E3 ubiquitin ligase complex (*Skp1-Cullin-F-box complex*) (Dharmasiri et al., 2005b; Dharmasiri et al., 2005a). This complex, consisting of *AtCUL1*, *RBX1* and *ASK1/ASK2*, is recruited by the receptor in an auxin-dependent manner (Quint and Gray, 2006), and stabilizes the interaction between TIR1 and Aux/IAA substrates. The interaction results in Aux/IAA ubiquitination and subsequent degradation by the proteasome, which implies that the regulation of protein stability is a crucial process in auxin signaling (Dharmasiri et al., 2005b; Tan et al., 2007). This rapid turnover of Aux/IAA proteins provides the ability to plants to modulate auxin-responses according to fast stimuli (Vanneste and Friml, 2009). There is an important redundancy in TIR1/AFB-type auxin receptors, since only a triple mutant (*tir1 afb2 afb3*) displays a visible reduction of lateral root number (Dharmasiri et al., 2005b).

To activate the transcription of auxin-regulated gene expression, auxin causes the destruction of Aux/IAA repressor proteins that dimerize with *ARFs* (*AUXIN RESPONSE FACTORS*). Once released from Aux/IAA proteins, ARFs bind to auxin-responsive promoter elements in target genes. In *Arabidopsis*, 23 genes encoding ARFs have been described, whereby ARF7 and ARF19 are involved in lateral root initiation. Consequently, the *arf7 arf19* double mutant fails to initiate lateral root primordia, similar to the *slr1* mutant (Fukaki et al., 2002; Vanneste et al., 2005). Moreover, the findings that the *arf7 arf19* double mutant is able to form few lateral roots suggests that further ARFs genes might contribute to lateral initiation (Fukaki et al., 2007).

### 2.1.1.3. Lateral root initiation

Lateral root initiation starts right after auxin-induced signaling, when the adjacent primed pericycle cells undergo anticlinal and asymmetrical division creating

two short cells flanked by two longer cells; this is defined as stage I (Malamy and Benfey, 1997; Casimiro et al., 2001). After a radial expansion, the central short daughter cells divide periclinally to form a primordium composed of inner and outer cell layers, which has been denominated as stage II (Malamy and Benfey, 1997). In stage III, the outer cells undergo another round of periclinal cell divisions to give rise to three cell layers in the lateral root primordium. The inner cells also divide periclinally to create a fourth cell layer; this is stage IV (Malamy and Benfey, 1997). In stage V, the lateral root primordium breaks through the parental cortex, and finally emerges at stage VIII (Malamy and Benfey, 1997).

Recently, components of the lateral root initiation process have been elucidated by transcriptome profiling of the *arf7 arf19* double mutant and the *slr1* mutant (Vanneste et al., 2005). A gene involved in the cell cycle regulation, *D-CYCLIN (CYCD3,1)*, displayed a lower expression in the *slr1* mutant. The overexpression of this cell cycle-regulating gene accelerated the transition from the G1 to the S phase, increasing anticlinal cell divisions, but it was unable to rescue the formation of lateral root primordia. The failure to activate the marker gene *ACR4 (ARABIDOPSIS CRINKLY4)* in pericycle founder cells demonstrated that cell proliferation *per se* was not the cause of lacking lateral root formation in the *slr1* mutant (De Smet et al., 2008; Dubrovsky et al., 2009). Thus, a fine level tuning of asymmetric cell divisions is required for lateral root initiation (Vanneste et al., 2005).

In the primary root auxin transport by PIN-type efflux carriers has a strong influence on lateral root initiation. The PIN family in *Arabidopsis thaliana* is composed of 8 members of plant-specific plasma membrane-localized proteins. The evident lack of lateral root formation in the *pin1 pin3 pin4 pin7* mutant (PIN quadruple mutant) suggested that auxin transport is likely to pattern the formation of lateral root primordia (Benková et al., 2003). This phenotypic disturbance can be phenocopied by an external application of the auxin efflux inhibitor 1-naphthylphthalamic acid (NPA), suggesting that asymmetric auxin transport and/or distribution play an important role in lateral root development (Benková et al., 2003). Indeed, acropetal auxin transport towards to the primary root tip is mediated by PINs localized in the vascular parenchyma and phloem, followed by AUX1-mediated auxin unloading to protophloem cells (Benková et al., 2003). After formation of short initial cells by anticlinal divisions (stage I), PIN1 is required to form cell plates (Geldner et al., 2004). After primordia emergence, PIN2 is expressed in epidermis cells towards the base of the lateral root (Benková et al., 2003). PIN3 expands its localization from the

base of the primordium to the columella cells of the newly formed meristem after stage V (Benková et al., 2003). PIN4 seems to share the same localization as PIN3, although being more restricted to the margins. PIN6 remains within the primordium during the whole process of lateral root initiation (Benková et al., 2003). PIN7 expression is restricted to inner and provascular cells at later stages of development (Benková et al., 2003). An important component that regulates the vesicle trafficking of PIN-type auxin carriers is called GNOM (Geldner et al., 2004). The *GNOM* gene encodes an ARF GDP/GTP exchange factor for small G-proteins of the ARF class (Geldner et al., 2004; Kleine-Vehn et al., 2008). The loss-of-function alleles of the *Arabidopsis* *GNOM* gene lead to severe defects in cell-to-cell alignment and reduced numbers of lateral roots (Geldner et al., 2004). Interestingly, in the weak alleles of *gnom* the pericycle cells are able to proliferate upon external auxin treatments, although the marker *ACR4* is not induced, which suggests that GNOM is required for the initial asymmetric cell division (Geldner et al., 2004; De Smet et al., 2008). Indeed, proper PIN1 polarity, which is GNOM-dependent, is required to establish an auxin gradient during primordial development (Benková et al., 2003; Geldner et al., 2004). In consequence, by modulating PIN protein trafficking, auxin regulates PIN abundance and activity at the cell surface providing a mechanism of feedback regulation of auxin transport (Paciorek et al., 2005). Additionally, PIN proteins are targets of phosphorylation by PINOID (PID) kinase and of dephosphorylation by the protein phosphatase 2A (PP2A), which seems to be essential to determine apical or basal PIN localization (Friml et al., 2004; Michniewicz et al., 2007).

Auxin can also be transported by *MULTI-DRUG-RESISTANT/P-GLYCOPROTEINS* (*ABCB/PGPs*). The ABCB/PGP P-glycoproteins, members of the ancient ATP-binding cassette (ABC) protein subfamily, are able to transport amphipathic and anionic molecules upon ATP-hydrolysis (Titapiwatanakun and Murphy, 2009). In *Arabidopsis* only a few ABCBs were characterized as auxin transporters. *PGP1* (*ABCB1*) and *PGP19* (*ABCB19*) are related to basipetal auxin transport and displayed a certain binding affinity to the auxin transport inhibitor NPA, but unlike PINs, the *pgp1* and *pgp19* mutant phenotypes cannot be completely mimicked by a treatment with this inhibitor (Lewis et al., 2007; Wu et al., 2007; Yang and Murphy, 2009). In the root, PGP1 and PGP19 appear to play a supportive role in controlling cellular auxin retrieval (Lewis et al., 2007; Titapiwatanakun et al., 2009). PGP4 also contributes to auxin transport in the root supporting AUX1 and PIN2 (Wu et al., 2007). Although the PGP1 and PGP19 proteins have a more stable localization at the plasma membrane,

their trafficking also depends on GNOM-like (GLN1) protein activity (Titapiwatanakun et al., 2009). The requirement of PGP1 and PGP19 for lateral root initiation remains a bit obscure, although the mutants *pgp* and *pin pgp* exhibit defects in lateral formation (Wu et al., 2007; Mravec et al., 2008). The complementary and additive effect of AUX1, PINs and PGPs proteins turns out to be a fine-tuning of polar auxin flows required for the correct development of lateral root primordia (Titapiwatanakun and Murphy, 2009).

The auxin maximum accumulating in the centre and consequently in the tip of lateral root primordia provides the signal for the degradation of IAA14 (Aux/IAA) proteins (Vanneste et al., 2005). The de-repression of ARFs (*ARF7/ARF19*) trigger the induction of genes related to the patterning of new lateral root primordia. The downstream genes regulated by ARF7 and ARF19 were recently identified by their ability to rescue the *arf7 arf19* mutant phenotype, overexpressing two LBD/ASLs which belong to a large family of transcription factors in *Arabidopsis* (Okushima et al., 2007). The direct activation of *LBD16/ASL18* (*LATERAL ORGAN BOUNDARIES-DOMAIN16 / ASYMMETRIC LEAVES2-LIKE18*) and *LBD29/ASL16* by ARFs suggest that the signaling cascade patterning lateral root primordia may also have duplicated or specialized, which reveals a whole regulatory network to develop a lateral root primordia (Okushima et al., 2007; De Smet and Jürgens, 2007).

The identification of the *puchi* mutant disturbed in cell division during early lateral root development confirmed an auxin-dependent patterning in lateral root primordia (Hirota et al., 2007). Auxin promotes the transcription of *PUCHI* through ARF-type transcription factor activation in all primordia cells, but does not affect the auxin distribution or primary transcriptional response to auxin in the early stages of lateral root formation (Hirota et al., 2007). The PUCHI protein was classified as a member of the AP2/EREBP family, which is a plant-specific family of transcription factors that contains other members related to shoot development and embryo patterning, such as *LEAFY PETIOLE* (*LEP*) or *DORNROESCHEN/ENHANCER OF SHOOT REGENERATION1* (*DNR/ESR1* and 2)(van der Graaff et al., 2000; Chandler et al., 2007; Cole et al., 2009).

In addition to auxin, other plant hormones might influence the patterning of new lateral root primordia. When pericycle cells were exposed to elevated cytokinin levels, due to an enhanced expression of the cytokinin biosynthesis gene *IPT* (*ISOPENTENYL TRANSFERASE*), plants exhibited a disturbed initiation and formation of lateral roots (Laplaze et al., 2007). These results corroborate the

findings that transactivation of the cytokinin-degrading enzyme *CYTOKININ OXIDASE1* in lateral root founder cells causes increased proliferation of laterals (Laplaze et al., 2007). According to the authors, cytokinins interfere at the early stages of lateral root development causing disturbances in PIN expression and, therefore, preventing the formation of an auxin gradient (Laplaze et al., 2007).

#### **2.1.1.4. Lateral root emergence**

Once a lateral root primordium has been initiated, it must form an autonomous meristem and emerge from the parental root tissue (Malamy and Benfey, 1997). Lateral root emergence also relies on auxin. The auxin derived from shoot apex seems to play a major role, since it was demonstrated in *Arabidopsis* that removal of leaves and cotyledons blocked lateral root emergence (Swarup et al., 2008). Auxin biosynthesis occurs in both, shoots and roots (Ljung et al., 2005). In *Arabidopsis*, auxin is mainly synthesized in the shoot and transported via the phloem or via polar auxin transport in the xylem parenchyma to the roots. Until the seedling is 4 days old both pathways are of similar importance (Ljung et al., 2005). Around 8 days after germination, phloem-mediated auxin transport becomes relatively more important (Ljung et al., 2005). Shoot-derived auxin is important for lateral emergence (Bhalerao et al., 2002). In the later stages of development, lateral roots acquire the ability to synthesize auxin on their own, which is important for the auxin pool size in the root (Ljung et al., 2005).

Although, there are two distinct auxin sources for lateral initiation and emergence, a competition for auxin seems to occur between these two processes. It has been shown by stochastic modeling and further validation in mutants with disturbed auxin transport that: i) in the initiation zone, close to the meristem, auxin reflux leads to an auxin accumulation up to a threshold; ii) auxin will give rise to a new primordium which depletes the auxin source in the initiation zone; iii) the primordium, now in the developed zone, consumes more auxin derived from the shoot; and iv) the primordia will emerge if their auxin content is higher than the emergence threshold (Lucas et al., 2008). Emerging lateral roots stop the consumption of auxin (Lucas et al., 2008). This suggests that root branching is controlled by mechanisms of lateral root inhibition due to a competition for auxin between lateral root initiation and emergence (Lucas et al., 2008).

A recent transcriptome profiling of auxin-treated roots revealed an increased expression of cell wall remodeling genes during lateral root development (Laskowski et al., 2006). Among those were pectin methylesterase and pectate lyase genes that are involved on pectin catabolism and breakdown (Laskowski et al., 2006). These observation suggested that the overlying cell layers need to undergo cell separation allowing primordium emergence (Laskowski et al., 2006). A concomitant expression of expansin, xyloglucan endotransglucosylase/hydrolase and polygalacturonase in the epidermal cells covering the lateral root primordia (Vissenberg et al., 2000; Van Sandt et al., 2007; Ogawa et al., 2009), support the view that an outgrowth of the primordium requires cell wall loosening to facilitate lateral root emergence (Laskowski et al., 2006; Swarup et al., 2008).

In the parental root, LAX3 (*LIKE AUX1-3*) is localized in cortical and epidermal cells adjacent to lateral root initials (Swarup et al., 2008). The mechanism of lateral root emergence starts with auxin originating from the dividing pericycle founder cells which induces cell wall remodeling gene expression in adjacent endodermal cells. This step is dependent on the degradation of the SH2/IAA3 repressor which is expressed mainly in the endodermis (Swarup et al., 2008). Then, the auxin from the primordium induces the expression of LAX3 that acts as an auxin influx carrier in cortical cells. In dependence of ARF7 and ARF19 as well as SLR/IAA14, LAX3 increases the cellular permeability for auxin (Swarup et al., 2008). As a result, the auxin originating from the lateral root primordium acts as a local signal which reprograms adjacent cells for cell wall loosening. In agreement with this hypothesis the *lax3* mutant is defective in lateral emergence, although the number of lateral root primordia is significantly higher compared to the wildtype (Swarup et al., 2008).

#### **2.1.1.5. Lateral root elongation**

The activation of the meristem in the lateral root primordium right after its breakthrough of the epidermal cell layer is required for an independent development. This process appears to profit from auxin, being produced in the lateral root meristem (Ljung et al., 2005). However, it is unknown whether the auxin biosynthesis only coincides with or is the cause of meristem activation in the lateral root. In the *alf3* mutant, lateral root primordia die in a premature state. This phenotype can be rescued by the external application of auxin into the growth medium demonstrating that auxin is required for meristem activation (Celenza et al., 1995).

Lateral root elongation relies on auxin transport either from shoot or the primary root tip. This was recently demonstrated by the disturbed acropetal auxin transport on *mdr1* mutants (*multi drug resistance1*) exhibiting a decreased elongation of laterals (Wu et al., 2007). The *MDR1-like ABC* transporter participates in auxin transport, is required for normal lateral elongation, and for producing an auxin maximum in the lateral root apex (Wu et al., 2007).

An impressive progress has been made in understanding lateral development over the past years. Recent research activities shed light on lateral root initiation and development based on a large number of intensive genetic and molecular studies trying to dissect the process of lateral root development in *Arabidopsis*. A next challenge will be to integrate auxin-dependent signaling pathways with other hormones and the nutritional status of the plant, which reflects an important component in root plasticity.

## **2.2. Root plasticity**

Plants evolved their ability to survive under challenging growth conditions by adapting their root system. According to the availability of nutrients or water in the soil, plants alter their root architecture in a way to increase the extractable soil volume. This response is particularly dependent on the plant species and the mobility of a nutrient in the soil (Hodge, 2006). The mechanisms by which plant roots sense nutrients availability in the soil solution are still largely unknown, however, first pieces of information on nutrient sensing and signaling are just becoming available. The most detailed pathways and, if relevant, their interference with nutrient transport processes are described in the following.

### **2.2.1. Nitrate signaling and nitrate-induced root plasticity**

In soils N is plant available in the forms of ammonium ( $\text{NH}_4^+$ ), nitrate ( $\text{NO}_3^-$ ), urea, amino acids and peptides (Miller et al., 2008). The abundance of these compounds is highly variable and this can dramatically affect root development. In *Arabidopsis*, the *NRT2;1* gene encodes a major component of the high-affinity  $\text{NO}_3^-$  transport system (HATS) in roots (Cerezo et al., 2001). *NRT2;1* is up-regulated under N limitation, but repressed by downstream N metabolites such as ammonium or amino acids (Krouk et al., 2006). High-affinity nitrate uptake is supported by the dual-

affinity NO<sub>3</sub><sup>-</sup>-transporter NRT1;1 (CHL1), which switches upon dephosphorylation to a low-affinity NO<sub>3</sub><sup>-</sup>-transporter (Liu and Tsay, 2003). When plants were cultivated under high N, NRT2;1 transcripts were strongly repressed in the *nrt1;1* mutant compared to wild-type plants, indicating that NRT1;1 may have a nitrate sensing function in the transcriptional regulation of NRT2;1 (Krouk et al., 2006).

Recently, a calcineurin B-like (CBL)-interacting protein kinase (CIPK), CIPK23, was found to be involved in early nitrate signaling. *CIPK23* was rapidly induced in the presence of nitrate (Ho et al., 2009). The analysis of a *cipk23* mutant indicated that this protein is a negative regulator of high-affinity phase by direct phosphorylation of Thr<sup>101</sup> residue in the NRT1;1 (Ho et al., 2009). Instead, CIPK8 protein positively regulates the low-affinity phase (Hu et al., 2009). Furthermore, the *nodule inception-like protein 7 (NLP7)* was also suggested to be part of the nitrate signaling pathway, by modulating nitrate assimilation in response to nitrate signals (Castaings et al., 2009). The *NLP7* transcription factor regulates the expression of *NTR2;1*, *NRT2;2* and the nitrate reductase gene *NIA* (Castaings et al., 2009). Thus, different levels of response can be triggered by these proteins, whereby CIPK23, CIPK8 and NLP7 are required for the regulation of nitrate transport and assimilation in plant roots.

The effect of nitrate nutrition on root development has been described in *Arabidopsis*. There, nitrate signaling triggers the elongation of already emerged lateral roots (Zhang et al., 1999). Under local supply of nitrate there was an increased elongation of lateral roots correlating with an enhanced cell proliferation in the lateral root meristem (Zhang et al., 1999). However, when high nitrate concentrations were locally supplied, the lateral roots delayed meristem activation in laterals, following a systemic inhibitory effect on lateral root elongation (Zhang et al., 1999; Zhang and Forde, 2000). The *nia1 nia2* double mutant presented a similar dual effect upon localized nitrate supply suggesting that the nitrate-ion itself acts as signal to influence root morphology (Zhang and Forde, 2000). *ANR1*, a member of the MADS-box transcription factor family, was shown to be a component of nitrate-stimulated lateral root elongation. *ANR1* transcript levels increased by nitrate and depended on NRT1;1 implicating that NRT1;1 acts upstream of ANR1. In split-root experiments, nitrate-exposed lateral roots elongated and this phenotype could not be mimicked by other nitrogen forms (Remans et al., 2006). The *nrt1;1 (chl1)* mutant exhibited a weaker lateral root elongation when *Arabidopsis* roots were cultivated in split-root plates with localized nitrate supply. In addition, the expression of *ANR1* was strongly reduced in the *nrt1;1 (chl1)* mutant (Remans et al., 2006). Therefore, apart

from its transport function, *NRT1;1* seems to have a sensor role for lateral growth into nitrate-rich patches, which was supported by *NRT1;1* and *ANR1* co-localization in root tips (Remans et al., 2006). This hypothesis was supported when *NRT1;1* was shown to be essential for changes in root morphology caused by the organic nitrogen form glutamate. Elevated L-glutamate supply in the medium can be sensed by the primary root tip and provoke root growth inhibition (Walch-Liu and Forde, 2008). The inhibitory effect of L-glutamate was reversed by external nitrate supply, independently of changes in glutamate uptake (Walch-Liu and Forde, 2008). The *nrt1;1* (*chl1*) mutant proved to be insensitive to the antagonistic effect of L-glutamate on primary root growth. However, when *NRT1;1* was overexpressed in the *nrt1;1* mutant the sensitivity was restored, suggesting *NRT1;1*-dependent nitrate signaling. Interestingly, the non-phosphorylated form *NRT1;1<sup>T101A</sup>* failed to restore the nitrate sensitivity suggesting that the *NRT1;1* is active as a sensor mainly in its phosphorylated form (Walch-Liu and Forde, 2008).

Using a systems biology approach and fluorescence-assisted cell sorting of GFP-tagged cell lines, transcriptome responses to nitrate allowed identifying a broad range of genes expressed in different cell layers in response to N signaling (Gifford et al., 2008). Among them, the microRNA167a/b, expressed in pericycle cells and the lateral root cap, was involved in a regulatory circuit with *ARF8* (*AUXIN RESPONSE FACTOR8*) mediating lateral root outgrowth (Gifford et al., 2008). The authors showed that *ARF8*, a repressor of lateral emergence, was induced by nitrate and blocked by a glutamine synthetase inhibitor during lateral initiation and subsequent emergence (Gifford et al., 2008). As a result, organic N rather than nitrate seems to generate a predominant signal regulating the repression of lateral root emergence (Gifford et al., 2008).

### 2.2.2. Ammonium transport and signaling in yeast and plants

In *Arabidopsis* and other crop plants, ammonium is taken up as a preferential N-source when both N forms are supplied at equimolar concentrations (Gazzarrini et al., 1999a; von Wirén et al., 2000). In plants, high-affinity ammonium uptake by roots is mediated by ammonium transporters of the AMT/Rh/MEP family. This family includes the Rh-type proteins, e.g. *human Rhesus blood group polypeptides*, which are expressed in erythroids (*RhAG*) and the kidney (*RhGK*), where they promote bi-directional ammonia transport (Marini et al., 2000). The first ammonium transporters

were identified from *Saccharomyces cerevisiae*, which harbours three closely related *MEP* (*METHYLAMMONIUM PERMEASE*) transporters (*Mep1*, *Mep2* and *Mep3*) (Marini et al., 1997).

In parallel the MEP-type *AmtB* protein was isolated from eubacteria and archaea (von Wirén and Merrick, 2004). The *Escherichia coli AmtB* transporter was the first member of this family to be purified and crystallized and therefore serves as a model for structural investigations (Khademi et al., 2004; Merrick et al., 2006). The crystal structure of *AmtB* showed a hydrophobic pore most likely forming an ammonia (NH<sub>3</sub>) channel, indicating that MEP-type proteins mainly transport the uncharged substrate species (Andrade et al., 2005).

Using yeast as a genetic model, several genes related to ammonium signaling were discovered. An important role in ammonium sensing has been attributed to the *Mep2* protein since this protein is required for pseudohyphal growth in response to very low ammonium availabilities (Lorenz and Heitman, 1998; Marini and Andre, 2000). By site-direct mutagenesis of residues lining along the ammonium conducting pore of *Mep2p*, it was possible to uncouple the signaling from the transport function, indicating that transport is required although not sufficient to sense ammonium (Rutherford et al., 2008). The intracellular C-terminus of *Mep2* in *Candida albicans*, which is dispensable for ammonium transport, was also found to be essential for filamentous growth in response to N starvation (Rutherford et al., 2008). By transcriptome profiling of yeast cells overexpressing *Mep2*, it was found that the *Npr1* (*NITROGEN PERMEASE REACTIVATOR 1*) kinase is necessary to activate *Mep2*-dependent ammonium transport, but not its localization or expression (Rutherford et al., 2008). Under poor-nitrogen supply, *Npr1* opposes the ubiquitination of *Gap1* (*GENERAL AMINO ACID PERMEASE1*) an amino acid sensor, suggesting that *Mep2* contributes greatly to filamentous growth occurring under amino acid deficiency (Boeckstaens et al., 2007; Van Zeebroeck et al., 2008). Nitrogen deficiency-induced filamentous growth can be controlled by different pathways, one of them involving the *mitogen-activated protein kinase* (*MAP*) kinase and *cyclic AMP-protein kinase A* (*cAMP-PKA*) (Van Zeebroeck et al., 2008). Most importantly, methylammonium (MeA), which is only metabolized to methyl-glutamine but not further, also activated the *Mep2*-PKA signaling cascade, however, only ammonium but not MeA caused the required changes in the *Mep2* C-terminus required for filamentous growth of yeast (Van Nuland et al., 2006). These results indicate that ammonium binding to the carrier triggers a conformational change and thereby

initiates signaling (Van Nuland et al., 2006). Plant ammonium transporters from *Arabidopsis* were not able to trigger the signaling cascade which indicates that ammonium sensing in yeast is different from that in higher plants (Van Nuland et al., 2006).

Among the *Arabidopsis* AMTs, *AtAMT1;1*, *AtAMT1;2* and *AtAMT1;3* are highly expressed in roots and up-regulated under N deficiency (Gazzarrini et al., 1999b; Von Wiren et al., 2000). The expression of *AtAMT2*, which is more closely related to the bacterial and yeast Amt/Mep proteins (Sohlenkamp et al., 2002) was higher in shoots than in roots, but also subjected to a N-dependent transcriptional regulation (Sohlenkamp et al., 2002). Uptake studies with <sup>15</sup>N-labeled ammonium in triple and quadruple mutants carrying insertions in different AMTs revealed that *AtAMT1;2* displayed the highest *in vivo* substrate affinity (236 μM), followed by *AtAMT1;3* and *AtAMT1;1* (60 μM and 51 μM, respectively) and finally by *AtAMT1;5* (4.5 μM) for which only correlative data were achieved (Yuan et al., 2007). While *AtAMT1;1*, *AtAMT1;3* and *AtAMT1;5* localize to the plasma membrane of rhizodermis cells, *AtAMT1;2* was found to be localized in the plasma membrane of endodermal and cortical cells; this reveals a spatial arrangement of AMT1-type transporters in order to assure ammonium uptake for efficient radial transport across the root tissue via the symplastic and apoplastic routes (Yuan et al., 2007).

Recently, a new type of posttranscriptional regulation was described for AMT1-type transporters. In the plasma membrane, *Arabidopsis* AMT1;1 forms trimers, and phosphorylation of a conserved Thr<sup>460</sup> residue in the cytosolic C-terminus causes trans-inactivation of neighboring subunits (Loque et al., 2007). In that way, a single phosphorylation event in the C-terminus of one subunit can lead to an allosteric regulation of the whole oligomer, which seems to be an efficient and fast mechanism to inactivate the protein complex (Loque et al., 2007). This phosphorylation event is triggered by external ammonium supply implying that AMT1;1 responds to external substrate fluctuations either directly, as a sensor, or indirectly, e.g. by depending on a receptor kinase-like protein (Lanquar et al., 2009). Whether this ammonium sensing mechanism around AMT1;1 is also relevant for changes in root architecture upon varying ammonium supplies remains to be investigated.

### 2.2.3. Phosphorus-regulated root plasticity

Plant responses to phosphorus (P) deficiency are agriculturally important due to its low availability in most soils. Numerous factors can influence P precipitation or fixation in the soil and thereby lead to an uneven distribution and spatial availability of P (Marschner, 1995). As a consequence, several morphological adaptations in the root morphology have been found and described that allow better exploiting P from the soil.

A major clue to acquire phosphate is a plant's ability to explore soil layers near to the soil surface through adaptive changes in root morphology (Lopez-Bucio et al., 2002). *Arabidopsis* plants respond to P deficiency with a redistribution of biomass allocation from the primary root to lateral roots (Lopez-Bucio et al., 2002). While the primary root is restrained from growth, lateral root growth increases in density and length, forming a shallow and highly branched root system (López-Bucio et al., 2003). Some mutants were isolated which displayed altered primary root growth under P deficiency. Among them, the *low phosphate root (lpr)* mutant was described to carry a point mutation in a multicopper oxidase gene (Svistoonoff et al., 2007). So far, it remains unknown what is the function of this abiotic stress-regulated enzyme in P-dependent changes in root morphology.

Recently, it has been proposed that cytokinins interfere with P starvation-responsive genes by regulating meristem activity. A hypothesis was raised in which an inhibition of cell cycle activity, but not of cell expansion and growth, reduces the expression of P starvation-responsive genes, suggesting that the cell cycle activity specifies the P demand in P-starved plants (Lai et al., 2007). Indeed, it has been previously reported that seedlings grown under P deprivation have an exhausted primary root meristem (Sanchez-Calderon et al., 2005). Thus, meristem activity is likely to be a target under P limitation. In agreement with this hypothesis, *PDR2* (*PHOSPHATE DEFICIENCY RESPONSE2*) is required for a proper expression of *SCR* (*SCARECROWN*), an essential regulator of root patterning and stem cell maintenance during root growth (Ticconi et al., 2009). Surprisingly, *PDR2* encodes a P5-type ATPase in *Arabidopsis*, and its localization in the ER together with *LPR1* seems to be important to adjust root meristem activity to external concentrations of P (Ticconi et al., 2009).

Auxin sensitivity seems to be vital for lateral root formation and emergence under P-limiting conditions. The expression of the auxin receptor *TIR1* (*TRANSPORT*

*INHIBITOR RESPONSE1*) increases upon P deprivation, and consequently accelerates the degradation of the Aux/IAA repressors and de-represses the transcription factor ARF19 required for lateral root formation and emergence (Perez-Torres et al., 2008). Interestingly, when plants overexpressing *TIR1* were grown under low P, they did not show meristem exhaustion suggesting that a TIR1-independent pathway might exist during root development under low P availability (Perez-Torres et al., 2008).

Despite the increase in lateral root density under P deprivation, it has been proposed that primary root growth under low P is independent of polar auxin transport (López-Bucio et al., 2005). In fact, mutants defective in auxin signaling or polar transport still showed changes in root morphology under P-limited conditions (López-Bucio et al., 2005). Furthermore, an altered auxin accumulation in roots grown on low P was suggested to cause the root phenotype in P-starved plants (Nacry et al., 2005). This suggestion appears contradictory, since polar auxin transport is essential for root branching. Nevertheless, further studies are needed to better understand the role of auxin in P signaling and altered root system architecture.

#### **2.2.4. Sulfur-regulated root plasticity**

A higher proliferation of roots under S starvation indicates that root morphology is also under control of the S nutritional status and presumably of S-signaling pathways. Sulfur-deficient plants elongate the primary root and stimulate lateral root growth (Kutz et al., 2002). *NIT3* (*NITRILASE3*), which is able to convert indole-3-acetonitrile to indole-3-acetic acid (IAA), was shown to be responsive to S deprivation (Kutz et al., 2002). Promoter analysis of *NIT3* revealed the presence of sulphur-responsive elements, which indicates that S starvation leads to an increase in auxin biosynthesis, and consequently, enhanced primary root growth and branching (Kutz et al., 2002). Furthermore, the auxin-inducible IAA18 and other Aux/IAA proteins are up-regulated under S starvation, suggesting a direct activation of auxin biosynthesis and signaling upon S deprivation (Nikiforova et al., 2003).

The plant hormone cytokinin is also a signaling component under sulfur deficiency. Exogenous cytokinins down-regulate the expression of *SULTR2;1* (a high-affinity sulphate transporter in the root) and up-regulate *APR1* (*APS REDUCTASE 1*) in the leaves, even though both genes are up-regulated under S deficiency (Ohkama

et al., 2002; Maruyama-Nakashita et al., 2006). Interestingly, when cytokinins were supplied exogenously to the cytokinin receptor mutant *cre1-1*, only a partial decrease of sulphate uptake was observed (Maruyama-Nakashita et al., 2004). These results indicate that *CRE1/AHK4* is involved in the repression of S deficiency-inducible genes and that cytokinins might be an important component in the root-shoot communication on the S nutritional status (Maruyama-Nakashita et al., 2004). Despite this important progress in understanding intracellular signaling components in the S deficiency stress response, any involvement of these components in morphological changes of S-deficient roots has not yet been reported.

### 2.2.5. Potassium-regulated root plasticity

A decreased number and length of lateral roots is a major change in the root system architecture when plants are subjected to potassium (K) deficiency. This response is also related with auxin signaling. Microarray analysis showed that the transcription factor *MYB77* is repressed upon K deprivation (Shin et al., 2007). Analysis of promoter regions of auxin-responsive genes revealed the presence of AuxREs in the *ARF7* promoter that share the same binding motif with MYB transcription factors. The authors further demonstrated that *MYB77* interacted through its C-terminus with *ARF7* controlling the lateral growth response upon K limitation (Shin et al., 2007). Interestingly, the *AtKUP4/TRH1* potassium transporter was recently suggested to be an auxin transporter. A mutant defective in *TINY ROOT HAIR 1 (TRH1)* is affected in root hair development and gravitropism, but an exogenous auxin supply can rescue the phenotype. Interestingly, wildtype plants grown under low K concentrations displayed unusual agravitropic responses similar to the *trh1* mutant (Vicente-Agullo et al., 2004). Furthermore, the *trh1* mutant exhibited a reduced efflux of radioactively labelled IAA in isolated root segments. In contrast, yeast cells heterologously expressing *TRH1* presented high efflux of radio-labelled IAA (Vicente-Agullo et al., 2004). These data indicate that the *AtKUP4/TRH1* potassium transporter is involved in auxin transport, although the underlying molecular mechanism remains unclear (Vicente-Agullo et al., 2004).

Transcriptome analysis further revealed that, after 6 h of K starvation, *Arabidopsis* roots induced the high-affinity K<sup>+</sup> transporter *HAK5*, which is expressed in the rhizodermis of primary and lateral roots. The up-regulation of *HAK5* under K deficiency went along with the formation of reactive oxygen species (ROS) and of

ethylene. During K deprivation, ROS accumulated preferentially in the elongation zone of primary roots (Shin and Schachtman, 2004). Moreover, external application of H<sub>2</sub>O<sub>2</sub>, which induces ROS, increased the expression of *HAK5*, indicating that ROS modulate *HAK5* expression and K uptake in K-deficient roots. Using the expression of *HAK5* as a marker for K starvation in Arabidopsis roots, ethylene was shown to act upstream of ROS signaling (Jung et al., 2009). However, it remains to be solved at what level the signaling cascade: K-deficiency – ethylene – ROS – *HAK5* expression interferes with root hair formation.

### 2.2.6. Iron signaling and iron acquisition

In well-aerated soils, the high abundance of Fe in soils does not correlate with its solubility due to the strong tendency of Fe to precipitate in the form of oxides or hydroxides (Marschner et al., 1986). This precipitation causes extremely low Fe availabilities that are far below those required to cover the Fe demand of plants. To cope with this situation, plants developed a set of physiological and morphological adaptations that are under control of different signaling pathways (Marschner et al., 1986).

Plants have evolved two different strategies for Fe-acquisition from the soil. In graminaceous monocots Fe acquisition is governed by Strategy II, which relies on the release of Fe-chelating substances by the root, so-called mugineic acid-type phytosiderophores (MAs) (Romheld and Marschner, 1986). These phytosiderophores are released under Fe deficiency and solubilize Fe<sup>(III)</sup> in the rhizosphere by chelation. The Fe(III)-phytosiderophore complex is then taken up by plant roots via the plasmamembrane transporter *YS1* (*YELLOW STRIPE1*)(Curie et al., 2001). The importance of this Fe acquisition pathway is emphasized by the *ys1* mutant phenotype in maize, which displays severe leaf chlorosis and is not capable to reach the reproductive growth phase (von Wiren et al., 1994). All other plants, except graminaceous monocots, induce the Strategy I responses to increase Fe acquisition by the plant roots (Romheld and Marschner, 1986), which consist of:(i) an acidification of the rhizosphere through an increased expression of plasma membrane-bound proton-ATPases thus enhancing the Fe<sup>(III)</sup> solubility; (ii) activation of the Fe<sup>(III)</sup>-chelate reductase *FRO2* (*FERRIC REDUCTASE OXIDASE*) increasing the concentration of soluble Fe<sup>(II)</sup> (Robinson et al., 1997; Robinson et al., 1999); (iii) upregulation of the plasma membrane Fe transporter *IRT1* (*IRON TRANSPORTER*

1) for Fe<sup>2+</sup> uptake (Korshunova et al., 1999; Vert et al., 2002). The majority of these components were described in *Arabidopsis*, a Strategy I plant, but Strategy II plants like rice also employ components of Strategy I e.g. when grown in flooded soils where Fe is mainly available in the ferrous form (Cheng et al., 2007).

The first molecular component related to Fe-deficiency signaling was identified in tomato, a Strategy I plant. *FER* (*FER-LIKE REGULATOR OF IRON UPTAKE*), which encodes a basic helix–loop–helix (BHLH) transcription factor, is predominantly expressed in roots and upregulated under low Fe availability (Ling et al., 2002; Brumbarova and Bauer, 2005). Plants with a constitutively upregulated expression of *FER* displayed abundant mRNA levels independent of the Fe nutritional status of the plant, nevertheless, the FER protein was detected only under Fe-deficiency conditions, indicating that *FER* expression underlies post-transcriptional control (Brumbarova and Bauer, 2005). The tomato mutant *chloronerva* is defective in the biosynthesis of NA, which is important for proper Fe trafficking within the plant. This mutant exhibits Fe-deficiency-induced chlorosis even though it accumulates high Fe levels due to an up-regulation of Strategy I genes. In this mutant, the FER protein accumulates even under Fe-sufficient conditions implying that the external Fe supply cannot cause FER repression (Brumbarova and Bauer, 2005). This observation suggested that FER might be regulated by a shoot-derived signal reflecting the Fe nutritional status (Brumbarova and Bauer, 2005). The homolog to *FER* in *Arabidopsis* has been named *FIT* (*FE-DEFICIENCY INDUCED TRANSCRIPTION FACTOR IRON UPTAKE*) and is a key component controlling Fe-deficiency responses in Strategy I plants (Bauer et al., 2007). *FIT* regulates *FRO2* and *IRT1* at the transcriptional level and *IRT1* presumably at the protein level too (Colangelo and Gueriot, 2004). Interestingly, overexpression of *FIT* was not sufficient to increase the expression of *FRO2* and *IRT1* indicating that FIT might act together with another factor to trigger Fe-deficiency responses in *Arabidopsis* (Wang et al., 2007). Indeed, microarray studies identified several basic helix–loop–helix (BHLH) transcription factors involved in Fe-deficiency responses. Transgenic plants constitutively expressing *BHLH38* or *BHLH39* and *FIT* displayed high transcript levels of *FRO2* and *IRT1*, suggesting that BHLH38 and BHLH39 physically interact with FIT under Fe-limited conditions (Yuan et al., 2008).

Evidence is accumulating that nitric oxide (NO) is involved in the regulation of Fe-deficiency responses (Graziano and Lamattina, 2007). It has been shown that Fe-deficient tomato roots accumulate high levels of NO, especially in rhizodermal cells,

which co-localizes with the expression of *LeIRT1* and *LeFRO1*. Moreover, the tomato *fer* mutant turned out to be insensitive to NO indicating that the FER protein is necessary to mediate the action of NO on the Fe-deficiency-induced signaling cascade (Graziano and Lamattina, 2007). It is interesting to note, that NO is also induced if Fe is in excess in plant cells. When Arabidopsis cells were cultured under high Fe supplies, NO rapidly accumulated in the plastids (Arnaud et al., 2006). This response went along with an elevated expression of *Fer1* (*FERRITIN1*), that encodes an Fe storage protein acting as a scavenger for Fe to avoid its accumulation and oxidative damage (Arnaud et al., 2006; Ravet et al., 2009). Employing a pharmacological approach, it has been shown that NO acts upstream to *AtFer1* (Arnaud et al., 2006). Thus, NO has a dual effect in Fe signaling, it is involved in regulating plant responses under Fe deficiency as well as under Fe excess.

Among the plant hormones, ethylene was shown to act as signal in Fe deficiency-induced responses. Using a pharmacological approach to reduce ethylene levels, tomato and Arabidopsis roots synthesized less ethylene and downregulated *IRT1* and *FRO2*; this effect could be reversed by an external application of 1-aminocyclopropane-1-carboxylic acid (ACC), an ethylene precursor. Thus, Fe limitation increases ethylene production which turned out to be a signal under Fe deficiency (Lucena et al., 2006). This signal has been shown to be a local response because it was not affected in the *ferric reductase defective3* (*frd3*) mutant, which is defective in xylem loading of the Fe<sup>(III)</sup>-chelator citrate required for Fe translocation to the shoot. As a consequence, *frd3* plants constitutively express Fe-deficiency responses (Durrett et al., 2007). However, the constitutive upregulation of Fe-deficiency responses in *frd3* could be suppressed by foliar Fe applications (Lucena et al., 2006). When the *frd3* mutant was treated with ACC, the expression of *IRT1* and *FRO2* remained upregulated, suggesting that ethylene is not a shoot-derived signal controlling Fe-deficiency responses in the root (Lucena et al., 2006).

Also cytokinins were shown to be involved as local signals controlling Fe acquisition in roots. When Arabidopsis roots were supplied with cytokinins, root growth was inhibited and Fe acquisition genes were repressed irrespective of the Fe nutritional status of the plant (Séguéla et al., 2008). Furthermore, an external supply of cytokinins to the *fit* mutant resulted in a repression of *IRT1* and *FRO2* to a similar extent as in wildtype plants, indicating that cytokinins repress Fe acquisition via a FIT-independent pathway (Séguéla et al., 2008) but involving the cytokinin receptors *CRE1/WOL/AHK4* and *AHK3* (Séguéla et al., 2008).

Iron deficiency also induces morphological changes at the level of the root system by triggering the development of additional root hairs that lead to an increase in root surface and thereby contribute to Fe acquisition. This coincides with an increase in the development of transfer cells in the rhizodermis and the formation of branched root hairs (Schmidt and Schikora, 2001). Using split root experiments, it was shown that the root hair branching typical for Fe deficiency was not induced by local Fe limitation as long as the shoot experienced Fe-sufficiency. Conversely, when *Arabidopsis* shoots suffered from Fe deficiency, local Fe deficiency led to the formation of root hairs, suggesting that root hair branching is dependent on a systemic and a local Fe deficiency signal (Schikora and Schmidt, 2001). Using mutants defective in ethylene signaling, like *ein2* and *etr1*, ethylene was proven to be an essential component in the signaling pathway coordinating the rhizodermal cell differentiation under Fe deficiency (Schmidt et al., 2000). Moreover, wildtype plants grown under Fe-sufficient conditions displayed ectopic root hair formation after exogenous ACC application (Schmidt et al., 2000).

Some Strategy I plants have the ability to form cluster roots under Fe-limiting conditions. These cluster roots are composed of numerous laterals with root hair sections formed along the root, where a high reductase activity was found (Rosenfield et al., 1991). Again, ethylene is involved in cluster root formation under Fe-limited conditions but its detailed function is still uncovered (Zaid et al., 2003). Likewise, sunflower plants have been shown to increase lateral root density under Fe-deprivation (Römheld and Marschner, 1981). This phenotype was reversed by an external application of Fe-chelates to the shoot, indicating that a systemic signal mediated these morphological changes in Fe-deficient roots. Despite the availability of several mutants in Fe signaling and acquisition, so far only little research has been conducted on the morphological adaptations of the root system to low Fe availability. Therefore, studies should also include approaches to describe whether Fe deficiency might affect the root system architecture at a qualitative and quantitative level.

### 2.3. Objectives of the thesis

The amount and form of nutrient supply in the soil has a profound role on the architecture of plants roots. Moreover, a few examples indicate that nutrient mobility influences plant root development (Hodge, 2006), even though it is still unclear which nutrients are able to trigger changes in the root architecture and what are the underlying molecular mechanisms that allow a plant root to sense a localized nutrient source. Based on the background that root plasticity appears to be a nutrient-specific response, the present thesis aimed to investigate and characterize the changes in root system architecture under localized nutrient supply and to identify molecular components involved. Therefore, two nutrients were chosen that differ in mobility and abundance in the soil solution and for which root morphological adaptations have not yet been investigated, namely iron (Fe) and ammonium (NH<sub>4</sub>). First, chapter 3 describes a detailed investigation on changes in root morphology triggered by a localized Fe supply. Although Fe is one of most abundant elements in the soil, its solubility is profoundly affected by chemical and physical characteristics of soil particles which may cause a heterogenous distribution in the soil. To investigate the role of localized Fe supply in the root morphology, a series of *in vitro* plant culture and molecular experiments were undertaken with Arabidopsis mutants which are defective in Fe acquisition or Fe translocation within the plant.

Chapter 4 describes a currently unrecognized adaptation of the root morphology to localized ammonium supply. Ammonium is positively charged and readily adsorbed by the negatively charged soil matrix, which makes ammonium a less mobile N form in the soil solution compared to nitrate (Miller et al., 2007). Taking a genetic approach with different mutants lacking the ability to transport ammonium, and employing analytical tools including <sup>15</sup>N uptake studies in agar plates, a particular involvement of certain ammonium transporters in ammonium-specific adaptations of the root system was investigated. Consequently, the question was tackled whether these morphological adaptations represent just a nutritional effect or a nutrient-sensing event.

The final chapter summarizes the previously described results and highlights the effect of nutrient availability on root system architecture over all nutrients that have been described so far. Furthermore, it is discussed in which nutrient transporters may act as transporters and sensors for nutrients at the same time.

### **3. Local Supply of Iron Distinctly Defines Lateral Root Number and Elongation in *Arabidopsis thaliana***

#### **3.1. Introduction**

In well-aerated and alkaline soils the availability of iron (Fe) to plants is far below that required for optimal growth (Marschner, 1995). With regard to the frequently occurring uneven distribution of organic matter but also of air- or water-conducting pores, Fe availability may vary locally and change in a gradual or patchy pattern within the root zone (Hinsinger et al., 2005). As a response to the low availability of soil Fe, plants have evolved a range of physiological and morphological responses that mobilize this micronutrient in the rhizosphere. Under limited Fe availability, non-graminaceous plant species, such as *Arabidopsis* induce plasma membrane-localized H<sup>+</sup>-ATPases that acidify the rhizosphere and thus favour subsequent Fe(III) reduction by a concomitantly expressed membrane-bound ferric Fe reductase. Ferrous Fe is then taken up into root cells by divalent metal cation transporters, among which IRT1 takes in a major role (Henriques et al., 2002; Vert et al., 2002). Both *IRT1* and the ferric reductase-encoding gene *FRO2* are rapidly up-regulated under Fe starvation and since an excess of intracellular Fe is toxic, the expression of both genes is co-ordinately down-regulated when enough Fe is supplied (Robinson et al., 1999; Connolly et al., 2003; Vert et al., 2003). Iron-dependent regulation is mediated by the basic helix-loop-helix (bHLH) transcription factor FIT (Bauer et al., 2007). In turn, *FIT* is also up-regulated in response to Fe deficiency suggesting that the Fe sensing event acts upstream of this transcription factor (Colangelo and Guerinot, 2004; Jakoby et al., 2004). It has been shown that the regulation of the high-affinity Fe uptake machinery in roots is regulated by local and systemic signals (Grusak and Pezeshgi, 1996; Giehl et al., 2009). Resupply of Fe to Fe-starved plants further induced the expression of *IRT1* and *FRO2* within 12 to 24 h demonstrating that Fe acts in the short run as an inducer of both genes (Vert et al., 2003). However, when plants were grown in a split-root set-up the expression and protein accumulation of IRT1 and FRO2 were enhanced in Fe-supplied but not in Fe-deficient root parts indicating that these components of Fe acquisition were also subject to a systemic regulation (Vert et al., 2003).

In addition to physiological responses, Fe deficiency also induces morphological changes by stimulating the ectopic formation of root hairs (Schmidt et al., 2000). It has been shown that Fe availability modulates the length, position and abundance of root hairs (Perry et al., 2007). Moreover, low Fe availability frequently leads to the formation of branched root hairs (Müller and Schmidt, 2004) through a signaling cascade probably involving auxin and ethylene (Schmidt et al., 2000; Schmidt and Schikora, 2001). Descriptions of other morphological changes under Fe deficiency go back to earlier reports in which subapical root zones of pepper started swelling and developed rhizodermal transfer cells (Landsberg, 1986), or sunflower increased lateral root density, which was reversed by an application of Fe chelates to leaves (Römheld and Marschner, 1981).

Lateral root development depends on the availability of certain plant nutrients. While mild nitrogen, sulphur or phosphorus deficiency generally lead to an extension of the root system and increased root-to-shoot ratios (Marschner, 1995; López-Bucio et al., 2003), the local supply of nitrate or phosphate to otherwise nitrogen- or phosphorus-deficient plants stimulates lateral root development (Drew, 1975; Zhang et al., 1999; Linkohr et al., 2002). Lateral root formation is a post-embryonic process (Dubrovsky et al., 2001) and results from the initiation, emergence and subsequent elongation of lateral roots (Casimiro et al., 2003; Péret et al., 2009). Nevertheless, lateral root structure differs in a nutrient-specific manner. For instance, a localized supply of nitrate or phosphate strongly stimulated lateral root elongation in *Arabidopsis*, whereas only local nitrate supply additionally increased lateral root density (Zhang et al., 1999; Linkohr et al., 2002). In both cases lateral root formation could not be explained by a nutritional effect but rather appeared as the consequence of a sensing event that was under control of local and systemic signals (Zhang et al., 1999; Remans et al., 2006).

To date, changes in lateral root structure in response to patchy micronutrient availabilities have not yet been described, even though profound changes in root architecture should be expected for those micronutrients that are sparingly soluble. Therefore, it was investigated how the local availability of Fe alters the architecture of *Arabidopsis* roots and which processes in lateral root formation might represent a primary target for the regulation by Fe. Furthermore, morphological responses in wild type plants were compared to those in the Fe transport-defective *Arabidopsis* mutants *irt1* and *frd3*, which led to the unexpected conclusion that the observed

architectural changes in lateral root development are primarily under the control of a local root-endogenous signalling system.

### 3.2. Material and methods

#### 3.2.1. Plant material and growth conditions

The wild-type (*Arabidopsis thaliana*) ecotypes used in this study were Wassilewskija (Ws-0), Columbia-0 (Col-0), Columbia-*glabrous1* (Col-*gl*) and Nossen (No-0). The wild-type *Arabidopsis* ecotypes were used as a proper experimental control according to the *Arabidopsis* background of the mutants described here. Seeds were surface sterilised in 70% (v/v) ethanol and 0.05% (v/v) Triton X-100. The seeds were planted in sterile plates containing half-strength Murashige and Skoog (1962) medium without iron (-Fe), supplemented with 0.5% sucrose, 2.5 mM MES (pH 5.6) and 1% (w/v) Difco Agar (Becton Dickinson). For the separated agar plates (SAP)- with localized Fe-supply containing different concentrations of Fe, the half-strength MS medium without iron (-Fe) was supplemented with 75  $\mu$ M of ferrozine [3-(2-pyridyl)-5,6-diphenyl-1,2,4-triazine sulfonate] (Sigma) to render traces of Fe contaminants in the agar unavailable (Jain et al., 2009). The agar segments were separated according to the conditions described in Zhang and Forde (1998) and the indicated concentrations of Fe(III)-EDTA were supplied at the middle segment and spread using a sterile glass stick one day before to transfer the *Arabidopsis* seedling in order to allow a proper distribution of the solution. For the homogeneous Fe supply, the Fe(III)-EDTA concentration were added in the same medium supplemented with ferrozine. The 7 day old seedlings were transferred to separated agar plates (SAP) containing agar medium as described above and Fe(III)-EDTA at indicated concentrations. Three seedlings per plate were transferred to segmented plates with the primary root touching the middle segment, oriented in a vertical position and cultured under a 22°C/19°C and 10/14 h light/dark regime at a light intensity 120  $\mu$ mol photons m<sup>-2</sup> s<sup>-1</sup>.

#### 3.2.2. Root growth measurements

After 15 days of incubation on SAP, root systems were scanned by an Epson Expression 10000XL scanner (Seiko, Epson) at 300 dpi resolution. Traces in the background of the images were removed by Adobe Photoshop 5.0 version LE software. Root growth measurements were taken from scanned images using

WhinRHIZO version Pro2007d software (Regents Instruments Canada Inc.). Lateral root primordia were counted using conventional light microscopy (Olympus BH, Germany). Developmental stages of lateral root initials were classified according to Malamy and Benfey (1999). All the experiments were performed at least twice and yielded similar results.

### 3.2.3. Histochemical analysis

For histochemical studies, seven-day-old Arabidopsis line *CYCB1::GUS* (*cycb1::uiad*) (Ferreira et al., 1994) germinated in half-strength MS Fe-free media were transferred to separated agar plates with the primary root apex touching the middle segment. Just before the primary root left the middle segment (3 days on treatment) and after it was growing for 4 days in contact with the third segment (7 days on treatments), root systems from the middle segment were excised and stained for GUS activity. For the staining, root samples were incubated overnight at 37°C in a GUS reaction buffer containing 0.4 mg mL<sup>-1</sup> of 5-bromo-4-chloro-3-indolyl-b-D-glucuronide, 50 mM sodium phosphate, pH 7.2, and 0.5 mM ferricyanide. After 12 h the roots were cleared and mounted as described by Malamy and Benfey (1997). For each treatment 30 to 40 roots were analysed. Before plants were transferred to treatments, a GUS staining analysis on roots growing in the top segment, revealed that  $1.0 \pm 0.01$  lateral roots were at the pre-emerged stage and  $1.43 \pm 0.53$  had already emerged.

### 3.2.4. Histochemical localization of iron

For localization of Fe(III) in wild-type and *frd3-1* roots, a Perl's staining protocol for Arabidopsis described by Stacey et al. (2008) was followed. Root segments from the middle segment were excised, rinsed three times with 10 mM EDTA followed by three times with ultra-pure water (18.2 Milli-Q cm<sup>-1</sup>). The samples were vacuum infiltrated with Perl's staining solution, composed of equal volumes of 4% (v/v) HCl and 4% (w/v) K-ferrocyanide and incubated for 15 min. Samples were left for another 15 min in the staining solution and rinsed three times with ultra-pure water. Stained samples were imaged using a stereo microscope (Zeiss Stemi 2000-C, Germany) equipped with a CCD digital camera (Sony DXC-390P). Representative pictures of all tested conditions were taken using Adobe Photoshop 5.0 version LE.

### 3.2.5. Expression analysis

For quantitative real-time PCR total RNA was extracted from root tissues grown in the middle plate segment using the Trizol RNA extraction kit (Invitrogen). RNA was quantified and treated with DNase I (Invitrogen). DNase-treated RNA was checked by agarose gel electrophoresis for genomic DNA contamination. One microgram of total RNA was reverse transcribed into cDNA using oligo(dT)<sub>24</sub> primers and the SuperScriptII Reverse Transcriptase Kit (Invitrogen).

Quantitative real-time PCR analysis was performed using an Eppendorf mastercycler realplex (Eppendorf, Germany) and QuantiTect SYBR Green qPCR Mix (Qiagen). Gene-specific primers were used for *IRT1* (*IRT1-For*, 5'-CGGTTGGACTTCTAAATGC-3'; *IRT1-Rev*, 5'-CGATAATCGACATTCCACCG-3'), *FER1* (*FER1-For*, 5'-AATCCCGCTCTGTCTCC-3'; *FER1-Rev*, 5'-AACTTCTCAGCATGCCC-3'), *FIT* (Séguéla et al., 2008) and *UBIQUITIN2 (UBQ2)* (*UBQ2-For*, 5'-CCAAGATCCAGGACAAAGAAGGA-3'; *UBQ2-Rev*, 5'-TGGAGACGAGCATAACACTTGC-3'). Relative transcript abundance was calculated by the Mastercycler ep realplex software package version 2.0.

### 3.2.6. Mineral element and chlorophyll analysis

Shoots of agar-grown plants were briefly rinsed with double distilled H<sub>2</sub>O and dried at 80°C. Samples consisting of approximately 30 shoots were digested with HNO<sub>3</sub> in polytetrafluoroethylene (PTFE) vials in a pressurised microwave digestion system (UltraCLAVE IV, MLS GmbH, Germany). Elemental analysis was performed by inductively coupled plasma mass spectrometry (ICP-MS, ELAN 6000, Perkin Elmer Sciex), equipped with a standard Scott-type spray chamber and a cross-flow nebuliser. The internal standard rhodium (10 mg L<sup>-1</sup>) was used to correct for the drift of the instrument. The certified reference material SRM 1575a ('pine needles'; National Institute of Standards and Technology/NIST) was used for quality control, and the recovery rate was >95%. Chlorophyll concentrations were determined by incubating shoot samples with spectrophotometric grade *N,N'*-dimethyl formamide (Sigma-Aldrich, Germany) at 4°C for 48 h. The absorbance at 647 nm and 664 nm was then measured in extracts according to Porra et al. (1989).

### 3.3. Results

#### 3.3.1. Localized supply of iron stimulates lateral root development in *Arabidopsis*

To investigate changes in root architecture of *Arabidopsis thaliana* in response to Fe, first the wild-type plants (No-0) *Arabidopsis* seeds were germinated on half-strength MS Fe-free media solidified with 1% agar. In order to remove the contamination of Fe from the agar (Jain et al., 2009) the seedling were transferred to segmented agar plates (SAP; Zhang and Forde, 1998) containing half-strength MS medium without iron (-Fe) supplemented with 75  $\mu\text{M}$  of Fe(II)-specific chelator ferrozine (described in the Material and Methods). Increasing concentrations of Fe(III)-EDTA were supplied either to all three segments (homogenous supply) or only to the middle segment (localized supply). Under homogenous supply root and shoot growth and in particular lateral root development in the upper, middle and lower root segment improved with increasing Fe concentrations up to 50  $\mu\text{M}$  with no considerable changes in phenotype beyond that concentration (Figure 1A, C-H); except at 500  $\mu\text{M}$  homogenous Fe supply when primary root length and the number of lateral roots in the bottom segment started to decline (Figure 1I, H). This is indicative of a particular sensitivity of the primary root tip to high Fe availabilities.

The local supply of 25  $\mu\text{M}$  Fe led to a strongly enhanced mean length of lateral roots in the Fe-treated agar segment (Figure 1B, E). Relative to 10  $\mu\text{M}$  Fe, 25  $\mu\text{M}$  localized Fe supply enhanced mean lateral root length by 15-fold resulting in a twofold higher lateral root length than under homogenous Fe supply. With further increasing Fe supply there was a gradual decrease in lateral root length down to the level of plants grown under homogenous Fe supply (Figure 1E). The marked morphological change at 25  $\mu\text{M}$  localized Fe supply was also reflected by the mean length of lateral roots in the upper root segment, although to a lesser extent (Figure 1C). This indicated that Fe-deficient basal root parts profited from the localized Fe availability in the root segment below, probably via acropetal Fe transport within the root. In contrast, the stimulation of lateral root number by local Fe was much weaker and only significant when referring to lateral root density (Figure 1F; Figure 2B). In fact, homogenous Fe supply led to a gradual increase in the number and mean length of lateral roots up to 25  $\mu\text{M}$  and, in contrast to lateral root length, lateral root number and density remained constant with further increases in Fe supply (Figure

1E, F). Mean lateral root length and number in the bottom segment responded in a similar way to either mode of Fe supply (Figure 1G, H). Taken together, these data indicated that mean lateral root length responded more sensitively to changes in localized Fe supply than lateral root number or density.

Since differences exist among chelating agents in the affinity and specificity for Fe and other metals (Chaney, 1988; Norvell, 1991) it was compared lateral root development under localized supply of 25  $\mu\text{M}$  Fe, either being chelated by ethylenediamine-tetraacetic acid (EDTA) or by N,N-di-(2-hydroxybenzoyl)-ethylenediamine- N,N-diacetic acid (HBED), two chelating agents with distinct affinities for Fe and other metal micronutrients (Chaney, 1988). However, lateral root length and number as well as chlorophyll concentrations were not significantly different irrespective of which Fe(III) chelator was used (Figure 3). Therefore, changes in root architecture observed were not due to an indirect effect of the Fe(III)-chelating agent and/or interactions of the chelator with other micronutrients.

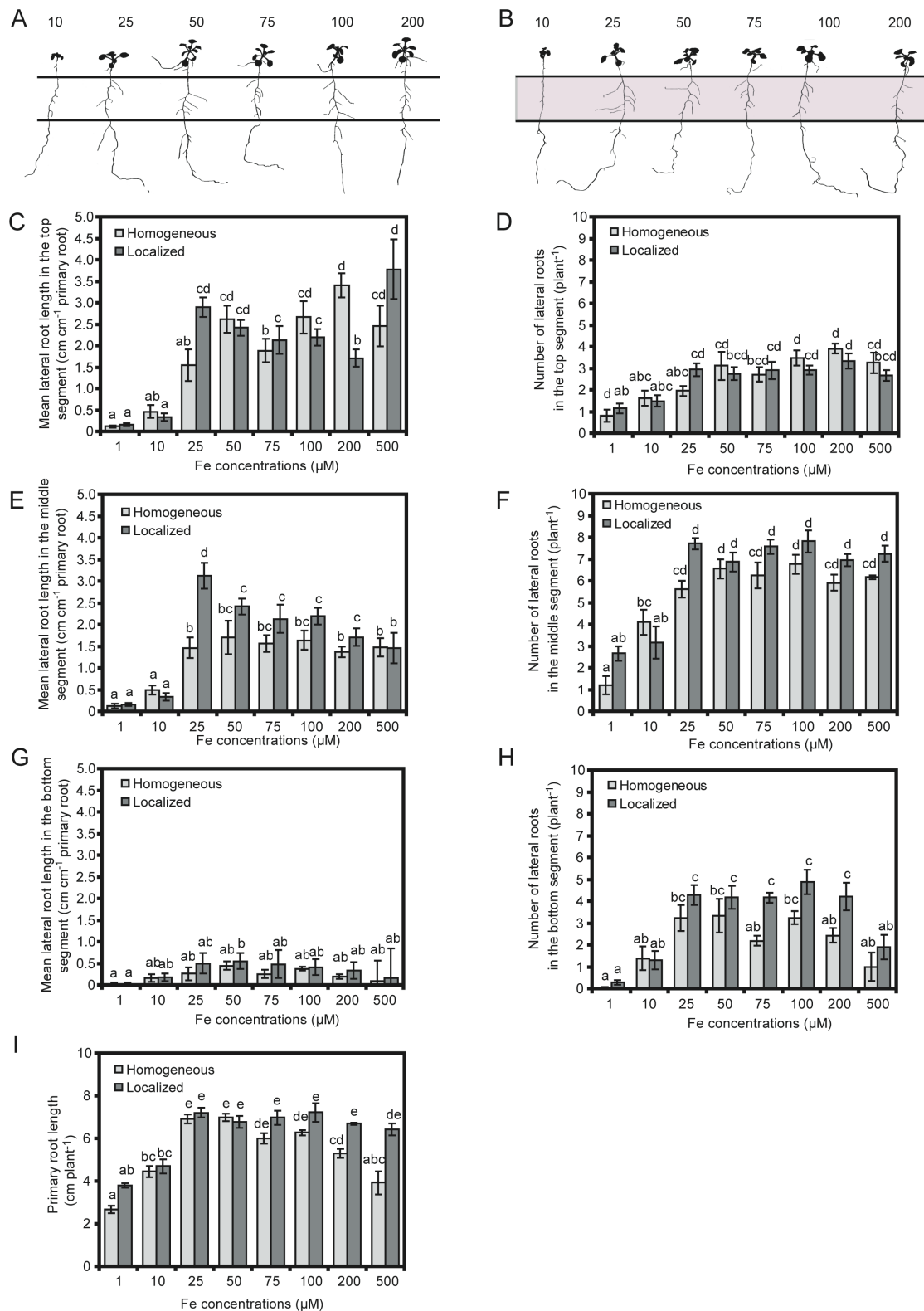


**Figure 1.** Effect of homogeneous and localized Fe supplies on lateral root development of *Arabidopsis* plants. **(A, B)** Root architecture of wild type plants (accession No-0) in response to Fe supply. Seedlings were grown on half-strength MS medium without Fe for 7 days before transfer to segmented agar plates (SAP) containing half-strength MS and 75 μM ferrozine. Fe(III)-EDTA was added at the indicated concentrations to all three segments **(A; homogeneous supply)** or only to the middle segment **(B; localized supply)**. Plants were scanned after 15 days of growth on Fe treatments. Horizontal lines represent the borders between the three segments. The grey colour in **(B)** indicates Fe being supplied only to the middle segment. Mean lateral root length in the **(C)** top, **(E)** middle and **(G)** bottom segment, and number of visible lateral roots (> 0.5 mm) in the **(D)** top, **(F)** middle and **(H)** bottom segment. **(I)** Primary root length over all three compartments as determined by image analysis. Bars indicate means ± SE, n = 8 plates each containing 3 plants. Different letters indicate significant differences among means ( $P < 0.05$  by Tukey's test).

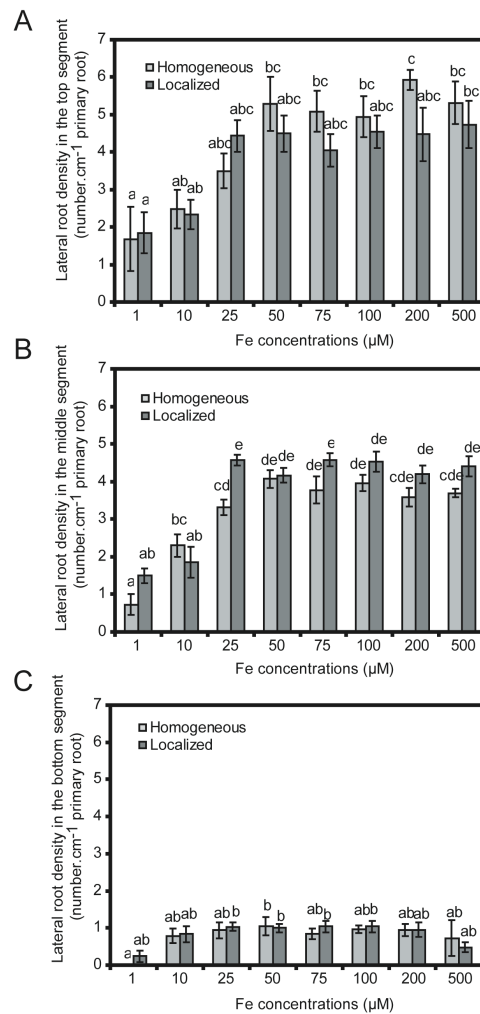


**Figure 2.** Effect of homogeneous and localized Fe supply on lateral root density of *Arabidopsis* plants. Seeds (accession No-0) were germinated on half-strength MS medium in the absence of Fe and 7 day-old seedlings were transferred to segmented agar containing half-strength MS and 75 μM of the Fe(II)-chelator ferrozine. Fe(III)-EDTA was added at the indicated concentrations to all three segments (homogeneous supply) or only to the middle segment (localized supply). Plants were scanned after 15 days of growth on Fe treatments and the lateral root density was calculated by image analysis in the top (A), middle (B) and bottom (C) plate segments. Bars indicate means ± SE, n = 8 plates with 3 plants per plate. Different letters indicate significant differences among means ( $P < 0.05$  by Tukey's test).

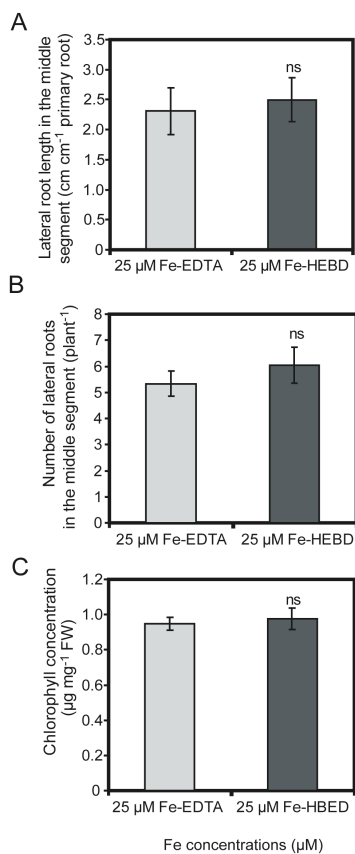


**Figure 3.** Effect of the Fe(III)-chelating agent on lateral root development in response to localized Fe supply.

(A) Number and (B) mean lateral root length and (C) chlorophyll concentrations in shoots of wild type plants (No-0) that were supplied with 25 μM Fe(III) chelated with either ethylenediamine-tetraacetic acid (EDTA) or by N,N-di-(2-hydroxybenzoyl)-ethylenediamine-N,N-diacetic acid (HBED) in the middle agar segment. Bars indicate means ± SE, n = 7-8 plates with 3 plants. ns denotes no significant difference according to Student's *t*-test ( $P < 0.05$ ).

### 3.3.2. Influence of the mode of iron supply on the nutritional status of the shoot

Homogenous or localized supply of 25 μM Fe resulted in the maximum production of shoot fresh biomass (Figure 4A). Above 25 μM no significant changes were observed, except that a homogenous supply of 500 μM Fe tended to repress growth while a localized supply of the same Fe concentration did not. Over a concentration range of 25 to 75 μM Fe, root biomass production was significantly greater under localized relative to homogenous supply (Figure 4B). Since in this concentration range primary root length was not significantly affected by either mode of Fe supply (Figure 1I) the enhanced root biomass production under localized Fe supply resulted almost exclusively from the formation of lateral roots (Figure 1E).

To address the question whether homogenous Fe supply confers an advantage to plants growing under low Fe availabilities, first it was determined the chlorophyll concentration as a measure of the Fe nutritional status of the shoot (Morales et al., 1990). Chlorophyll levels reached maximum values at 25 μM Fe under both modes of Fe supply (Figure 4C). Thus, despite the spatially restricted Fe supply an enhanced elongation of lateral roots into the Fe-containing patch enabled

the plants to satisfy the Fe demand of their shoots as efficiently as under homogenous Fe supply. With respect to their tight correlation with shoot and root biomass values chlorophyll concentrations sensitively reflected the Fe nutritional status.

Moreover, the mode of Fe delivery did not significantly affect the shoot concentrations of Fe or other nutrients, since element concentrations that were altered with increasing Fe supply showed similar changes under homogenous and localized Fe supply (Table 1). As an exception to that, more Zn accumulated under elevated levels of localized relative to homogenous Fe supply. This result might be indicative of the involvement of IRT1 or further metal transporters with poor substrate specificity (Korshunova et al., 1999; Vert et al., 2002) in the uptake of Zn in Fe-deficient root segments outside of the region of Fe supply. Thus, the shoot nutrient profile indicated that the morphological changes observed in the roots were not due to an undesirable effect of the mode of Fe supply on the accumulation of other essential macro- or microelements.

**Table 1.** Concentration of nutrients in shoots of Arabidopsis (accession No-0) plants grown for 15 days under different concentrations of Fe, supplied either homogeneously across all three segments (homogeneous) or only in the middle segment (localized). Shown are means and  $\pm$ S.E. (n = 4 replicates of 30 shoots). Different letters indicate significant differences among means ( $P < 0.05$  by Tukey's test). Concentrations of S, P, K, and Ca are given in mg g<sup>-1</sup>; and the concentrations of Mg, Fe, B, Mn, and Zn are in  $\mu$ g g<sup>-1</sup>.

Fe concentrations ( $\mu$ M)	S	P	K	Ca	Mg	Fe	B	Mn	Zn
Homogeneous supply									
10	15.50 $\pm$ 1.0 b	11.71 $\pm$ 1.5 ab	55.37 $\pm$ 1.1 a	4.68 $\pm$ 0.7 ab	2.19 $\pm$ 0.34 b	137 $\pm$ 24 ab	219 $\pm$ 27 b	198 $\pm$ 48 abc	708 $\pm$ 13 d
25	10.61 $\pm$ 0.5 ab	13.17 $\pm$ 0.4 b	52.88 $\pm$ 0.8 a	4.95 $\pm$ 0.1 ab	1.96 $\pm$ 0.02 ab	188 $\pm$ 20 ab	114 $\pm$ 7 a	221 $\pm$ 15 bc	400 $\pm$ 15 c
50	9.77 $\pm$ 0.6 ab	14.06 $\pm$ 0.8 b	54.64 $\pm$ 1.4 a	5.07 $\pm$ 0.1 b	1.87 $\pm$ 0.03 ab	151 $\pm$ 11 ab	109 $\pm$ 12 a	176 $\pm$ 6 abc	233 $\pm$ 30 b
200	8.63 $\pm$ 0.1 a	12.15 $\pm$ 1.6 ab	55.56 $\pm$ 1.1 a	3.96 $\pm$ 0.2 a	1.66 $\pm$ 0.06 a	235 $\pm$ 9 b	122 $\pm$ 14 a	138 $\pm$ 4 a	110 $\pm$ 20 a
Localized supply									
10	15.51 $\pm$ 1.7 c	10.38 $\pm$ 1.0 a	56.04 $\pm$ 3.7 a	4.95 $\pm$ 0.8 ab	2.20 $\pm$ 0.24 b	102 $\pm$ 13 a	195 $\pm$ 30 b	223 $\pm$ 71 bc	704 $\pm$ 79 d
25	11.34 $\pm$ 1.1 b	11.81 $\pm$ 0.4 ab	53.31 $\pm$ 1.9 a	4.95 $\pm$ 0.2 ab	2.08 $\pm$ 0.14 b	167 $\pm$ 26 ab	119 $\pm$ 15 a	248 $\pm$ 45 c	463 $\pm$ 93 c
50	10.15 $\pm$ 0.6 ab	12.69 $\pm$ 0.6 ab	53.37 $\pm$ 1.5 a	4.68 $\pm$ 0.6 ab	1.85 $\pm$ 0.11 ab	189 $\pm$ 38 ab	119 $\pm$ 22 a	167 $\pm$ 9 ab	330 $\pm$ 32 bc
200	9.86 $\pm$ 0.2 ab	12.19 $\pm$ 0.4 ab	51.86 $\pm$ 0.9 a	4.56 $\pm$ 0.4 ab	1.85 $\pm$ 0.05 ab	181 $\pm$ 16 ab	112 $\pm$ 16 a	142 $\pm$ 8 ab	294 $\pm$ 17 b

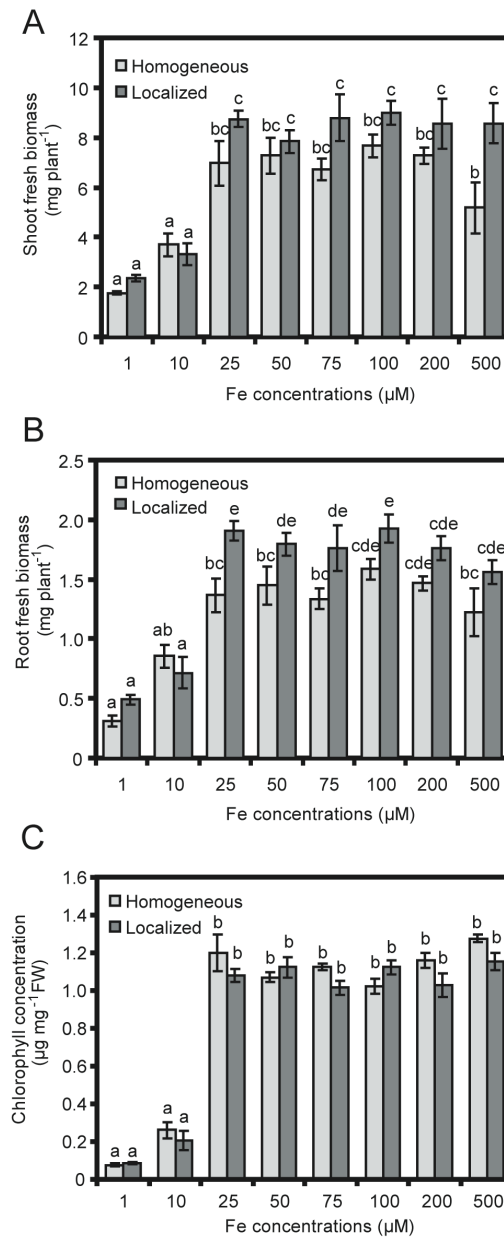


**Figure 4.** Effect of the mode of Fe supply on the growth of *Arabidopsis* seedlings. Fresh weight of (A) shoots or (B) roots, and (C) chlorophyll concentrations in shoots of seedlings grown for 15 days either on homogeneous or localized supply of different concentrations of Fe. Bars represent means  $\pm$  SE,  $n = 4$  replicates with 30 shoots each replicate. Different letters indicate significant differences among means ( $P < 0.05$  by Tukey's test).

### 3.3.3. Effect of localized Fe supply on early lateral root development

To investigate the effect of localized Fe supply on the early development of lateral roots, it was taken the advantage of transgenic plants expressing the  $\beta$ -glucuronidase (GUS) reporter under the control of the *CYCB1;1* promoter (Ferreira et al., 1994). This reporter stains meristematic cells allowing to track root primordia before their emergence. Since this reporter is in the Col-0 background, it was re-determined the lateral root response to increasing Fe supplies in this line and found the maximum lateral root length at 50  $\mu$ M localized Fe supply (data not shown) instead of 25  $\mu$ M as observed for No-0 (Fig. 1E). Then, the primary root tip of Fe-deficient *CYCB1;1::GUS* seedlings were exposed to localized Fe supply and determined the developmental stage of pre-emerged lateral root initials according to the classification described by Malamy and Benfey (1997) after 3 and 7 days. It is important to note that at day 0 there was not yet any lateral root to be counted since the primary root tip just started entering the middle agar segment. Three days after transfer to different Fe supplies the number of lateral root initials was similar under both Fe treatments at any concentration, and the number of emerged lateral roots remained low (Figure 5A). After 7 days, when the primary root tip had reached the Fe-deficient segment in the bottom, 1-2 additional lateral roots had been formed, and the majority of initiated lateral root primordia was emerged (Figure 5B). At 10  $\mu$ M Fe supply, i.e. non-promoting conditions for lateral root development, homogenous Fe supply was more favourable for lateral root emergence than localized supply (Figure 5B). This was most likely due to the delivery of Fe from the upper to the middle root segment under homogenous Fe supply. However, at 50 and 200  $\mu$ M localized Fe supply, not only lateral root number increased, but most notably, the proportion of emerged lateral roots was enhanced. Taken together, this suggests that the local presence of Fe has a lower impact on the priming and initiation of lateral root development, but rather stimulates the emergence and elongation of already initiated lateral root primordia. This view is also supported by the more pronounced effect of localized Fe on lateral root length over number (Fig. 1E,F).

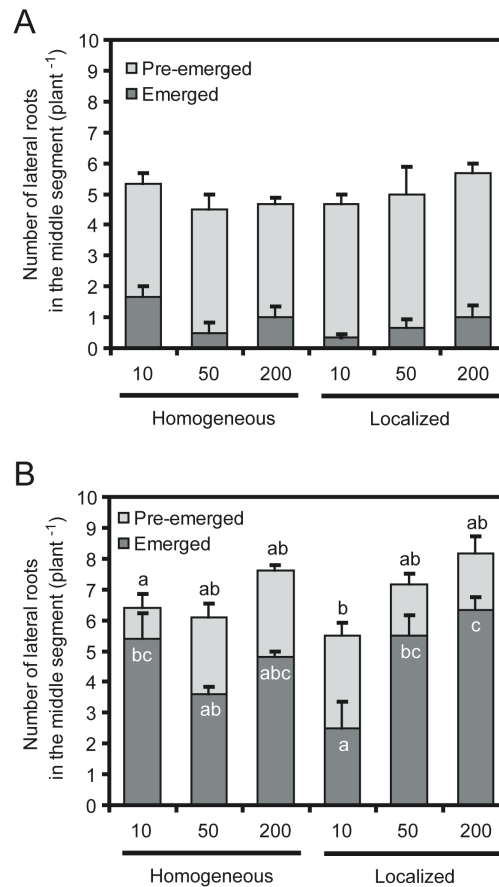


**Figure 5.** Effect of localized Fe supply on lateral root initiation and emergence. **(A, B)** *CYCB1;1::GUS* transgenic seedlings were germinated on Fe-deficient medium and transferred to segmented agar plates supplemented with 75 μM ferrozine and with the indicated Fe(III)-EDTA concentrations only in the middle segment (localized supply) or in all three segments (homogeneous supply). The primary root tip was placed to the middle segment and after 3 **(A)** or 7 **(B)** days roots from the middle segment were excised and stained for GUS activity. The total number of pre-emerged (light grey) and emerged (dark grey) lateral roots was counted under the microscope. Bars represent means ± SE, n = 15-20 seedlings. In **(A)** no significant differences were obtained ( $P < 0.05$  by Tukey's test). In **(B)** different letters indicate significant differences among means for pre-emerged (black letters) and emerged (white letters) lateral root initials ( $P < 0.05$  by Tukey's test).

### 3.3.4. Involvement of IRT1 in the differential response of the number and length of lateral roots to localized iron supply

Based on the observation that *Arabidopsis* plants proliferate lateral roots preferentially in Fe-containing agar patches (Figure 1), it was investigated whether the Fe transporter IRT1 was involved in the differential regulation of number and length of lateral roots under localized Fe supply. Similar to No-0, also in Ws-0 lateral root number steeply increased with localized Fe supply and reached its maximum at 25  $\mu\text{M}$  (Figure 6A). Above 25  $\mu\text{M}$  Fe the number of emerged lateral roots remained the same. In contrast, *irt1* plants developed very few lateral roots up to 100  $\mu\text{M}$  Fe supply and then tended to increase lateral root number with further increases in Fe supply. At 600  $\mu\text{M}$  Fe, *irt1* plants were able to initiate the same number of lateral roots as wild type plants (Figure 6A). Similar to the No-0 accession, Ws-0 plants also responded to local Fe availability by increasing lateral root length in a concentration-dependent manner. For Ws-0, however, maximum lateral root length was observed around 75  $\mu\text{M}$ , indicating that there is a considerable natural variability for this trait among different accession lines of *Arabidopsis*. Relative to its wild type, *irt1* was not able to reach a comparably high length of lateral roots in the Fe-treated segment. Even at 600  $\mu\text{M}$  Fe the lateral root length of *irt1* plants remained far below the maximum observed at 75  $\mu\text{M}$  in the wild type (Figure 6B).

Chlorophyll concentrations in wild type plants attained a maximum between 50 and 200  $\mu\text{M}$  Fe and decreased with a further increase in supply (Figure 6C). In contrast, chlorophyll concentrations in *irt1* plants indicated a Fe-deficient status at any Fe supply and showed a shift in their Fe response towards higher Fe supplies, so that chlorophyll concentrations followed the same concentration-dependent pattern as lateral root number or length. Thus, IRT1 appears as an essential component for the differential response of the number and the length of lateral roots to increasing concentrations of localized Fe supply.

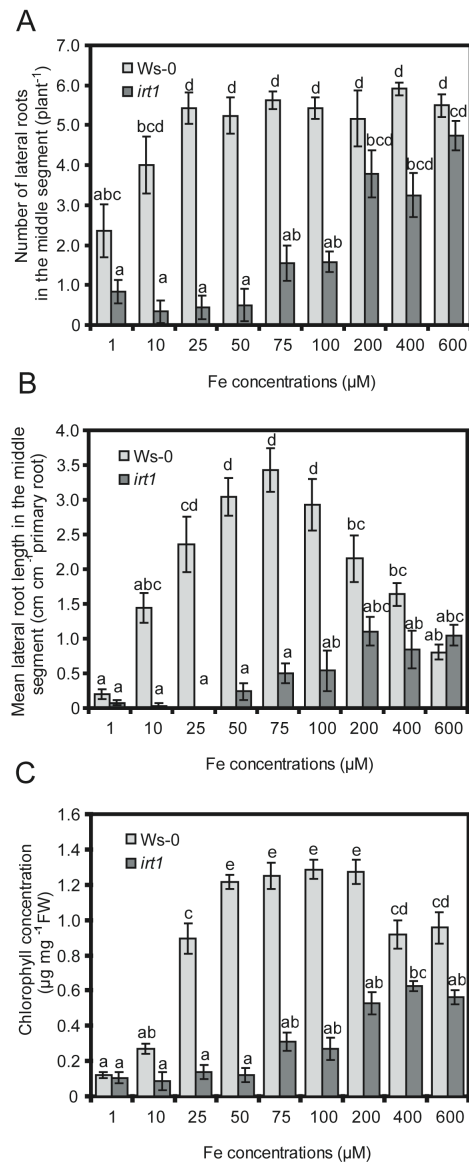


**Figure 6.** Lateral root development in wild type and *irt1* plants in response to localized Fe supply. **(A)** Number and **(B)** mean length of lateral roots in wild type (*Ws-0*) and *irt1* mutant plants as affected by the Fe concentration supplied to the middle segment. Wild type and *irt1* seeds were germinated on Fe-free, half-strength MS medium for 7 days. Seedlings were then transferred to segmented agar plates supplied with Fe in the middle segment at the indicated concentrations. After 15 days the number and mean length of visible lateral roots (> 0.5 mm) in the middle segment were determined by image analysis. **(C)** Shoot chlorophyll concentrations were determined after 15 days of growth. Bars represent means  $\pm$  SE,  $n = 7$  replicates consisting of 3 plants. Different letters indicate significant differences among means ( $P < 0.05$  by Tukey's test).

### 3.3.5. Influence of FIT on lateral root development under localized iron supply

Considering the central role of FIT in regulating physiological Fe stress responses in Arabidopsis (Colangelo and Guerinot, 2004; Jakoby et al., 2004) and the additional role of its tomato ortholog LeFER in root hair formation (Ling et al., 2002), it was assessed the involvement of this Fe-regulated transcription factor in changes of root architecture in response to localized Fe supply. In *fit* mutant plants the number of lateral roots was significantly lower than in wild type plants at concentrations up to 50  $\mu\text{M}$  of localized Fe supply and achieved a similar number only at 200  $\mu\text{M}$  Fe. Over the whole range of locally supplied Fe concentrations mean lateral root length of *fit* mutant plants showed no increase (Figure 7B). It is important to note here that lower lateral root length of *fit* plants above 25  $\mu\text{M}$  Fe relative to the wild type reflected a similar situation to that seen in *irt1* mutant plants (Figure 6). As it has been demonstrated that *fit* plants suffer from impaired Fe uptake due to lower *IRT1* and *FRO2* expression (Colangelo and Guerinot, 2004), this observation may indirectly support a role of IRT1/FRO2-dependent Fe acquisition in increasing lateral root length under localized Fe supply. To investigate whether FIT overexpression can provoke a morphological response and increase lateral root length, 35S::FIT lines were tested for lateral root responses to local Fe supply. However, the constitutive expression of *FIT* did not significantly affect the root architecture, and lateral root number as well as length in response to localized Fe supply were identical in Col-0 and 35S::FIT lines (Figure 7). Considering the lack of a root architecture-related phenotype in 35S::FIT lines and the similar response of *fit* and *irt1* insertion lines, it is suggested that FIT has no direct, Fe acquisition-independent role in the adaptation of lateral root morphology to a localized availability of Fe.

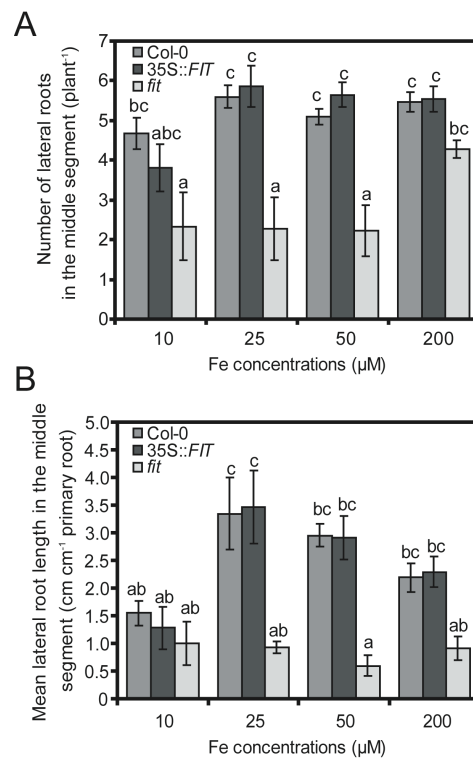


**Figure 7.** Lateral root development in response to localized Fe supply in transgenic plants with deregulated expression of *FIT*.

**(A)** Number and **(B)** mean lateral root length in wild type (*Col-0*), *35S::FIT* and *fit* mutant plants as affected by the Fe concentration supplied to the middle segment. Seeds were germinated on Fe-free, half-strength MS medium for 7 days. Then, seedlings were transferred to segmented agar plates supplied with Fe in the middle segment at the indicated concentrations. After 15 days, the number of visible lateral roots (> 0.5 mm) and mean lateral root length in the middle segment was determined by image analysis. Bars indicate means  $\pm$  SE,  $n = 7-12$  plates with 3 plants per plate. Different letters indicate significant differences among means ( $P < 0.05$  by Tukey's test).

### 3.3.6. Influence of *FRD3* on lateral root development and the expression of Fe-responsive genes

Root architectural changes in response to differing spatial availabilities of nutrients might result either directly from the local presence of the nutrient or indirectly from an altered nutritional status of the plant that is communicated to the roots. For most of the nutrients characterized so far a sharp distinction between these regulatory factors has turned out to be difficult to achieve. In the case of Fe, the *Arabidopsis ferric reductase defective3 (frd3-1)* and its allelic mutant *manganese accumulator1 (man1; also known as frd3-3)* showed a constitutive upregulation of the Fe acquisition machinery in roots despite accumulating more Fe in the root compared to wild type plants (Delhaize, 1996; Rogers and Guerinot, 2002; Green and Rogers, 2004). These mutants thus represent useful tools to investigate whether the morphological root responses described herein are under the control of local or

systemic regulation. Under homogenous supply of Fe, *Col-gl* and *frd3-1* plants behaved very similar with regard to lateral root development. Both lines showed a parallel increase in lateral root number except at 200  $\mu\text{M}$  Fe where *frd3-1* mutants significantly increased lateral root number beyond the level of wild type plants (Figure 8A). In a similar concentration dependency, lateral root length increased in both lines even though *frd3-1* mutants tended to achieve their maximal length already at lower Fe supplies than wild type plants (Figure 8C). Since these two differences might be a consequence of a higher Fe accumulation in *frd3-1* roots (Green and Rogers, 2004), the roots were subjected to Perl's staining, allowing to visualize local Fe accumulations (Stacey et al., 2008). Indeed, under homogenous Fe supplies, Perl's reagent detected higher Fe levels in *frd3-1* than in wild type roots (Figure 10).

At 1  $\mu\text{M}$  of localized Fe supply *frd3-1* mutant plants developed approximately two lateral roots more than the corresponding wild type in their Fe-treated root segments, thereafter lateral root number did not change with Fe supply in both genotypes (Figure 8B). Interestingly, lateral root length followed the same concentration-dependent manner in both lines (Figure 8D). Thus, the differential response between the number and length of lateral roots as it was observed in wild type plants remained conserved despite the loss of FRD3. A similar growth response was observed in *man1 (frd3-3)* mutant plants (data not shown). These observations gained importance with respect to the chlorophyll levels which reflected a significantly lower Fe nutritional status in *frd3-1* mutant than in wild type plants at  $> 10 \mu\text{M}$  Fe supply (Figure 8F) and were accompanied by a chlorotic shoot phenotype (data not shown). This was not the case under homogenous Fe supply (Figure 8E), where plants could profit from additional Fe being acquired by upper root segments. Thus, the earlier response of *frd3-1* mutant plants to a local supply of 1  $\mu\text{M}$  Fe was not affected by the Fe nutritional status of the shoot. This indicated that the quantitative traits in lateral root development as determined here were independent of a FRD3-mediated regulation by the Fe nutritional status of the shoot.

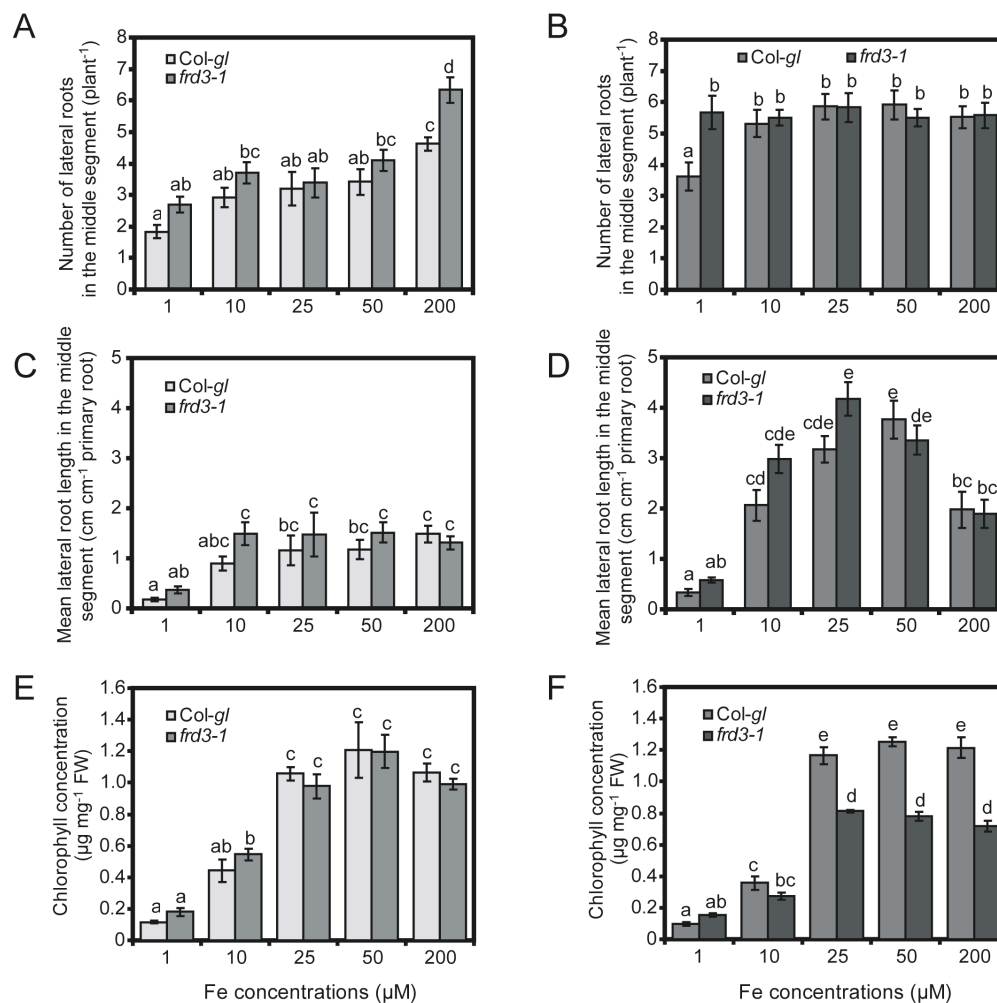


**Figure 8.** Lateral root development in wild type and *frd3-1* plants in response to homogenous or localized Fe supply.

(A, B) Lateral root number, (C, D) lateral root length and (E, F) chlorophyll concentration in the shoots of wild type (*Col-gl*) and *frd3-1* mutant plants. Seeds were germinated on Fe-free, half-strength MS medium for 7 days before transfer to segmented agar plates homogeneously supplied with Fe(III)-EDTA to all three segments (A, C, E) or locally supplied only to the middle segment (B, D, F). Plant roots were scanned and the chlorophyll concentration determined after 15 days on Fe treatments. Bars represent means  $\pm$  SE,  $n = 7-12$  plates with 3 seedlings per plate. Different letters indicate significant differences among means ( $P < 0.05$  by Tukey's test).

Additionally, it was compared *IRT1* gene expression levels in wild type and *frd3-1* plants under both modes of Fe supply. Under homogeneous Fe supply *IRT1* mRNA accumulation followed the same dependency on Fe supply in both lines, but at a concentration of  $\geq 25 \mu\text{M}$  Fe mRNA levels remained at a slightly higher level in *frd3-1* plants (Figure 9A). When Fe was supplied locally, *IRT1* mRNA levels showed a distinct and sharp increase (Figure 9B) supporting its responsiveness to local Fe supplies (Vert et al., 2003). Similar to the situation under homogenous supply of Fe, *IRT1* transcript levels remained at a higher level in *frd3-1* roots only under Fe

concentrations of  $\geq 25 \mu\text{M}$  (Figure 9A, B). In the same concentration range, also *FIT* transcript levels were higher in *frd3-1* plants when locally supplied with Fe (Figure 9C, D). With respect to the chlorophyll levels (Figure 8F), this gene expression study indicated that locally supplied *frd3-1* plants experienced more severe Fe deficiency at  $\geq 25 \mu\text{M}$  Fe than wild type plants which should theoretically result in a stronger Fe deficiency signal from the shoot to the root (Vert et al., 2003). Nevertheless, Fe-dependent repression of lateral root length followed the same concentration dependency in both lines (Figure 8D) supporting the view that lateral root length was not subject to a systemic, *FRD3*-dependent regulation.

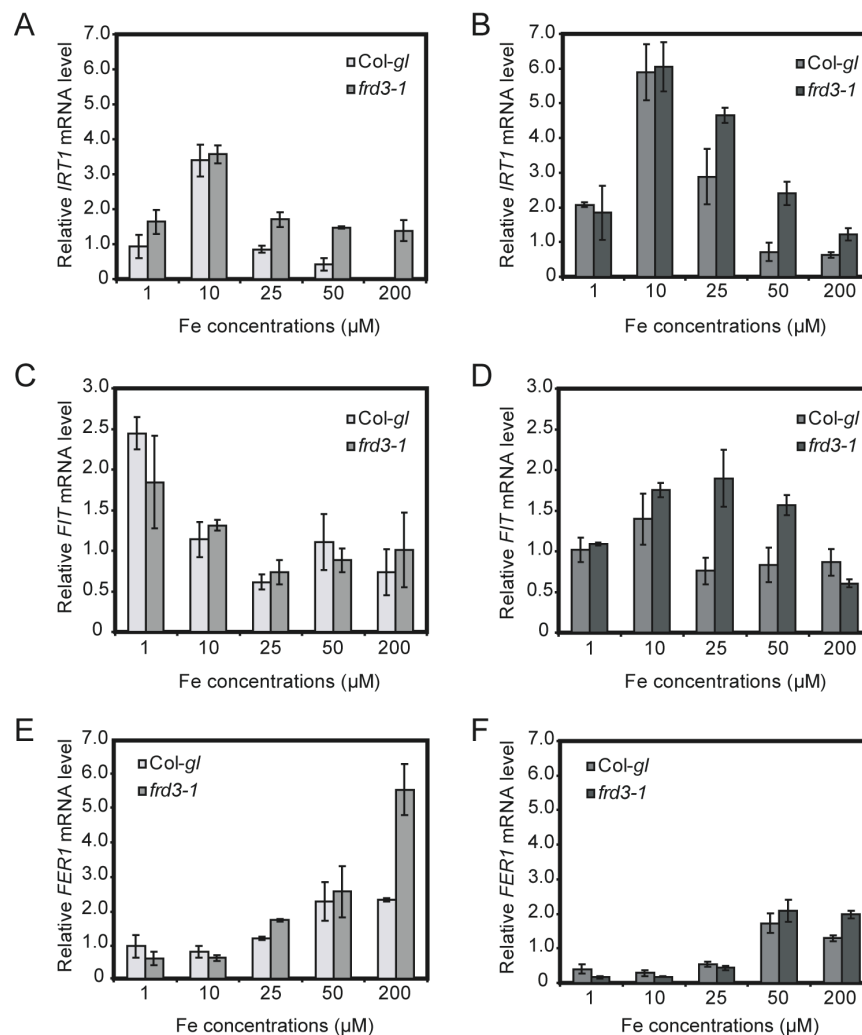
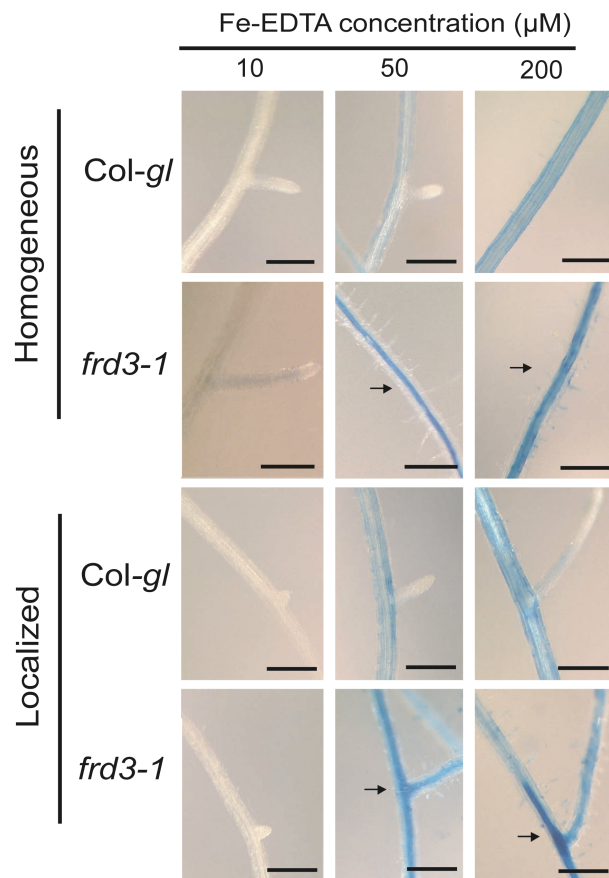


**Figure 9.** Effect of homogenous or localized Fe supply to wild type or *frd3-1* plants on the expression of Fe-regulated genes.

Transcript levels of (A, B) *IRT1*, (C, D) *FIT* or (E, F) *FER1* as determined by qRT-PCR in roots of *Col-gl* wild type and *frd3-1* mutant plants. Root segments were harvested from the middle segment of plants growing for 15 d under homogenous (A, C, E) or localized (B, D, F) supply of Fe at the indicated concentrations. Bars represent means  $\pm$  SE, n = 3-4.

**Figure 10.** Histochemical localization of Fe(III) in wild-type and *frd3-1* roots.

Roots of wild-type and *frd3-1* plants, grown on either homogeneous or localized supply of 10, 50 or 200  $\mu\text{M}$  Fe-EDTA during 7 days, were washed with EDTA and ultra-pure water (18.2 Milli-Q  $\text{cm}^{-1}$ ) and subsequently vacuum infiltrated with Perl's stain solution (equal volumes of 4% [v/v] HCl and 4% [w/v] K-ferrocyanide) for 15 min. Shown are representative plants for each genotype and treatment (n=10 plants each). Bar = 150  $\mu\text{m}$ . Arrows indicate Fe(III) localization close to the vasculature in *frd3-1* roots supplied with 50 or 200  $\mu\text{M}$  Fe-EDTA.



### 3.4. Discussion

#### 3.4.1. Localized Fe supply differentially regulates lateral root number and lateral root length

This study shows that the localized availability of Fe exerts a dual effect on lateral root development in *Arabidopsis*. Firstly, a direct comparison of lateral root growth responses to homogenous or localized supply of Fe revealed a twofold increase in lateral root length of wild type plants grown on 25  $\mu\text{M}$  localized Fe supply relative to plants grown on homogenous Fe supply, while lateral root number was much less affected (Figure 1E, F). Thus local Fe supply mainly stimulated the elongation process in lateral root development. Secondly, high local Fe supplies evoked an inhibition of mean lateral root length (Figure 1E, 6B) but not of lateral root number (Figure 1F, 6A). A growth-inhibitory effect of Fe has recently been reported for primary roots and suggested as the major cause for root shortening under local P deficiency, because low P levels might indirectly increase Fe availability and thus favor Fe accumulation to toxic levels (Ward et al., 2008). Indeed, under certain conditions P negatively affects Fe availability by precipitation reactions outside or inside the plant tissue (Marschner, 1995) and these results with homogenous Fe supply also showed a negative effect of high Fe concentrations on primary root development (Figure 1I). In contrast, when high concentrations of Fe (200-500  $\mu\text{M}$ ) were locally supplied the primary root elongation was not inhibited, although lateral root elongation had already decreased (Figure 1E, I). Since phosphate concentrations in the medium were the same and elemental analysis revealed that shoot phosphate concentrations were not affected by either mode of Fe supply at any Fe concentration (Table 1), the Fe-mediated inhibition of lateral root growth observed here was most likely independent of any interactions with P. Given that lateral root length showed an optimum in its response to local Fe supplies, whereas lateral root number was insensitive to high Fe supplies, these two morphological root traits are subject to a differential regulation by local Fe supplies. This was corroborated in three different *Arabidopsis* accession lines (No-0, Ws-0, and Col-*g/l*) with varying but distinct optimum concentrations for highest mean lateral root length (Figures 1E, 6B, 8D).

Due to the extremely low concentrations of soluble Fe at neutral to alkaline pH (Marschner 1995), there is a particular need for plants to coordinate physiological

with morphological mechanisms to enhance Fe acquisition. This has been demonstrated for subapical root zones of strategy I plants, where an enhanced proton extrusion and Fe(III) reducing capacity coincide with the formation of ectopic root hairs (Römheld et al., 1984; Müller and Schmidt, 2004). With regard to elongation of lateral roots, their directed growth towards soil patches with higher Fe solubility, like acidic microsites, might thus represent an additional morphological component in the coordination with physiological responses to a low and heterogeneous distribution of Fe.

### 3.4.2. The local regulation of lateral root development by iron

When *Arabidopsis* plants are challenged by Fe deficiency, strategy I responses are induced to improve Fe acquisition from the rhizosphere (Marschner, 1995). These responses have been described to be subject to a local control, in which Fe acts as a local inducer (e.g. for *IRT1* and *FRO2* expression), and a systemic control, in which a shoot-derived signal represses Fe acquisition genes (Vert et al., 2003). Several lines of evidence in this study indicate that the impact of Fe on lateral root development is different and primarily subject to a local rather than a systemic regulation: i) Lateral root elongation followed an optimum response to local Fe supplies and decreased at elevated external Fe levels (Figure 1E), even though the Fe nutritional status of the shoots did not change (Figure 4C, Table 1). Under homogenous Fe supply the repression of lateral root length was absent, further supporting the conclusion that the elongation process was regulated by the local Fe availability. These two observations emphasise that the Fe-dependent regulation of this morphological trait differs from that of the physiological traits, where a long-distance Fe signal from the shoot regulates Fe acquisition genes in roots (Vert et al., 2003; Lucena et al., 2006; Enomoto et al., 2007); ii) Under localized Fe supply lateral root elongation in *frd3-1* mutants did not significantly differ from the wild type plants, although *frd3-1* shoots suffered from Fe deficiency (Figure 8D, F). Since FRD3 acts as a citrate loader into the xylem required for root-to-shoot translocation of Fe, *frd3-1* plants accumulate Fe in roots while the shoot remains Fe deficient (Durrett et al., 2007), thereby causing a weaker repression of strategy I responses in roots upon Fe resupply (Figure 9; Rogers and Guerinot, 2002). Thus, Fe-mediated repression of lateral root elongation under localized Fe supply was independent of FRD3, suggesting feedback control by Fe in a local rather than systemic regulatory

loop; iii) In contrast to wild type plants, the *irt1* mutant showed a poor stimulation of lateral root elongation as localized Fe concentrations were increased (Figure 6B), although lateral root initiation was stimulated to wild type levels after excessive Fe supply (Figure 6A). Thus, a lack of IRT1 in the initiation process could be compensated for by excessive Fe supply; however, this was not the case for lateral root elongation as even at highest Fe supply the elongation never achieved wild type levels (Figure 6A, B). Meanwhile, *IRT1* transcript levels showed a more pronounced upregulation under localized compared to homogenous Fe supply (Figure 9A, B), confirming the previously postulated control of *IRT1* by local Fe supply (Vert et al., 2003) in addition to its systemic up-regulation under Fe deficiency that is mediated via FIT. Thus IRT1, which is preferentially expressed in the rhizodermis of Fe-deficient roots (Vert et al., 2002), might take in a role as an Fe sensor or as an Fe transporter that confers local Fe regulation and that is located upstream of the Fe sensing event required to stimulate lateral root elongation.

The Fe-dependent regulation of lateral root number might primarily depend on the achievement of a certain Fe threshold level within the innermost root cells. Evidence for that mainly derived from the experiments with the *frd3-1* mutant, which had a higher number of lateral roots relative to wild type plants when grown at 1  $\mu$ M local Fe supply (Figure 8B) or at 200  $\mu$ M homogenous Fe supply (Figure 8A). Notably, the latter went along with strongly elevated levels of *FER1* expression (Figure 9 E, F) and root Fe, as put into evidence by Perl's staining (Figure 10), supporting the notion that lateral root initiation is not repressed by high local Fe supplies. These *frd3-1* responses were most likely a consequence of the inhibited root-to-shoot translocation of Fe, as in the *frd3-1* roots Fe accumulates to higher levels in the vascular cylinder than in wild type roots (Figure 10; Green and Rogers, 2004). Taking into account that *frd3-1* plants just weakly down-regulated the Fe acquisition response (Figure 9; Rogers and Guerinot, 2002), it might well be that *frd3-1* roots reached those internal Fe levels that are required for lateral root initiation at an earlier stage. Interestingly, a recent cell type-specific transcriptome profiling approach indicated that Fe deficiency might be sensed in the innermost root cells since most of the Fe-dependent changes in gene expression were detected in the root stele (Dinnyeny et al., 2008). This supports the view that local Fe availabilities are integrated with systemic Fe nutritional signals in inner root cells to trigger lateral root initiation and elongation, while in particular the fine-tuning of lateral root length responds to local Fe signals involving IRT1 and thus the contribution of outer root

cells. In this context, it has also been shown that localized supply of nitrate to *Arabidopsis* plants exerts a stimulation of lateral root elongation via a dual regulatory system, involving both local and systemic signalling pathways (Zhang and Forde, 1998; Zhang et al., 1999). In contrast to Fe-mediated lateral elongation, however, the inhibitory effect of nitrate on LR elongation is conferred by systemic inhibition (Zhang et al., 1999).

The fact that morphological traits such as an increased formation of branched root hairs (Müller and Schmidt, 2004) or lateral root elongation (Figure 1A, D) and physiological responses, such as the up-regulation of *IRT1* and *FRO2* expression, respond to local Fe supply further supports the idea of an Fe sensor in roots (Giehl et al., 2009). In yeast cells an intracellular Fe sensing circuit has been characterized which involves the transcription factors Aft1p and Aft2p that act upstream of Fe(III) reductase and Fe(II) transporter genes and downstream of a mitochondrial signal related to Fe-S cluster biosynthesis (Rutherford et al., 2005; Kumánovics et al., 2008). In *Arabidopsis* roots evidence for a local Fe sensor comes from these experiments which show a stronger up-regulation of *IRT1* under local Fe supply (Figure 9B), as well as from split-root experiments in which *IRT1* and *FRO2* expression increased only in those roots exposed to Fe (Vert et al., 2003). Therefore, here it was suggested *IRT1* as a component involved in local Fe sensing or the transduction of a local Fe signal, however, further experimental evidence is required to verify this hypothesis.

## **4. Ammonium triggers lateral root branching in Arabidopsis in an AMT1;3-dependent manner**

### **4.1. Introduction**

In most soils plant nutrients are not homogeneously distributed, particularly if they derive from organic matter and precipitation or adsorption to the soil matrix restrict their solubility and transport to the root surface (Ettema and Wardle, 2002; Hinsinger et al., 2005). Plants may respond to a spatially restricted availability of nutrients with an alteration of the root system architecture displaying enhanced lateral root development into nutrient-rich patches. This response is nutrient specific and only observed if overall nutrient availability is limited. Early experiments with barley showed that locally concentrated supplies of nitrate or phosphate but not potassium stimulated lateral root growth within the nutrient-rich soil patch, while lateral root formation was suppressed in nutrient-poor zones (Drew, 1975; Drew and Saker, 1975; 1978). In the case of phosphate, a low availability appears to be sensed in the root apex, where cell elongation and meristem activity become strongly reduced and thereby avoid further root development into phosphate-depleted soil zones (Svistoonoff et al., 2007; Desnos, 2008). In the case of nitrate, the role of the apical root meristem in nitrogen sensing remains unclear, however, lateral roots also elongate into nitrate-containing soil zones if the remaining root system is nitrogen deficient (Drew, 1975; Remans et al., 2006). In Arabidopsis, nitrate-driven lateral root growth depends on the expression of the MADS-box transcription factor ANR1, which acts downstream of the dual-affinity nitrate transporter NRT1;1 (Zhang and Forde, 1998; Remans et al., 2006). Since an Arabidopsis mutant defective in nitrate reductase activity still responded to a local supply of nitrate, while local supply of ammonium or glutamine failed to elicit the same growth response, it has been concluded that local lateral root elongation is controlled by nitrate itself (Zhang et al., 1999).

Even though ammonium sensing responses could not be observed in Arabidopsis (Zhang et al., 1999), there are a few reasons why they should be expected. Firstly, ammonium is less soluble than nitrate and partly adsorbed to the soil matrix so that roots growing towards the ammonium source would decrease

diffusion distances (Miller et al., 2007). Secondly, at low external concentrations ammonium is a preferential nitrogen source for most plants (Gazzarrini et al., 1999). Thirdly, motile *Chlamydomonas* cells show mechanisms of ammonium sensing by actively moving towards a localized source of either ammonium or its non-metabolizable substrate analog methylammonium (Ermilova et al., 2007) and finally, yeast cells sense ammonium. When grown under low ammonium supply yeast cells produce pseudohyphae which are nuclear-free hyphal structures that better allow foraging of a nitrogen-poor substrate (Lorenz and Heitmann, 1998). Pseudohyphal differentiation depends on Mep2 which has the greatest substrate affinity of the three ammonium transporters in yeast (Marini et al., 1997) and is able to rapidly activate a protein kinase A-mediated signaling pathway (van Nuland et al., 2006). Specific point mutations in Mep2 uncoupled ammonium signaling from transport suggesting a role as a transceptor, a protein that acts as a transporter and receptor at the same time (Lorenz and Heitmann, 1998; Thevelein et al., 2005). However, AMT-type ammonium transporters from *Arabidopsis* were not able to substitute for a lack of Mep2 with regard to pseudohyphal differentiation in yeast (van Nuland et al., 2006).

*Arabidopsis* possesses six AMT-type ammonium transporters with five of these genes being expressed in roots, while *AMT1;4* is the only one expressed in pollen (Yuan et al., 2007; 2009). *AMT1;1* and *AMT1;3* are expressed in rhizodermal and cortical cells where they confer high-capacity and high-affinity ammonium uptake with an *in-vivo*  $K_m$  of 50 and 61  $\mu\text{M}$ , respectively (Loqué et al., 2006; Yuan et al., 2007). Correlative evidence indicated that *AMT1;5*, which is also expressed in rhizodermal root cells, contributes only 5-10% of the overall ammonium uptake capacity at an even higher substrate affinity. In contrast, *AMT1;2* represents a lower-affinity transporter expressed in endodermal and cortical cells that most likely finds a major role in the uptake and retrieval of ammonium from the root apoplast (Yuan et al., 2007). *AMT1;1* and *AMT1;2* are allosterically regulated by C-terminal phosphorylation which trans-inhibits the activation of AMT1 subunits in a trimeric complex (Loqué et al., 2007; Neuhäuser et al., 2007). C-terminal phosphorylation of *AMT1;1* is rapidly triggered by external ammonium supply and causes a decrease in ammonium uptake by roots (Lanquar et al., 2009). A working model has been set up in which the external ammonium signal is conferred to the cytosolic side either via a membrane-anchored receptor-like kinase or via *AMT1;1* itself, presuming that *AMT1;1* acts as a transceptor (Lanquar et al., 2009). Any relation between AMTs and root morphology has not yet been reported.

Against this background it was investigated changes in the lateral root architecture of *Arabidopsis* plants grown under local ammonium supply and observed that local ammonium stimulates lateral root initiation and leads to highly branched lateral roots, while further elongation of pre-emerged root initials becomes arrested. Employing different growth systems for the morphological analysis of lateral root branching and measuring in parallel the uptake of  $^{15}\text{N}$ -labeled ammonium, it was confirmed that ammonium-induced lateral root initiation cannot be explained by a nutritional effect alone. Monitoring lateral root branching in transgenic lines with altered *AMT* gene expression indicated a particular involvement of *AMT1;3* in ammonium-triggered lateral root formation. Moreover, a rigorous comparison of lateral root growth responses between ammonium and nitrate throughout a large set of experiments identified a complementary action of ammonium and nitrate in guiding lateral root development.

## 4.2. Material and methods

### 4.2.1. Plant Material

The following lines were used: *amt1;1-1*, *amt1;3-1*, *amt1;3-1-35S::AMT1;3* (Loqué et al., 2006), *amt1;2-1*, *amt2;1-1*, *qko (amt1;1, amt1;2, amt1;3, amt2;1)*, *qko+11* and *qko+13* (Yuan et al., 2007), *CYCB1:GUS* (Ferreira et al., 1994). The *qko-DR5:GFP* line was generated introducing the *DR5rev:GFP* construct (Vanneste and Friml, 2009) into the *qko* background by *Agrobacterium*-mediated transformation via floral dip. If not otherwise stated the *Arabidopsis thaliana* ecotype Columbia-0 (*Col-0*) was used as a wild-type. The *AMT1;3* TA and TD mutants were kindly provided by Dr. Lixing Yuan. The *AMT1;3* pore mutations (D202N, Asp202Asn) and *AMT1;3* C-terminal mutations (Y471stop, Tyr471Met and Y473stop, Tyr473Met) were generated by *in vitro* mutagenesis based on PCR with QuickChange Multi kit (Stratagene). As template, *AMT1,3* fragment cloned into pCR4-TOPO (Invitrogen) was used to generate each mutation according to the manufactured instructions. The primers used were *AMT1,3* D202N-For, TTTAGCACCGGAGCCATTAACCTTTGCTGGCTCC; Y471STOP-For CGTCACGGTGGCTTTGCTTAGATCTACCATGATAATGATG; and Y473STOP-For GGTGGCTTTGCTTATATCTAGCATGATAATGATGATGAGTC. The mutations were confirmed by sequencing analysis and the fragments were sub-cloned into the vector pPT-Hyg, which then were used to transform *qko* plants.

### 4.2.2. Plant *in vitro* culture

Seeds were surface-sterilized with 70% ethanol and germinated on MGRL medium (Fujiwara et al., 1992) containing 5 mM MES (2-[morpholino]ethanesulphonic acid; Sigma, Germany; pH 5.7), 0.5% sucrose, and 1% Difco Agar (Becton, Dickinson and Company). For transfer to vertically-split agar plates (Remans et al., 2006) plants were supplemented with 0.5 mM nitrate, while for transfer to horizontally-split agar plates (Zhang and Forde, 1998) plants were pre-cultured in the absence of nitrogen. Plants were pre-cultured on vertically-oriented plates for 10 days, transferred to fresh plates containing the same solid medium supplemented locally with  $\text{NH}_4\text{Cl}$  or  $\text{KNO}_3$  at indicated concentrations and KCl to balance  $\text{Cl}^-$  or  $\text{K}^+$  concentrations in all segments of the plate. The medium was supplemented with 5-10 mM MES according to the increasing concentrations of  $\text{NH}_4\text{Cl}$  or  $\text{KNO}_3$  supplied to the HN plate side under vertically-split agar plates in order to avoid changes in the pH which was kept constant at 5.7. Root system architecture was assessed after 15 days of growth in a growth chamber with a 10/14 h day/night regime at 22°/19°C and a light intensity of 120  $\mu\text{mol photons m}^{-2}\text{s}^{-1}$  on horizontally- or vertically-split agar plates. Supply of  $^{15}\text{N}$ -labelled  $\text{NH}_4\text{Cl}$  or  $\text{KNO}_3$  (1% labelled by  $^{15}\text{N}$ -Chemotrata Chemiehandels-gesellschaft mbH Leipzig, Germany) to the agar medium was followed by analysis of accumulated  $^{15}\text{N}$  in roots or shoots by isotope-ratio mass spectrometry coupled with an elemental analyzer (Thermo Electro Finnigan, Bremen, Germany).

### 4.2.3. Heterologous expression of AMT1;3 mutants in yeast

The ORF of AMT1;3 was amplified by PCR and cloned in pDR195 yeast vector (described in Yuan et al., 2007). The pore mutation in AMT1;3 D202N and the C-terminal AMT1;3 mutations (Y471stop and Y473stop) were cloned into yeast vector pDR196 that was used to transform the *triple mep* yeast mutant-strain 31019b (Marini et al., 1997). Yeast transformation was modified from the protocol described by Gietz and Schiestl (1995). Yeast cells were cultivated overnight in liquid YPD medium (10 g  $\text{L}^{-1}$  BACTO yeast extract, Becton Dickson & Co, Sparks, Maryland, USA, 20 g  $\text{L}^{-1}$  BACTO peptone, Becton Dickson, 2% glucose). After the cells culture reached the OD of 0.4-0.5, they were centrifuged at 2000 g at RT for 7 min. The yeast cell were then washed once by sterile destilated MQ water and were resuspended in TE/LiAc solution (100 mM lithium acetate, 10 mM Tris-HCl pH 7.5, 2 mM EDTA). To perform each transformations, around 15-20  $\mu\text{g}$  of salmon sperm

DNA was denatured four times at 95 °C for 5 min. followed each time by incubation at 4 °C for 5 min. In the same Eppendorf tube, 1 µg of plasmid DNA, 70 µL of 5% PEG4000, 10 µL of TE/LiAc solution and 19 µL of the cell suspension were added. This mixture was incubated at 28 °C for 30 min., followed by 42 °C for 15 min. and completing by 28 °C for more 30 min. After centrifugation, the pellet was re-suspended in 100 µL of sterile MQ water and a serial dilution was performed for plating the yeast cells. Growth complementation assays were performed on YNB medium (1.7 g L<sup>-1</sup> DIFCO yeast nitrogen base without amino acids and ammonium sulfate, Becton Dickinson & Co, 20 g L<sup>-1</sup> agar, Bacteriological agar Nr. 1, Oxoid Ltd, Basingstone, UK, 2% glucose) supplemented with 2% of glucose and a nitrogen source (0.2, 2 mM ammonium chloride, 1 mM Arg or 100 mM MeA - a non-metabolizable substrate analog methylammonium) and buffered at pH 5.5 by 50 mM MES-Tris. Yeast cell were incubated at 28 °C for 3 days.

#### 4.2.4. Root growth measurements

Root systems were scanned at a resolution of 300 dpi (Epson Expression 10000XL scanner, Seiko), and the background noise was removed from images using Adobe Photoshop version 5.0 LE (Adobe Systems Inc., California). Root growth was determined by analysing scanned images by WinRHIZO version Pro2007d (Regents Instruments Inc., Canada). The number of emerged lateral roots (> 0.5 mm) was determined by image analysis except for experiments with *CYCB1::GUS* plants (Figure 13 and Table 2) where analysis required histochemistry and microscopy. All the experiments were performed at least twice with similar results.

#### 4.2.5. Histochemical analysis and microscopy

For histochemical studies the Arabidopsis lines *CYCB1::GUS* (*cycb1::uid*, Ferreira et al., 1994) reporter plants were incubated overnight at 37°C in GUS reaction buffer (1 mg/mL of 5-bromo-4-chloro-3-indolyl-b-D-glucuronide in 100 mM sodium phosphate, pH 7.0) and the stained seedlings were cleared according to Malamy and Benfey (1997). Lateral root initials were classified and grouped as emerged (> stage VII) or pre-emerged (stages I-VII). Fixed (6h in 4% formaldehyde in phosphate or PBS buffer, pH 6.5) roots expressing the *cycb1::uid* marker were analyzed and lateral root formation was assessed under a light microscope (Zeiss Axiovert 200 M, Jena, Germany). The Arabidopsis lines *DR5::GUS* (Ulmanov et al.,

1997) and *qko-DR5::GUS* were grown under splitted agar conditions and the localization of the promoter activity was conducted using an inverted fluorescence microscope equipped with ApoTome (Zeiss Axiovert 200 M, Jena, Germany).

#### 4.2.6. Gene expression analysis

For quantitative real-time PCR total RNA was extracted from root tissues grown on individual segments in split-agar plates using the Trizol RNA extraction kit (Invitrogen). RNA was quantified and treated with DNase I (Invitrogen). DNase-treated RNA was checked by agarose gel electrophoresis for genomic DNA contamination. One microgram of total RNA was reverse transcribed into cDNA using oligo(dT)<sub>24</sub> primers and the SuperScriptII Reverse Transcriptase Kit (Invitrogen). Quantitative real-time PCR analysis was performed using an Eppendorf mastercycler realplex (Eppendorf, Germany) and QuantiTect SYBR Green qPCR Mix (Qiagen). Gene-specific primers were used for *AMT1;1* (*AMT1;1*-For, 5'-TCCTAATGGTGATGGTGGACAA -3'; *AMT1;1*-Rev, 5'-TGTTGGAAATGGCAGCGA-3'), *AMT1;3* (*AMT1;3*-For, 5'-GTTGGTGGCATAGCAGGTTT -3'; *AMT1;3*-Rev, 5'-CGGAACGAGTATCTTAGTGAAGG- 3') and *UBIQUITIN2* (*UBQ2*) as reference gene as described in Yuan et al., (2007). Relative transcript abundance was calculated by the Mastercycler ep realplex software package version 2.0.

#### 4.2.7. Accession Numbers

Arabidopsis Genome Initiative locus identifiers for the genes mentioned in this article are At4g13510 (*AMT1;1*), At1g64780 (*AMT1;2*), At3g24300 (*AMT1;3*) and At2g38290 (*AMT2;1*).

### 4.3. Results

#### 4.3.1. Lateral root formation is stimulated by local ammonium supply

To investigate ammonium sensing responses in plants, *Arabidopsis Col-0* plants were placed on horizontally-split agar plates (Zhang and Forde, 1998) to which ammonium or nitrate was supplemented to the middle agar segment. After 15 days of growth the total lateral root length in the middle segment showed a dose-response curve with a threefold increase at 0.5 mM nitrate but a less than twofold increase at 0.8 mM ammonium where lateral root length found its maximum (Figure 11C and 11D). Thereby, the average length of the newly emerged lateral roots in the middle plate segment was stimulated by 132% under nitrate but only by 35% under local ammonium supply (Figure 12C and 12D). In contrast, exposing the middle part of the primary root axis to increasing N concentrations increased lateral root number only by 1.4 roots plant<sup>-1</sup> under nitrate but by 2.0 roots plant<sup>-1</sup> under local ammonium supply (Figure 12I and 12J). Since the total primary root length was negatively affected by elevated levels of local ammonium supply (Figure 12M and 12N), it was calculated lateral root densities for each segment (Figure 11G to 11L). Lateral root density is a reliable measure for lateral root number that corrects for treatment-dependent variations in the length of the parent root (Dubrovsky et al., 2009). In the middle segment lateral root density significantly increased under local ammonium but not under local nitrate supply (Figure 11I and 11J). In the nitrogen-deficient upper root segment, lateral root length and density slightly increased with the supply of either nitrogen form but did not decrease at elevated concentrations (Figure 11A, 11B, 11G, 11H). Lateral roots formed in the bottom segment also responded to external nitrogen supply with an increase in total or average lateral root length and density under nitrate or ammonium supply (Figure 11E, 11F, 11K, 11L, Figure 12E and 12F). Thus, local nitrate or ammonium supply to the middle segment stimulated lateral root development in the bottom segment to a lower but still significant extent, which might be a consequence of nitrogen transport in the root apoplast or symplast between the middle and the bottom root segment. Nevertheless, it is important to note that the major difference between the local responses to ammonium and nitrate was the more prominent increase in lateral root number and density by ammonium, while lateral root length was mainly stimulated by nitrate.

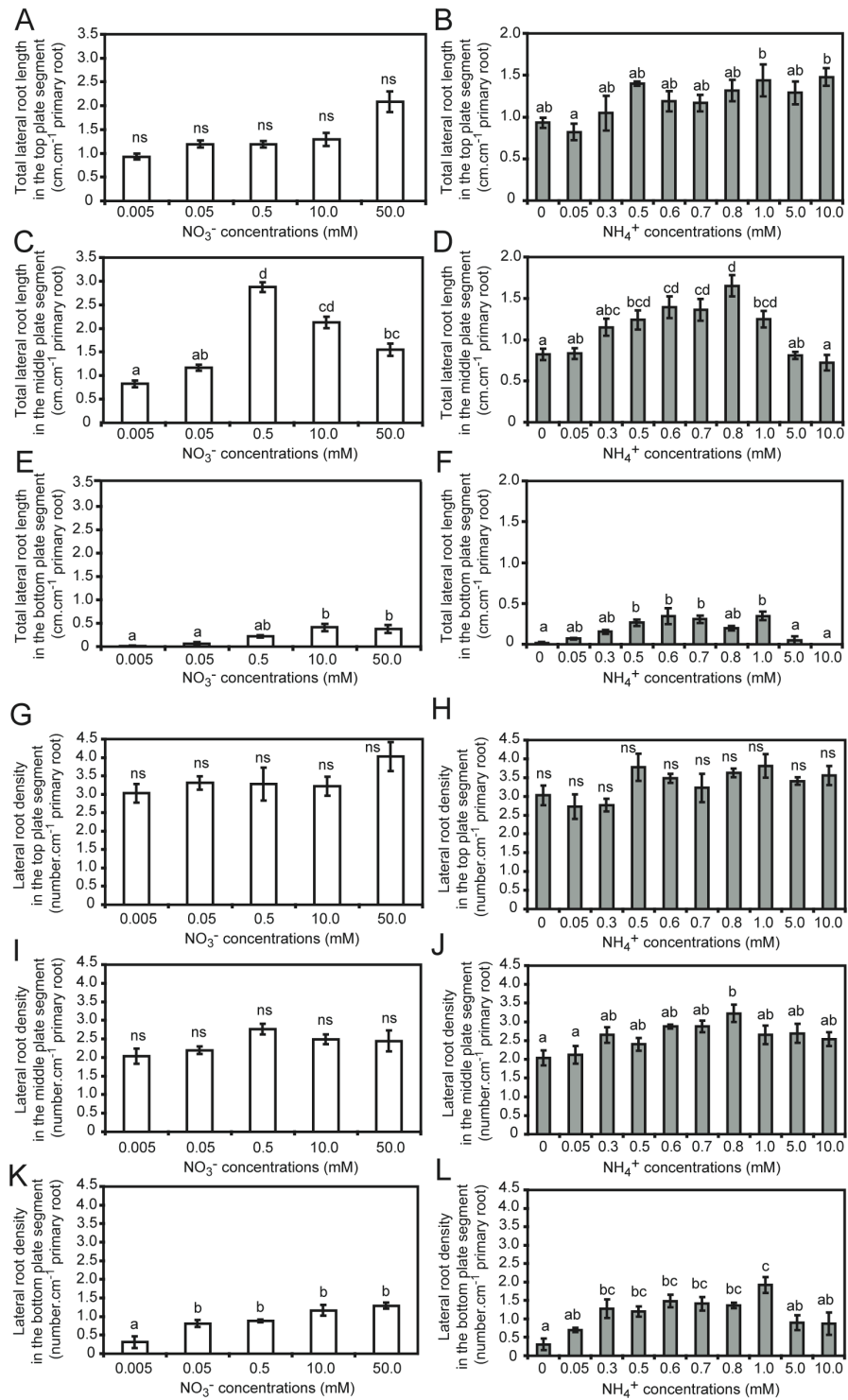


**Figure 11.** Lateral root development is differently affected by local nitrate and ammonium supply.

(A) to (F) Total lateral root length per unit of primary root in the top (A) and (B), middle (C) and (D), and bottom (E) and (F) root compartment. (G) to (L) Lateral root density in the top (G) and (H), middle (I) and (J), and bottom (K) and (L) root compartment. Arabidopsis plants were grown for 15 days on horizontally-split agar plates and supplemented with increasing concentrations of nitrogen in the form of KNO<sub>3</sub> (A, C, E, G, I, K) or NH<sub>4</sub>Cl (B, D, F, H, J, L) only in the middle compartment. Bars represent mean values ( $\pm$  SE) of 21 individual plants per treatment and different letters denote significant differences among means at  $P < 0.05$  (Tukey's test).

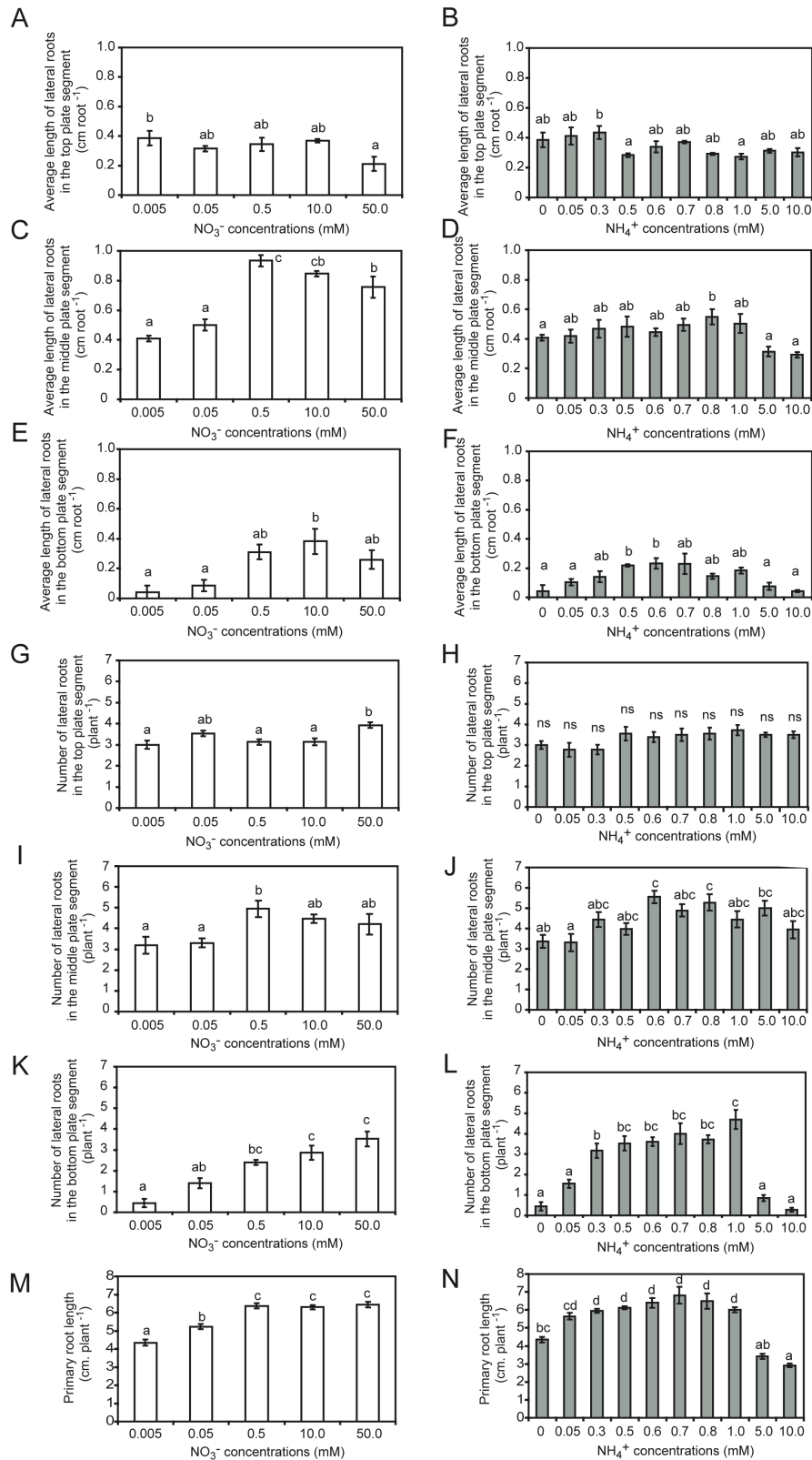


**Figure 12.** Primary and lateral root development under local nitrate and ammonium supply. **(A) to (F)** Average lateral root length in the top **(A)** and **(B)**, middle **(C)** and **(D)** and bottom **(E)** and **(F)** root compartment. **(G) to (L)** Lateral root number in the top **(G)** and **(H)**, middle **(I)** and **(J)** and bottom **(K)** and **(L)** root compartment. **(M)** and **(N)** Primary root length. Arabidopsis plants were grown for 15 days on horizontally-split agar plates and supplemented with increasing concentrations of nitrogen in the form of nitrate **(A, C, E, G, I, K, M)** or ammonium **(B, D, F, H, J, L, N)** only in the middle compartment. Bars represent mean values ( $\pm$  SE) of 21 individual plants per treatment and different letters denote significant differences among means at  $P < 0.05$  (Tukey's test).

Then it was monitored in a time-course experiment the lateral root development under local supply of glutamine as an alternative reduced nitrogen source. However, neither lateral root length nor number or density in the middle segment increased above that observed in control (KCl) treatments (Figure 13A to 3C). A simultaneous supply of glutamine with ammonium did not significantly alter lateral root length in the short term but after 15 days tended to repress the ammonium-stimulated increase in lateral root number and density. These observations indicated that the stimulatory effect of local ammonium supply on lateral root formation could not be mimicked by glutamine. Moreover, the difference between ammonium and control treatments confirmed that ammonium preferentially stimulated lateral root number and density not only in comparison to nitrate (Figure 11) but also in comparison to nitrogen deficiency (Figure 13). Thus, the lateral root phenotype observed under ammonium was not merely caused by the absence of nitrate.

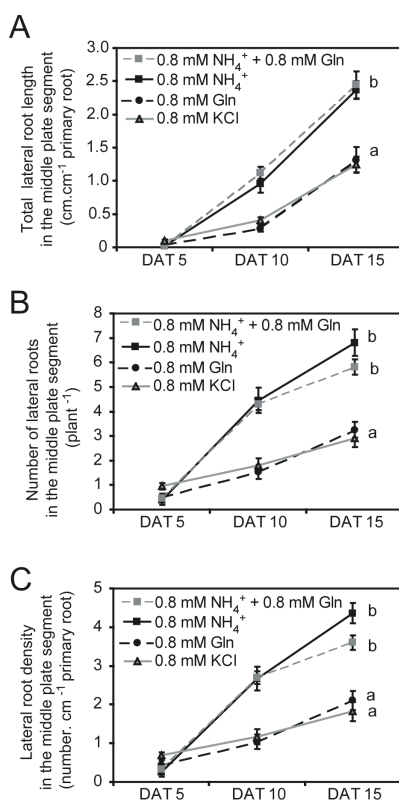


**Figure 13.** Influence of glutamine on lateral root development under localized ammonium supply.

**(A)** Total lateral root length per unit of primary root, **(B)** lateral root number and **(C)** lateral root density in the middle root compartment. Arabidopsis plants were grown for 15 days on horizontally-split agar plates and supplemented with 0.8 mM KCl, 0.8 mM NH<sub>4</sub>Cl, 0.8 mM glutamine or 0.8 mM NH<sub>4</sub>Cl + 0.8 mM glutamine in the middle compartment. Roots were scanned 5, 10 or 15 days after transfer. Bars represent mean values ( $\pm$  SE) of 21 individual plants per treatment and different letters denote significant differences among means at  $P < 0.05$  (Tukey's test).

To investigate whether the different number or density of lateral roots under the two N forms was primarily caused by differences in lateral root initiation or emergence (Péret et al., 2009), the *CYCLINB1::GUS* reporter line was employed thereby allowing the early developmental stages of lateral root primordia to be traced (Colon-Carmona et al., 1999). When these plants were grown in horizontally-split agar plates under localized ammonium supply there was a significantly higher number of lateral roots than under nitrate. This was mainly due to a greater number of pre-emerged lateral root initials (Figure 14). Under local glutamine supply the number of pre-emerged initials approached that of ammonium but still remained at a significantly lower level. These observations suggested that ammonium triggers lateral root development predominantly via the stimulation of their initiation rather than their emergence.

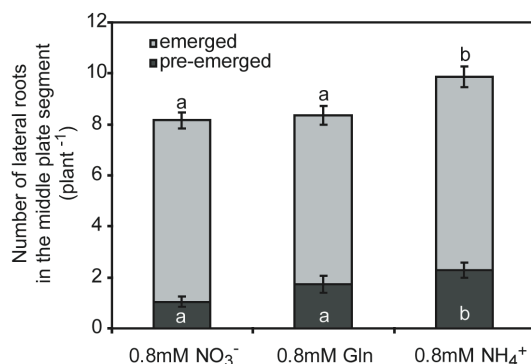


**Figure 14.** Localized ammonium supply increases the number of pre-emerged lateral root initials.

*CYCB1::GUS* lines were germinated on N-deficient medium before transfer to horizontally-split agar plates supplemented with 0.8 mM of either nitrate, ammonium or glutamine in the middle root compartment. Lateral roots in the middle root compartment were classified into pre-emerged initials (stages I – VII) versus emerged lateral root initials (stages  $\geq$  VIII; Malamy and Benfey, 1997). Plants were assessed 12 days after transfer. Bars represent means ( $\pm$  SE),  $n=20-25$ , and different letters denote significant differences among means within each developmental stage at  $P < 0.05$  (Tukey's test).

### 4.3.2. Ammonium-induced lateral root branching is subject to systemic repression

To overcome the limitations of the horizontally-split plate system, i.e. restricted higher-order lateral root branching and the mixed nutritional situation in the primary root axis as it is divided into three segments with different nitrogen supplies, *Arabidopsis* roots were transferred to vertically-split agar plates. Here, the first-order lateral root was guided into nitrogen-supplemented agar while the remainder of the root continued to grow either on the same nitrogen concentration or under nitrogen deficiency. In agreement with the study by Remans et al. (2006), localized nitrate supply stimulated growth of second-order lateral roots as indicated by their increase in length and density on high N (HN), but both measures were strongly repressed when the other agar patch with the main root system (LN side) was additionally supplemented with nitrate (Figure 15A,C and D). There was no significant effect on first-order lateral root length (Table 2, HN plate side). In contrast, under local ammonium supply second-order lateral root lengths were lower than those under nitrate supply, but second-order lateral root density and third-order lateral root development were strongly stimulated (Figure 15B to 15F, Table 2). When the remaining root system also grew in the presence of ammonium (LN plate side) third-order lateral root length and density on the high N plate side (HN) were significantly decreased, indicating that the third-order lateral root phenotype was subject to systemic regulation (Figure 15E, F). To verify the influence of the external nitrogen supply, lateral root formation was also assessed on the side with the primary root (Table 2, LN plate side). The lengths of the primary root and first-order laterals were hardly or not affected by additional supply of either nitrogen form, but second-order lateral root length steeply increased in the presence of nitrate. The length of both second- and third-order lateral roots increased in the presence of ammonium, and this was associated with an increase in second-order lateral root number in the presence of either N form (Table 2). This observation confirmed that ammonium provoked a local stimulation of higher-order lateral root branching that was subject to systemic repression by the nitrogen supplied to the other root fraction.

Simultaneously, nitrogen uptake was monitored by supplementing  $^{15}\text{N}$ -labeled nitrate or ammonium only to the high N (HN) side. Cumulative  $^{15}\text{N}$  uptake was slightly higher in ammonium- than in nitrate-supplied plants and additional supply of N to the other agar patch did not significantly decrease root  $^{15}\text{N}$  accumulation from either N

form (Figure 15G). As expected,  $^{15}\text{N}$  accumulation in roots on the low N (LN) side was lower than on the HN side and additional  $^{14}\text{N}$  supply to these roots decreased  $^{15}\text{N}$  accumulation to a similar extent for both N forms (Figure 15H).  $^{15}\text{N}$  accumulation in shoots followed the same trend (Figure 15I). Referring to the total tissue N concentration, as determined by the analysis of  $^{15}\text{N}$  and  $^{14}\text{N}$ , additional supply of either N form to the LN side significantly increased N concentrations in the LN root fraction as well as in the shoot (Figure 15H and 15I). Thus, the inhibition of third-order lateral root formation on the HN side after additional ammonium supply to the other root fraction was most likely subject to systemic regulation of the N nutritional status of the root fraction on the LN side and/or the shoot wild-type.

**Table 2.** The presence of ammonium and nitrate triggers lateral root development. Total length and total numbers of first-, second- or third-order lateral roots as well as primary root length of *Arabidopsis* wildtype plants grown on vertically-split agar plates for 15 days on either local nitrogen supply (0.8 mM NO<sub>3</sub><sup>-</sup> or NH<sub>4</sub><sup>+</sup> on HN side with 5 μM NO<sub>3</sub><sup>-</sup> on the LN side; LN vs. NO<sub>3</sub><sup>-</sup> and LN vs. NH<sub>4</sub><sup>+</sup>) or homogenous nitrogen supply (0.8 mM NO<sub>3</sub><sup>-</sup> or NH<sub>4</sub><sup>+</sup> on both sides; NO<sub>3</sub><sup>-</sup> vs. NO<sub>3</sub><sup>-</sup> and NH<sub>4</sub><sup>+</sup> vs. NH<sub>4</sub><sup>+</sup>). Values represent means (± SE) of 12-20 individual plants and different letters denote significant differences among means at *P* < 0.05 (Tukey's test).

	HN plate side						LN plate side						Primary root length (cm.plant <sup>-1</sup> )
	Lateral root length (cm.plant <sup>-1</sup> )			Lateral root number (plant <sup>-1</sup> )			Lateral root length (cm.plant <sup>-1</sup> )			Lateral root number (plant <sup>-1</sup> )			
	First-order	Second-order	Third-order	First-order	Second-order	Third-order	First-order	Second-order	Third-order	First-order	Second-order	Third-order	
LN vs NO <sub>3</sub> <sup>-</sup>	10.60 ±0.45b	35.84 ±3.92b	0.79 ±0.19a	25.64 ±1.56c	4.00 ±0.82a	46.60±3.35b	1.97±1.02a	n.d	32.45±2.09n.s	4.36±1.70a	13.96±0.59b		
NO <sub>3</sub> <sup>-</sup> -vs-NO <sub>3</sub> <sup>-</sup>	8.54 ± 0.95b	11.24 ±3.52a	0.12 ±0.10a	13.60 ±1.89ab	2.41 ±0.24a	58.81±4.51b	27.58±4.87c	n.d	38.25±4.36n.s	59.25±11.5b	12.79±0.44a		
LN vs NH <sub>4</sub> <sup>+</sup>	4.81 ±0.34a	7.45 ±0.58a	2.57 ±0.24b	22.06 ±0.40bc	18.88 ±0.41c	28.88±1.68a	1.85±0.24a	0.03±0.01a	28.06±1.70n.s	8.24±1.09a	11.05±0.52a		
NH <sub>4</sub> <sup>+</sup> vs NH <sub>4</sub> <sup>+</sup>	5.09 ±0.43a	4.46 ±1.35a	0.66 ±0.22a	11.23 ±3.80a	9.65 ±3.21b	20.29±2.97a	7.80±2.37b	0.57±0.05b	37.00±3.46n.s	59.33±5.48b	11.17±0.82a		

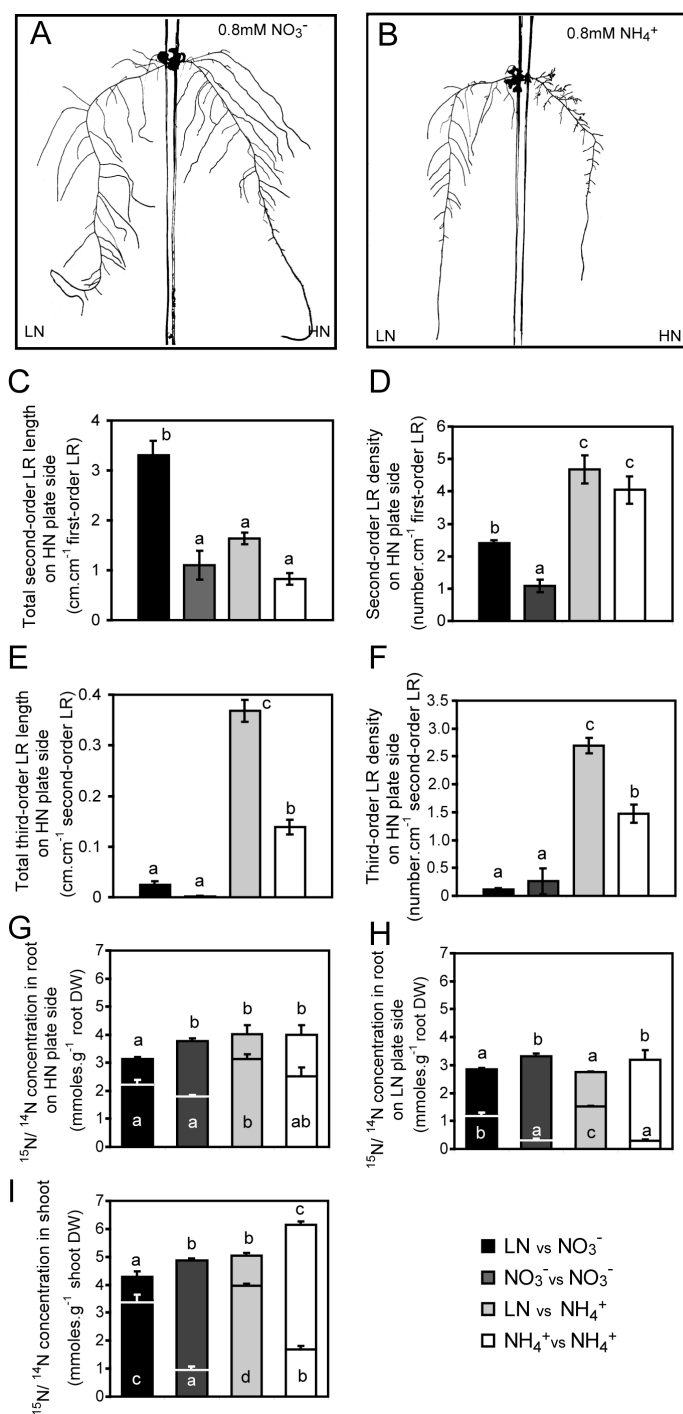


**Figure 15.** Local ammonium supply induces third-order lateral root branching.

(A) and (B) Typical root morphology of wild-type plants grown on vertically-split agar plates with the first lateral root growing into a high N compartment (HN) with (A) 0.8 mM KNO<sub>3</sub> or (B) 0.8 mM NH<sub>4</sub>Cl and the remainder of the roots growing in 5 μM KNO<sub>3</sub> (low nitrogen, LN). (C) to (F) Quantitative assessment of root morphology, (C) second-order lateral root length, (D) second-order lateral root density, (E) third-order lateral root length, (F) third-order lateral root density. (G) to (I) <sup>15</sup>N uptake from <sup>15</sup>N-labeled nitrate or ammonium applied to the HN side and its distribution in plants. Concentrations of total nitrogen (<sup>14</sup>N+<sup>15</sup>N, outer bars) and <sup>15</sup>N (inner bars) in (G) roots grown on the HN side, or (H) roots grown on the LN side, and (I) shoots are indicated. Plants were grown on vertically-split agar plates for 15 days on either local nitrogen supply (5 μM NO<sub>3</sub><sup>-</sup> on the LN side with 0.8 mM NO<sub>3</sub><sup>-</sup> or NH<sub>4</sub><sup>+</sup> on HN side; LN vs. NO<sub>3</sub><sup>-</sup> and LN vs. NH<sub>4</sub><sup>+</sup>) or homogenous nitrogen supply (0.8 mM NO<sub>3</sub><sup>-</sup> or NH<sub>4</sub><sup>+</sup> on both sides; NO<sub>3</sub><sup>-</sup> vs. NO<sub>3</sub><sup>-</sup> and NH<sub>4</sub><sup>+</sup> vs. NH<sub>4</sub><sup>+</sup>). Bars represent mean values (± SE) of 10-20 individual plants and different letters for total nitrogen (<sup>14</sup>N+<sup>15</sup>N, outer bars) and <sup>15</sup>N (inner bars) denote significant differences among means at *P* < 0.05 (Tukey's test).

Recently, glutamine has been described as a repressor of lateral root emergence (Gifford et al., 2008). Indeed, addition of a local equimolar supply of glutamine together with ammonium decreased third-order lateral root length and density, while glutamine by itself poorly triggered third-order lateral root formation (Figure 16A, B). The simultaneous supply of glutamine significantly decreased the cumulative uptake of  $^{15}\text{N}$ -labelled ammonium (Figure 16C). This might be due to a systemic repression, considering the proposed role of glutamine as a metabolic signal for N sufficiency or to a direct down-regulation of *AMT1* genes by glutamine (Rawat et al., 1999).

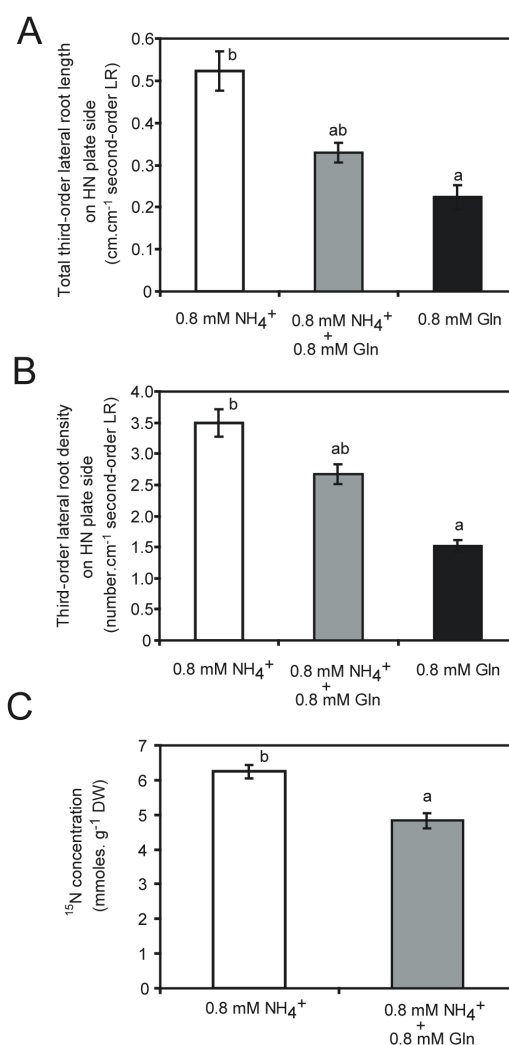


**Figure 16.** Glutamine represses ammonium-induced third-order lateral root branching. **(A)** Third-order lateral root length, **(B)** third-order lateral root density, and **(C)**  $^{15}\text{N}$  concentrations in roots from  $^{15}\text{N}$ -labelled ammonium supplied to the high N (HN) side. Wild-Type plants were grown for 15 days on vertically-split agar plates with the first lateral root growing into a high N compartment (HN) with 0.8 mM  $^{15}\text{N}$ -labelled  $\text{NH}_4\text{Cl}$ , 0.8 mM  $^{15}\text{N}$ -labelled  $\text{NH}_4\text{Cl}$  together with 0.8 mM glutamine or 0.8 mM glutamine alone, while the remainder of the roots was growing without N supply. Bars represent mean values ( $\pm$  SE) of 10-15 individual plants and different letters denote significant differences among means at  $P < 0.05$  (Tukey's test).

To verify a systemic effect of glutamine, increasing glutamine concentrations were added to the LN compartment of the split-root design. Measurement of lateral root development on the HN side of the plate revealed a strong decrease of first (data not shown), second and third-order lateral root length and density (Figure 17A and 17B). Neither  $^{15}\text{N}$  accumulation nor total N concentrations in ammonium-supplied roots differed significantly from control plants grown in the absence of glutamine on LN plate side (Figure 17C), indicating that inhibition of third-order lateral root formation could not be explained exclusively by a glutamine-mediated repression of ammonium uptake (Rawat et al., 1999). Total N concentrations in the LN root fraction or in shoots increased at the expense of ammonium- $^{15}\text{N}$  due to higher glutamine uptake (Figure 17D and 17E). Thus, glutamine or glutamine-derived nitrogen most likely acted as a metabolic repressor of ammonium-induced third-order lateral root formation which was most likely independent of an inhibition of local ammonium uptake.

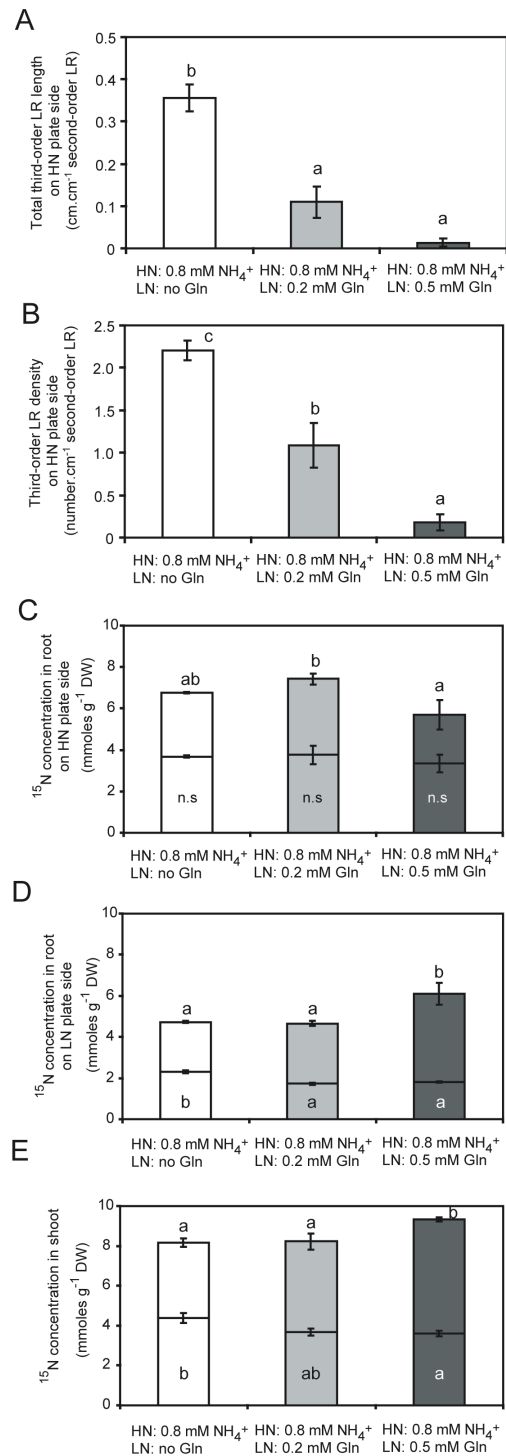


**Figure 17.** Systemic repression of ammonium-induced third-order lateral root branching by glutamine.

**(A)** Third-order lateral root length, **(B)** third-order lateral root density, and **(C to E)** <sup>15</sup>N uptake from <sup>15</sup>N-labeled ammonium applied to the HN side and its distribution in plants. Concentrations of total nitrogen (<sup>14</sup>N+<sup>15</sup>N, outer bars) and <sup>15</sup>N (inner bars) in **(C)** roots from the high N (HN), **(D)** roots from low N (LN) side of the plate, and **(E)** shoots are indicated. Wild-Type plants were grown for 15 days on vertically-split agar plates with the first lateral root growing into a high N (HN) compartment supplied with 0.8 mM <sup>15</sup>N-labeled NH<sub>4</sub>Cl. Increasing concentrations of glutamine were added to the remainder of the roots growing in a low N compartment (LN). Bars represent mean values of 8-12 individual plants and different letters denote significant differences among means at  $P < 0.05$  (Tukey's test); n.s. not significant.

### 4.3.3. Ammonium and nitrate regulate lateral root development in a complementary way

To investigate whether nitrate and ammonium have a differential effect on lateral root initiation or emergence, the *CYCLINB1::GUS* reporter line was grown in vertically-split agar plates and the effect of a combined ammonium nitrate supply was compared to that of the single nitrogen forms. Taking into account pre-emerged lateral root initials the localized ammonium supply increased the density of second-order laterals as well as the length, number and density of third-order laterals relative to the nitrate treatment (Table 3). In contrast, ammonium nitrate-grown plants had even greater lateral root numbers, but resulted in a similar density of second-order laterals comparable to ammonium-supplied plants due to a concomitant increase in the length of first-order lateral roots. With regard to third-order lateral roots, ammonium nitrate enhanced third-order lateral root number even more than ammonium supply alone, pointing to an additive effect of both N forms. Due to the lower second-order lateral root length, third-order lateral root density remained highest under ammonium. The comparison between nitrate- and ammonium nitrate-grown plants clearly showed that the higher lateral root numbers and densities conferred by ammonium supply were independent of any effects on the parent root (Table 3) and that ammonium also stimulated higher-order lateral root branching in the presence of nitrate. Thus, nitrate and ammonium promoted lateral root development in a complementary manner, in which ammonium was the dominant trigger for lateral root initiation.

**Table 3.** Ammonium and nitrate stimulate lateral root development in a complementary manner. Length, number and density of first-, second- or third-order lateral roots of *Arabidopsis CYCB1::GUS* plants grown under local supply of ammonium, nitrate or ammonium nitrate in vertically-split agar plates. Pre-emerged and emerged lateral roots (<0.5 mm) were determined after histochemical staining. Numbers represent mean values ( $\pm$  SE) of 12-21 individual plants per treatment, and different letters denote significant differences among nitrogen treatments at  $P < 0.05$  (Tukey test).

	Lateral root length (cm.plant <sup>-1</sup> )			Lateral root number (plant <sup>-1</sup> )			Lateral root density (number.cm <sup>-1</sup> )		
	First-order	Second-order	Third-order	Second-order	Third-order	Second-order	Third-order		
0.8 mM NO <sub>3</sub> <sup>-</sup>	10.60 $\pm$ 0.45b	35.83 $\pm$ 3.92b	0.79 $\pm$ 0.20a	33.83 $\pm$ 2.54a	24.27 $\pm$ 2.31a	3.33 $\pm$ 0.38a	0.78 $\pm$ 0.12a		
0.8 mM NH <sub>4</sub> <sup>+</sup>	4.81 $\pm$ 0.49a	8.01 $\pm$ 0.75a	2.88 $\pm$ 0.26b	25.66 $\pm$ 1.65a	49.08 $\pm$ 3.87b	5.47 $\pm$ 0.60b	6.52 $\pm$ 0.54b		
0.4 mM NH <sub>4</sub> NO <sub>3</sub>	11.39 $\pm$ 0.98b	41.04 $\pm$ 7.71b	1.42 $\pm$ 0.29a	55.88 $\pm$ 4.19b	71.83 $\pm$ 8.41c	5.14 $\pm$ 0.24b	2.10 $\pm$ 0.42a		

#### 4.3.4. The ammonium transporter-defective mutant *qko* shows decreased ammonium-triggered lateral root branching

It was investigated the role of ammonium uptake in lateral root branching employing the *Arabidopsis qko* mutant, which is defective in four root-expressed *AMMONIUM TRANSPORTER (AMT)* genes (*amt1;1*, *amt1;2*, *amt1;3*, *amt2;1*) and shows a 90-95% reduction of high-affinity ammonium influx in short-term uptake studies (Yuan et al., 2007). Fifteen days after transfer to horizontally-split agar plates, first-order lateral root length in *qko* was 32% lower than in the wild-type, whereas the visible number or density of first-order lateral roots formed in response to ammonium decreased by 48% or 53%, respectively (Figure 18A to 18C). The analysis of  $^{15}\text{N}$  concentrations in entire seedlings after 15 days of growth in the presence of  $^{15}\text{N}$ -labeled ammonium in the middle segment, revealed a 32% decrease in cumulative ammonium uptake in *qko* (Figure 18D). The comparison between wild-type and *qko* plants thus confirmed that local ammonium supply exerted a stronger stimulation of lateral root initiation than of elongation and that the ammonium-induced changes in root architecture depended on AMT-type ammonium transport proteins or their uptake capacity. Under local ammonium supply on vertically-split agar plates, it was observed that second-order and third-order lateral root formation in *qko* were strongly reduced (Figure 18F, 18G and 18H), which went along with a weaker biomass production (Figure 18I), whereas the growth response to nitrate was similar to the wild-type (Figure 18E, 18G and 18H). Since the loss of lateral root branching in *qko* under localized ammonium supply (Figure 18C, 18F, 18G and 18H) coincided with lower cumulative ammonium uptake (Figure 18D), a nutritional effect of ammonium-derived nitrogen had to be considered. In this case a higher concentration of locally supplied ammonium should restore lateral root branching in *qko* due to ammonium uptake via low-affinity transport systems (Loqué and von Wirén, 2004). However, increasing external ammonium supply showed that even 5 mM ammonium did not restore wild-type levels of either the length or density of third-order lateral roots in *qko* (Figure 19A and 19B). In wild-type plants third-order lateral root development decreased under high local ammonium supplies probably due to ammonium-induced systemic inhibition (Figure 16). At 5 mM ammonium supply, cumulative  $^{15}\text{N}$  uptake in *qko* was 21% higher than under 0.8 mM. This was almost at the same level as in wild-type plants supplied with 0.8 mM (Figure 19C) where they showed a vigorous

third-order lateral root development. Thus, higher local ammonium supplies could not restore lateral root formation in *qko*, indicating that lateral root formation depends on the presence of AMT proteins per se rather than on the quantity of absorbed ammonium.

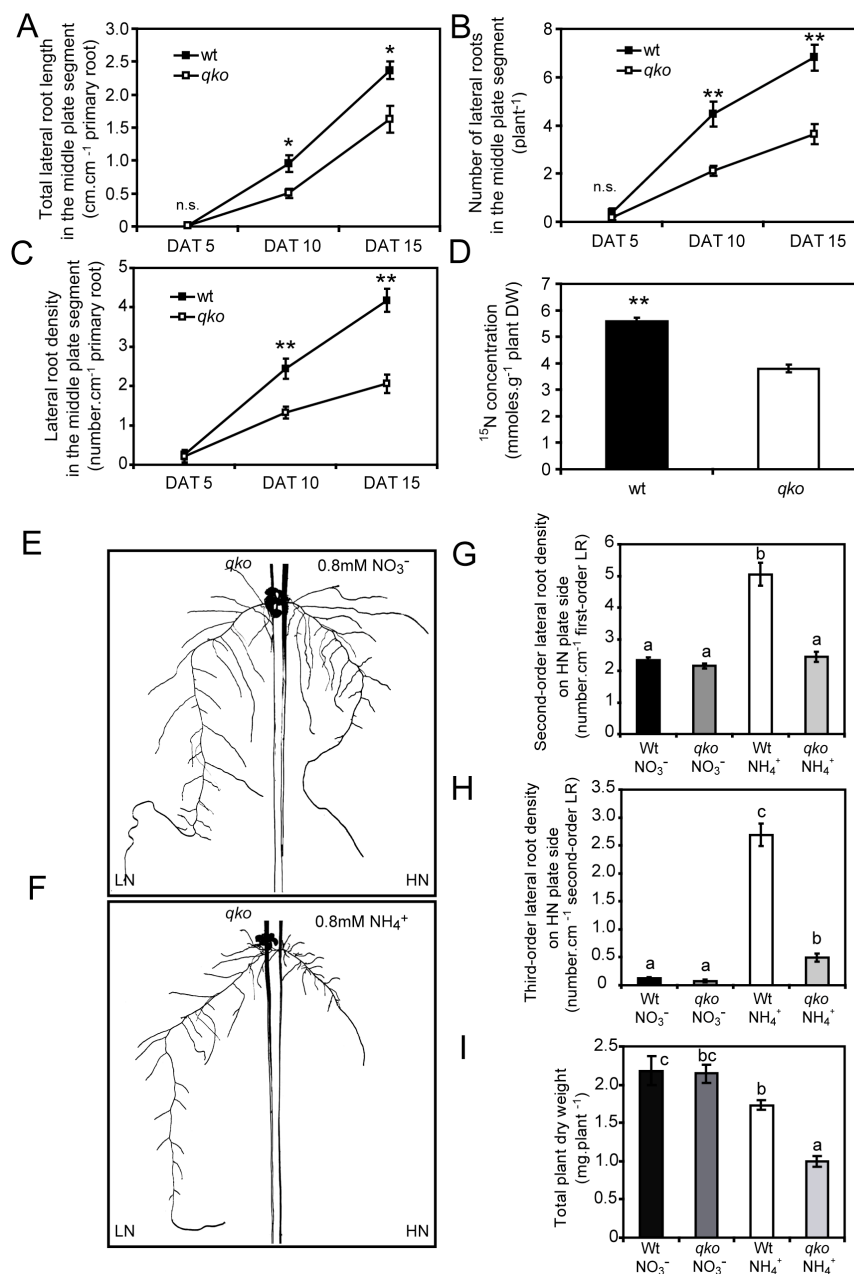


**Figure 18.** Third-order lateral root branching by local ammonium supply requires *AMMONIUM TRANSPORTER* (*AMT*) genes.

(A) to (D) Time course of lateral root development on horizontally-split agar plates. (A) Lateral root length, (B) lateral root number, (C) lateral root density, and (D) <sup>15</sup>N concentration in roots from <sup>15</sup>N-labeled ammonium supplied to the middle root compartment. Wild-Type and *qko* (*amt1;1*, *amt1;2*, *amt1;3*, *amt2;1*) plants were grown for 15 days on horizontally-split agar plates. Bars represent mean values ( $\pm$  SE) and asterisks denote significant differences between lines at \*  $P < 0.05$  or \*\*  $P < 0.001$  (Student's *t*-test),  $n = 10-12$  individual plants per treatment; n.s., not significant. (E) to (H) Root morphology of *qko* plants grown on vertically-split agar plates with the first lateral root growing into (E) 0.8 mM NO<sub>3</sub><sup>-</sup> or (F) 0.8 mM NH<sub>4</sub><sup>+</sup> and the remainder of the roots growing in 5  $\mu$ M NO<sub>3</sub><sup>-</sup> (LN). (G) Second-order lateral root density and (H) third-order lateral root density of roots grown in the high N (HN) compartment. (I) Total plant dry weight of plants grown for 12 days under localized nitrate or ammonium supply. Bars represent mean values ( $\pm$  SE) of 12-20 individual plants per treatment. Different letters denote significant differences among means at  $P < 0.05$  (Tukey's test).

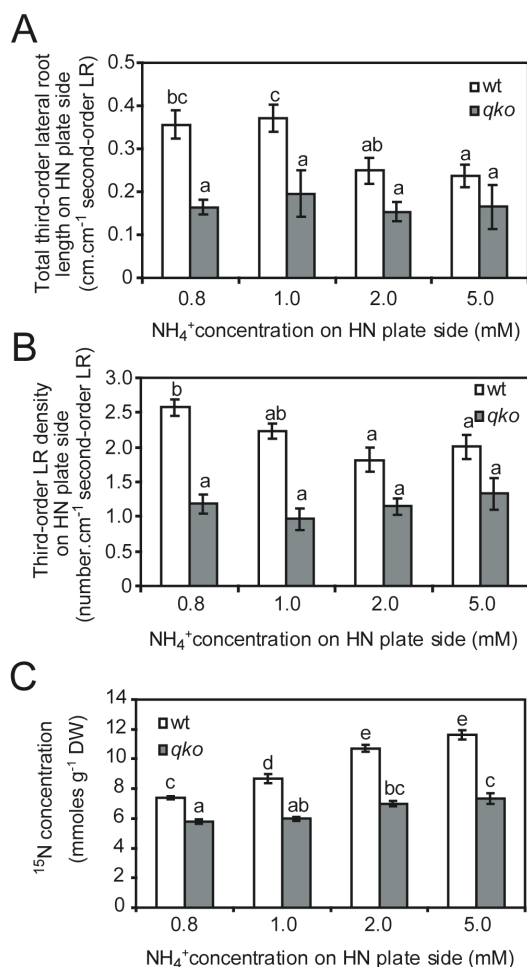


**Figure 19.** Millimolar ammonium supply cannot restore third-order lateral development in *qko*.

**(A)** Third-order lateral root length, **(B)** third-order lateral root density, and **(C)** <sup>15</sup>N concentrations shoot plus root samples from <sup>15</sup>N-labeled ammonium supplied to the HN compartment. Wild-Type and *qko* (*amt1;1*, *amt1;2*, *amt1;3*, *amt2;1*) plants were grown on vertically-split agar plates with a localized supply of increasing ammonium concentrations. Bars represent means ( $\pm$  SE) and different letters denote significant differences at  $P < 0.05$  (Tukey's test);  $n = 10-15$ .

#### 4.3.5. The role of AMT1;3 in lateral root branching

Considering that Arabidopsis plants express five AMT-type ammonium transporters in roots (Yuan et al., 2007) and that AMT1;5 which is still functional in *qko* is not responsible for lateral root branching (Figure 18), it was investigated the role of the four remaining AMTs in third-order lateral root formation by phenotyping the corresponding single T-DNA- or transposon-tagged insertion lines. With respect to third-order lateral root length, none of the single insertion lines differed from its corresponding wild-type (Figure 20A to 20D). Only the *amt1;3-1* insertion line yielded a significantly lower third-order lateral root density than its wild-type Ws-0

background. In fact, lateral root density in *amt1;3-1* decreased by 30% and thus still remained at a higher relative level than that of *qko* plants, which was 50-75% below wild-type levels (Figure 18 and 19). To verify an effect of AMT1;3, *amt1;3-1* plants expressing a 35S::AMT1;3 construct (Loqué et al., 2006) were assayed and observed to completely restore wild-type levels of third-order lateral root density (Figure 21A and 21B). Interestingly, cumulative  $^{15}\text{N}$ -ammonium uptake was similar in all lines (Figure 21C) supporting the notion that the lower third-order lateral root density in *amt1;3-1* was not related to impaired acquisition of ammonium-derived N.

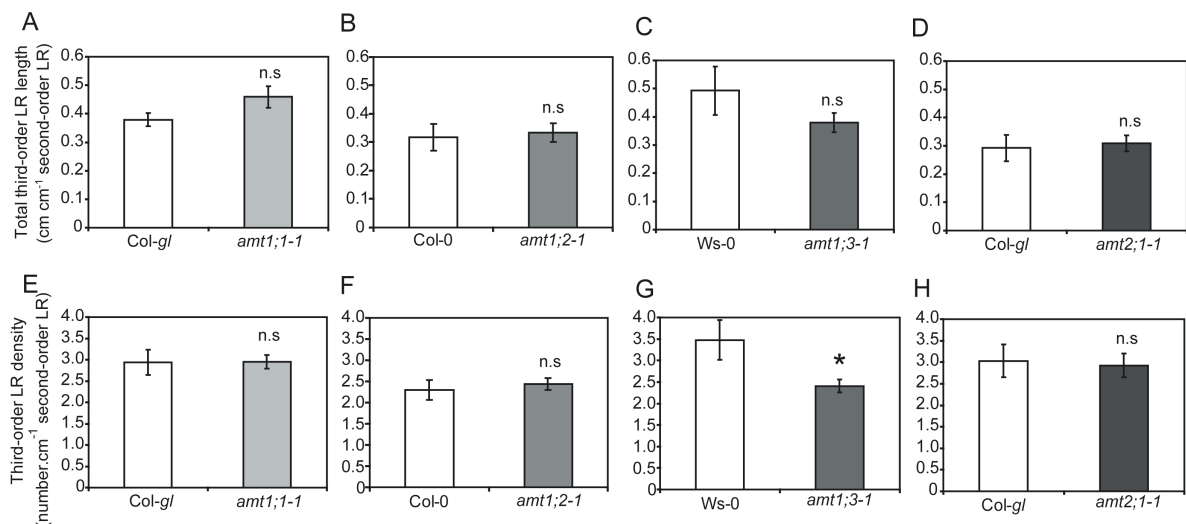


**Figure 20.** Third-order lateral development in single *AMT* insertion lines.

(A) to (D) total third-order lateral root length, (E) to (H) third-order lateral root density of plants grown for 15 days on vertically-split agar plates with a localized supply of 0.8 mM ammonium. (A) and (E) Col-gl and *amt1;1-1* (Loqué et al., 2006); (B) and (F) Col-0 and *amt1;2-1* (Yuan et al., 2007); (C) and (G) Ws-0 and *amt1;3-1* (Loqué et al., 2006); (D) and (H) Col-gl and *amt2;1-1* (Yuan et al., 2007). Bars represent means ( $\pm$  SE) and different letters denote significant differences at  $P < 0.05$  (Student's t-test);  $n = 12-20$ .

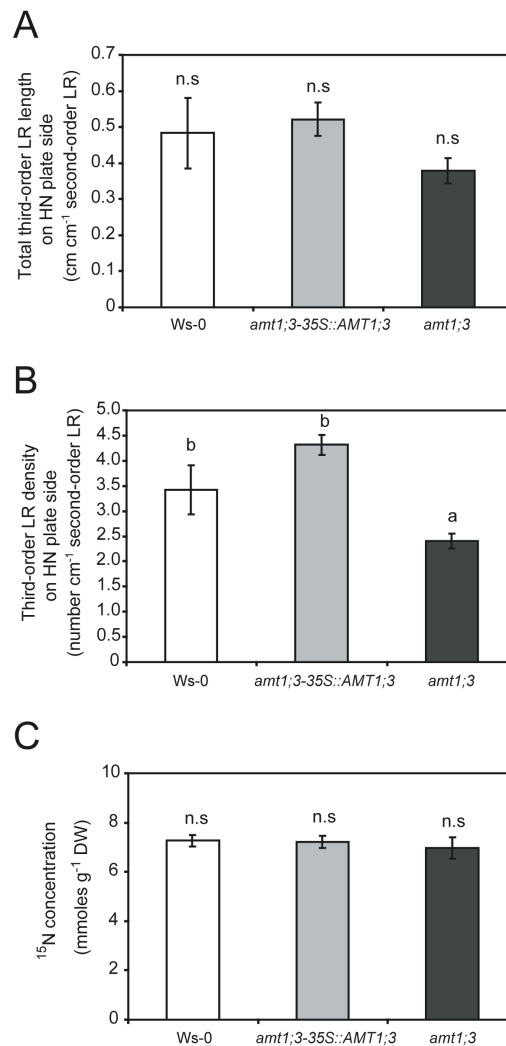


**Figure 21.** Third-order lateral development in the 35S:AMT1;3-transformed *amt1;3-1* insertion line.

(A) Total third-order lateral root length, (B) third-order lateral root density, and (C) <sup>15</sup>N concentrations in shoot plus root samples from <sup>15</sup>N-labeled ammonium supplied to the HN compartment. Ws-0, *amt1;3-1* and 35S:AMT1;3 plants were grown for 15 days on vertically-split agar plates with a localized supply of 0.8 mM ammonium. Bars represent means ( $\pm$  SE) and different letters denote significant differences at  $P < 0.05$  (Tukey's test);  $n = 12-20$ .

Since Ws-0 plants showed a slightly higher third-order lateral root formation than other Arabidopsis accession lines (Figure 20), the role of AMT1;3 was assessed in the Col-0 background employing the *qko* line with reconstituted expression of AMT1;3 (*qko+13*) and compared against *qko+11* expressing AMT1;1, which is the only other AMT transporter showing an overlapping cell type-specific expression pattern in roots and comparable biochemical transport properties (Loqué et al., 2006; Yuan et al., 2007). Third-order lateral root length and third-order lateral root density of *qko+13* plants achieved wild-type levels, whereas *qko+11* plants did not restore third-

order lateral root formation (length and density) and remained at a similar level as wild-type plants (Figure 22A, C). In contrast, there was no significant effect of either AMT on average third-order lateral root length (Figure 22B). In agreement with their similar ammonium uptake capacities as determined in short-term transport studies and the same biomass production as wild-type plants on ammonium-based medium (Yuan et al., 2007), *qko+11* and *qko+13* both accumulated ammonium-derived N to the same extent (Figure 22D), clearly exceeding the  $^{15}\text{N}$  accumulation by *qko* plants. Thus, although both transporters conferred a similar ammonium uptake capacity only AMT1;3, but not AMT1;1, was able to trigger third-order lateral root proliferation and this action was independent of the genetic background. It was also verified whether pruning of the primary root affects higher-order lateral root branching as it favors the comparison of two more balanced root fractions (Remans et al., 2006). However, similar results were obtained showing that AMT1;3 is able to restore third-order lateral root formation (Table 4), indicating that primary root pruning had minimal impact on higher-order lateral root branching.

It was tested whether the successful complementation of third-order lateral root formation by *AMT1;3* was caused by a higher mRNA expression level in the split-root system. However, at harvest *AMT1;3* expression levels were even lower in the N-deficient root fraction and similar to those of *AMT1;1* under local ammonium supply (Figure 23A). To further consider changes in *AMT* gene expression during third-order lateral root development, ammonium-supplied root fractions were harvested in a time-course study from split plates. Interestingly, *AMT1;1* transcript levels steeply increased and peaked two days after transfer of plants to vertically-split agar plates before decreasing again, whereas *AMT1;3* transcript levels remained at a constantly low level during the whole period of third-order lateral root formation (Figure 23B). Thus, a higher gene expression level was unlikely to account for AMT1;3-triggered third-order lateral root formation.

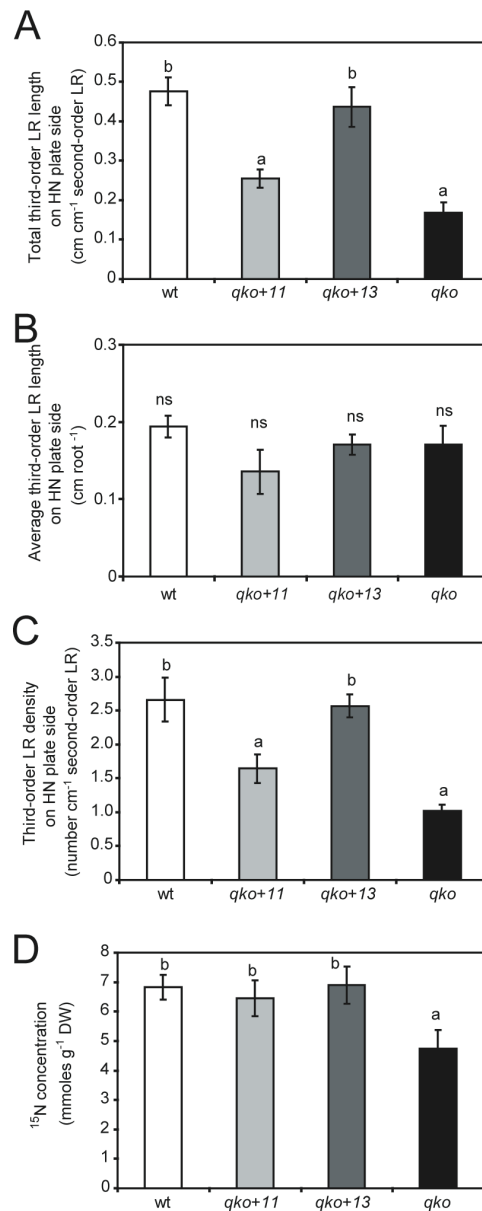


**Figure 22.** Reconstituted expression of *AMT1;3* but not of *AMT1;1* restores third-order lateral development in *qko*.

(A) Total third-order lateral root length, (B) average third-order lateral root length, (C) third-order lateral root density and (D) <sup>15</sup>N concentrations in whole plant (shoot+root) from <sup>15</sup>N-labeled ammonium supplied to the high N compartment. Wild-Type, *qko* (*amt1;1*, *amt1;2*, *amt1;3*, *amt2;1*), *qko+11* (*amt1;2*, *amt1;3*, *amt2;1*) or *qko+13* plants (*amt1;1*, *amt1;2*, *amt2;1*; Yuan et al., 2007) were grown for 15 days on vertically-split agar plates with a localized supply of 0.8 mM ammonium. Bars represent means (± SE) and different letters denote significant differences at  $P < 0.05$  (Tukey's test);  $n = 15-20$ .

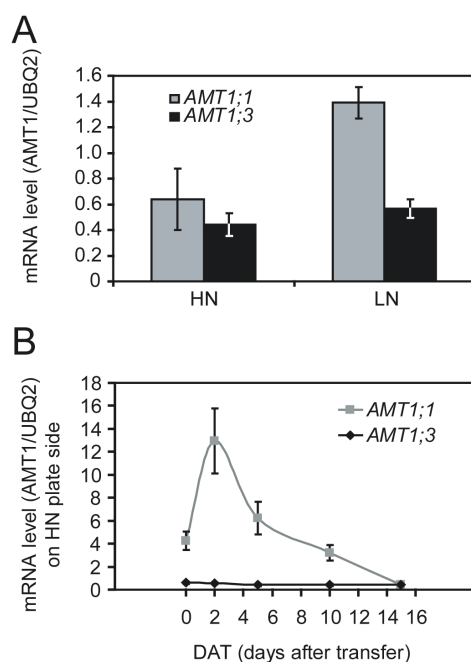


**Figure 23.** *AMT1;1* and *AMT1;3* are differently regulated under localized ammonium supply.

**(A)** Relative mRNA abundance of *AMT1;1* and *AMT1;3* in roots from the low N (LN) compartment or the high H (HN) compartment supplemented with 0.8 mM ammonium. Wild-Type plants were grown on vertically-split agar plates for 15 days. mRNA abundance was quantified by qRT-PCR relative to the constitutively expressed polyubiquitin control gene (*UBQ2*) **(B)** Time-course of the *AMT1;1* and *AMT1;3* mRNA abundance on the HN plate side during 15 days of lateral root exposure to localized ammonium supply. Bars represent means ( $\pm$  SE);  $n = 3-4$ .

Recently, the C-terminus of *AMT1;1* was shown to play a role in allosteric regulation and functionality of a trimeric AMT complex (Loqué et al., 2007). Presuming a similar role of the C-terminus in *AMT1;3*, it was introduced a T to D amino acid substitution at position 471, which corresponds to a T460D substitution in the *AMT1;1* protein, where it mimics phosphorylation and leads to loss of functionality in *AMT1;1* (Loqué et al., 2007). Expression of this C-terminus variant in the *qko* background led to a comparable low cumulative  $^{15}\text{N}$ -ammonium uptake as in *qko* (Figure 14A), indicating that the T471D substitution was inactive *in planta*. Thus, this variant was suitable to investigate a functional coupling between ammonium transport and lateral root branching in *AMT1;3*. The total third-order lateral length and density in the C-terminally inactivated *AMT1;3* variant did not significantly differ from *qko*. By contrast, introduction of a T to D substitution at the same position to mimic a non-phosphorylated state of the *AMT1;3* C-terminus did not significantly decrease third-order lateral root formation relative to wild-type plants and decreased

ammonium uptake only by 15% (Figure 24B and 24C). Consequently, loss of functional ammonium transport by C-terminal inactivation in *AMT1;3* went along with a loss of third-order lateral root formation.

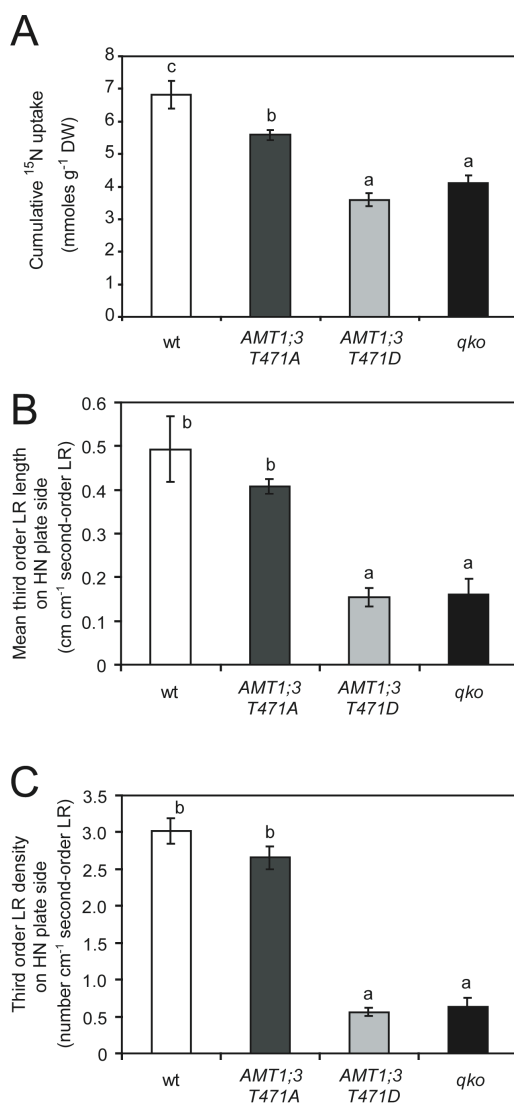


**Figure 24.** C-terminal inactivation of *AMT1;3* leads to loss of third-order lateral development.

**(A)** <sup>15</sup>N concentrations in plants (shoot plus root samples) from <sup>15</sup>N-labeled ammonium supplied to the high N compartment, **(B)** Total third-order lateral root length, **(C)** third-order lateral root density. Wild-type, *qko* (*amt1;1*, *amt1;2*, *amt1;3*, *amt2;1*), *qko+13 TA* plants (*amt1;1*, *amt1;2*, *amt2;1*; *AMT1;3 T471A*) and *qko+13 TD* plants (*amt1;1*, *amt1;2*, *amt2;1*; *AMT1;3 T471D*) were grown for 15 days on vertically-split agar plates with a localized supply of 0.8 mM ammonium. Bars represent means ( $\pm$  SE) and different letters denote significant differences at  $P < 0.05$  (Tukey's test);  $n = 15-20$ .

In yeast the Mep2 protein has been assigned as ammonium sensor responsible for pseudohyphal growth under N limitation conditions. By mutations in the ammonium conducting pore and in the intracellular C-terminus of Mep2, it was possible to uncouple ammonium signaling from ammonium transport in yeast

(Rutherford et al, 2008). Since a *trans*-inactivation of AMT1;3 by mimicked phosphorylation could not uncouple ammonium signaling for lateral growth from ammonium transport (Figure 24), a site-direct mutagenesis was performed in AMT1;3 by targeting lining residues in pore region or introducing a stop-codon in the C-terminus right after those amino acids that are essential for transporter regulation. By growth complementation assays in yeast and modeling analysis, the amino acid substitution D198N in AMT1;1 has been shown to cause a lack of ammonium transport without changing the stability of the protein (Loqué et al., 2007). Moreover, in AMT1;1 the C-terminal Y467 and Y469 residues are essential for the ammonium transport function due to its interaction with the neighboring loop, whereas Y467 is a conserved residue in AMT1 subfamily proteins being responsible for *trans*-inactivation of adjacent monomers in the trimeric AMT complex (Loqué et al., 2007). By targeting the equivalent residues in the AMT1;3 protein, the pore mutation D202N resulted in a non-functional transporter when expressed in yeast (Figure 25). The C-terminally truncated version Y471stop led to the absence of ammonium transport probably due to *trans*-inactivation of the other transporters, comparable to the situation in AMT1;1. In contrast to AMT1;1, the addition of a stop-codon at the corresponding residue Y473 in AMT1;3 yielded to a functional transporter in yeast (Figure 25). This observation suggested that the C-terminus of AMT1;3 most likely possesses a differential regulation from that in AMT1;1.

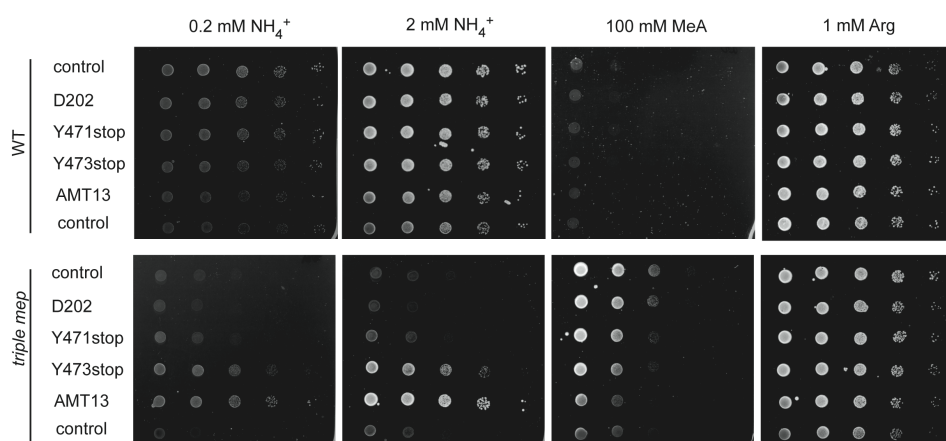


**Figure 25.** Functional analysis of AMT1;3 mutations in yeast.

The *triple mep* yeast mutant (strain 31019b) and wild-type were transformed with the vectors pDR196-control, pDR196-AMT1;3 D202N (pore mutation), pDR196-AMT1;3 Y471stop and pDR196-AMT1;3 Y473stop (C-terminal mutations). The AMT1;3 was cloned in the pDR195 and the additional control was used (pDR195-control in the bottom). The yeast transformants were selected in YNB medium supplemented with 1 mM arginine (Arg). From the preculture yeast cells, 10  $\mu$ L of cell suspensions were spotted in a serial dilution of one to fivefold on YNB medium supplemented with 2% glucose and either 0.2, 2 mM ammonium chloride, 1 mM Arg or 100 mM MeA (non-metabolizable substrate analog methylammonium). Yeast cells were incubated at 28  $^{\circ}$ C for 3 days. The growth complementation assay was performed twice with similar results.

To confirm these results *in planta*, the same AMT1;3 variants were expressed in the *qko* background and a detailed investigation of their root morphology under local ammonium supply was performed. Plants expressing the pore mutation AMT1;3 D202N were not able to form third-order lateral roots and had a <sup>15</sup>N-ammonium uptake capacity that was comparable to that in *qko* (Figure 26). Moreover, the AMT1;3 variant Y471stop and the mutation Y473stop did not significantly differ from *qko* with regard to total third-order lateral length and density and agreed with a comparable cumulative uptake of <sup>15</sup>N-ammonium (Figure 26). So far, these results indicate that a functional cytosolic C-terminus and functional ammonium transport by AMT1;3 are essential for ammonium-triggered lateral root growth.

**Table 4.** Reconstituted expression of *AMT1;3* restores third-order lateral development in *qko* also when primary roots are pruned. Total second- and third-order lateral root length and density on the ammonium-supplied side (HN, high N) and on the N-deficient side (LN, low N). Wildtype (Col-0), *qko* (*amt1;1*, *amt1;2*, *amt1;3*, *amt2;1*), *qko+11* (*amt1;2*, *amt1;3*, *amt2;1*) or *qko+13* plants (*amt1;1*, *amt1;2*, *amt2;1*, *amt1;3*, *amt2;1*; Yuan et al., 2007) were grown for 15 days on vertically-split agar plates with a localized supply of 0.8 mM ammonium. Values represent means ( $\pm$  SE) and different letters denote significant differences  $P < 0.05$  (Tukey's test); n = 15-20.

	HN plate side			LN plate side		
	Total lateral root length (cm.cm <sup>-1</sup> LR)	Lateral root density (number.cm <sup>-1</sup> LR)	Total lateral root density (number.cm <sup>-1</sup> LR)	Total lateral root length (cm.cm <sup>-1</sup> LR)	Lateral root density (number.cm <sup>-1</sup> LR)	Total lateral root density (number.cm <sup>-1</sup> LR)
<i>wt</i>	Second-order 2.06 $\pm$ 0.13n.s	Third-order 0.47 $\pm$ 0.03b	Second-order 5.02 $\pm$ 0.22a	Third-order 2.83 $\pm$ 0.36c	Second-order 1.84 $\pm$ 0.18n.s	Third-order 0.11 $\pm$ 0.05n.s
<i>qko</i> +AMT1;1	2.12 $\pm$ 0.12n.s	0.26 $\pm$ 0.02a	6.21 $\pm$ 0.49b	1.76 $\pm$ 0.16ab	1.51 $\pm$ 0.12n.s	0.09 $\pm$ 0.03n.s
<i>qko</i> +AMT1;3	1.84 $\pm$ 0.07n.s	0.44 $\pm$ 0.05b	5.33 $\pm$ 0.30ab	2.50 $\pm$ 0.19bc	1.43 $\pm$ 0.10n.s	0.05 $\pm$ 0.02n.s
<i>qko</i>	2.21 $\pm$ 0.34n.s	0.15 $\pm$ 0.02a	4.24 $\pm$ 0.38a	1.02 $\pm$ 0.11a	1.55 $\pm$ 0.24n.s	0.02 $\pm$ 0.01n.s
						2.81 $\pm$ 0.15n.s
						0.17 $\pm$ 0.02n.s

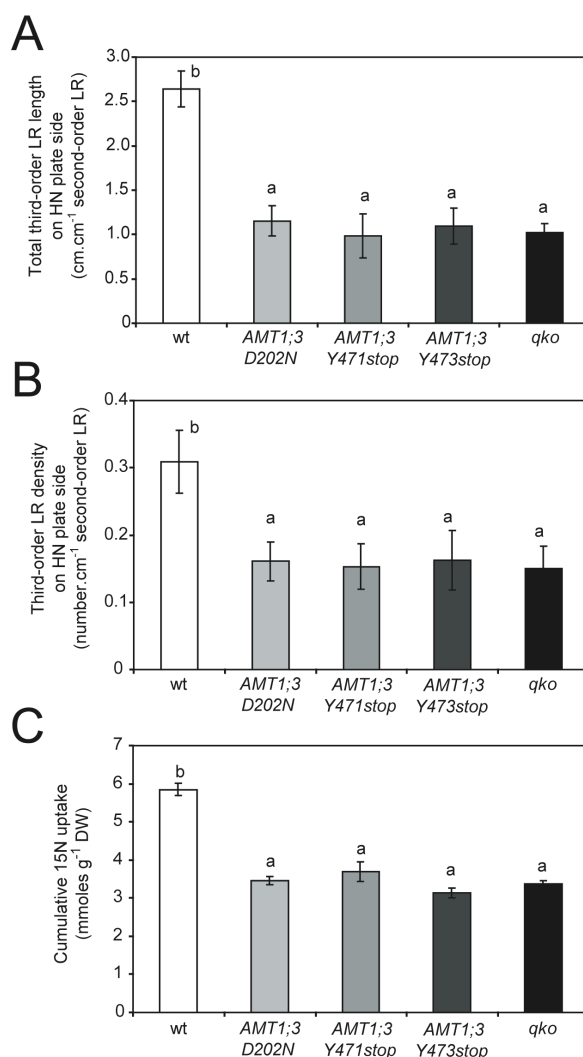


**Figure 26.** Reconstituted expression of *AMT1;3* but not of *AMT1;1* restores third-order lateral development in *qko*.

(A) Total third-order lateral root length, (B) average third-order lateral root length, (C) third-order lateral root density and (D) <sup>15</sup>N concentrations in whole plant (shoot+root) from <sup>15</sup>N-labeled ammonium supplied to the high N compartment. Wild-type, *qko* (*amt1;1*, *amt1;2*, *amt1;3*, *amt2;1*), *qko*+13 *D202N* plants (*amt1;1*, *amt1;2*, *amt2;1*; *AMT1;3 D202N*), *qko*+13 *Y471stop* (*amt1;1*, *amt1;2*, *amt2;1*; *AMT1;3 Y471stop*), *qko*+13 *Y473stop* (*amt1;1*, *amt1;2*, *amt2;1*; *AMT1;3 Y473stop*) and *qko* plants were grown for 15 days on vertically-split agar plates with a localized supply of 0.8 mM ammonium. Bars represent means ( $\pm$  SE) and different letters denote significant differences at  $P < 0.05$  (Tukey's test); with  $n = 8-10$  for root growth measurements and  $n=12-15$  for cumulative <sup>15</sup>N concentrations.

#### 4.3.6. Ammonium promotes lateral root initiation to local auxin signalling

The synthetic *DR5::GUS* reporter has been described as a suitable marker for auxin accumulation in early lateral root primordia, where an internal auxin pulse in pericycle cells triggers their conversion into founder cells (Dubrovsky et al., 2008; Péret et al., 2009). In agreement with previous studies using auxin reporters (Péret et

al, 2009) or mapping the auxin distribution at high-resolution in the root apex (Pettersson et al., 2009) *DR5::GUS* expression was localized first at the level of the pericycle and then in apical cells of the newly formed lateral root primordium. Interestingly, the activity of the auxin reporter was much stronger under local supply of ammonium than under nitrate in second- (Figure 27A and 27C) and third-order laterals at any stage before lateral root emergence (Figure 27B and 27D). According to the *DR5::GUS* reporter, ammonium represents a potent trigger for lateral root initiation through an auxin signal that primes pericycle founder cells or acting on lateral root initiation process (Casimiro et al., 2001, Dubrovsky et al., 2008, Péret et al, 2009). In order confirm this results, auxin concentration was measured in *Arabidopsis* wild-type and *qko* mutant grown in split-agar plates treated by ammonium or nitrate. The wild-type roots showed a comparable auxin concentration when grown either in ammonium or nitrate on HN plate side (Figure 27E). In contrast, the reminiscent root system grown on N-free plate side (LN) presented four-fold increasing auxin concentration when ammonium was supply to the HN compared to nitrate (Figure 27E). Hence, the root morphological changes observed on HN plate side treated by ammonium or nitrate is not caused by IAA abundance in the root, but might result from altered IAA distribution in root cells (tissues) that regulate lateral root development. Interestingly, in either plate side (HN and LN) the *qko* mutant roots have a similar auxin concentration to wild-type roots grown on local supply of nitrate. However, *qko* roots presented higher auxin concentration in the HN-ammonium treated plate side and resembles the wild-type auxin concentrations in the LN compartment (Figure 27E). All together, this results indicated that a local AMT-dependent transport or signalling is required to maintain a lower auxin-levels when ammonium, but not nitrate, is present. Taking into account the stronger activity of *DR5* promoter under local ammonium supply, it is possible to speculate that an AMT-mediated ammonium signalling likely affect auxin transport/signalling-components. In order to verify this hypothesis, the *DR5::GFP* reporter was introduced into *qko* mutant background. In the second-order lateral root tip, *qko* mutant displayed a higher *DR5* promoter activity when compared to wild-type *DR5::GFP* lines, which becomes more evident when an auxin transport-inhibitor 1-N-naphthylphthalamic acid (NPA) was added to the HN plate side (Figure 27F). In ammonium-induced third-order lateral roots of wildtype plants, the auxin reporter was expressed in the vascular system at the site of pre-emerged lateral roots and in the newly formed meristem of the lateral root primordium (Figure 27F). In the lateral root emerging-primordia of *qko*, however,

expression of the auxin reporter was weaker and the typical pattern of auxin distribution into the lateral root primordium was absent (Figure 27F). This data confirmed that auxin transport (or signalling) is disturbed in the *qko* mutant and that a local ammonium supply into the root most likely changed auxin distribution in an AMT-dependent signalling. Considering that NPA treatment is still able to cause IAA increases in the apical root meristem in *qko* developed lateral roots and that NPA blocks basipetal auxin transport (Casimiro et al., 2001) it can be speculated that the *qko* seems to be affected in auxin transport from the shoot, although, a detail investigation is needed.

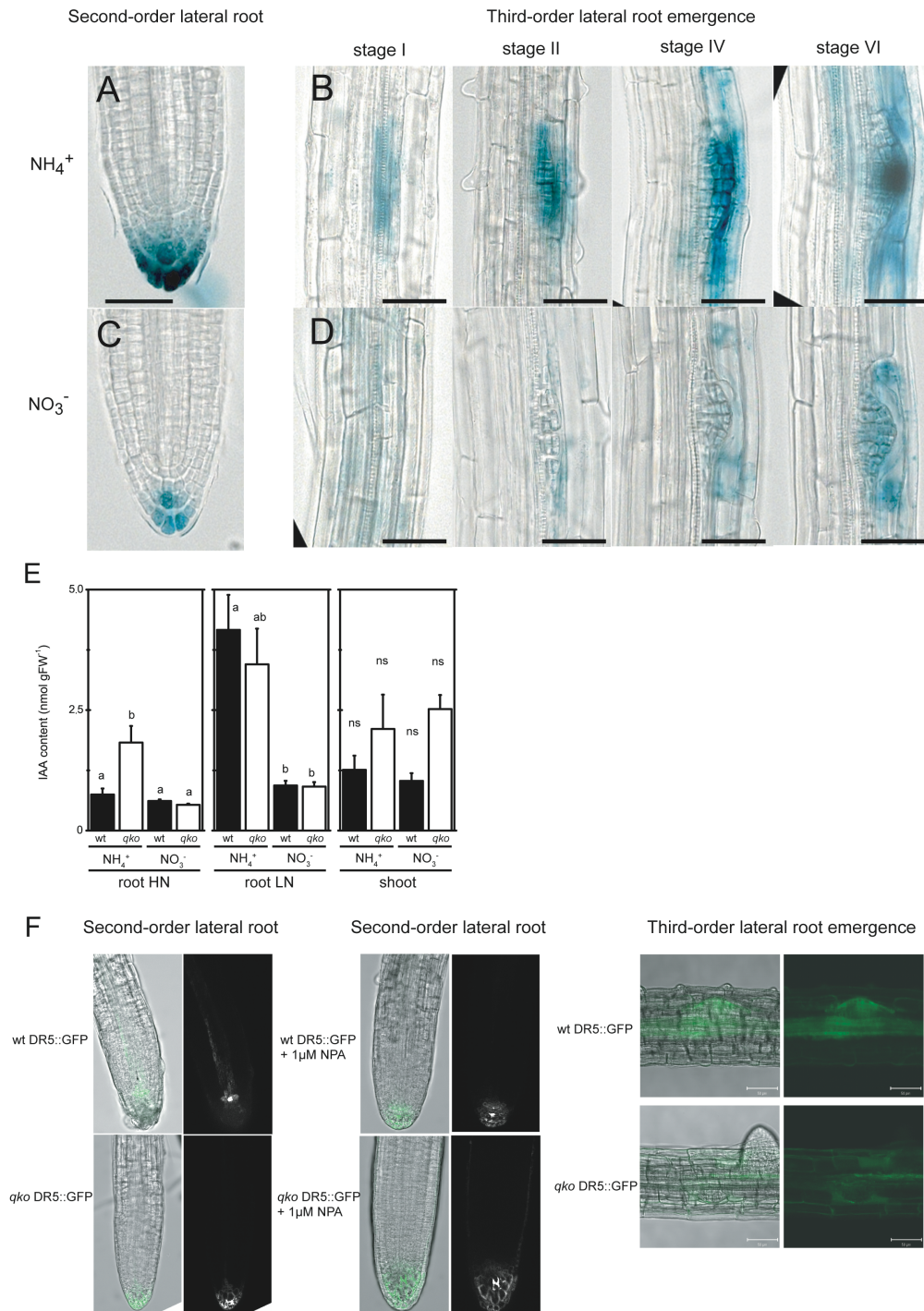


**Figure 27.** Auxin distribution is altered under localized ammonium supply.

The expression of the auxin reporter *DR5::GUS* in wild-type under ammonium-supplied second- (**A**) and third- (**B**) order lateral root or nitrate-supplied second- (**C**) and third- (**D**) order laterals after 12 days of exposition on HN plate side. Local auxin content (**E**) in roots on HN (ammonium or nitrate-treated roots), LN (without N supply) and shoot from wild-type and *qko* mutant. Bars represent means ( $\pm$  SE) and different letters denote significant differences at  $P < 0.05$  (Tukey's test);  $n = 3-4$ . Auxin reporter *DR5::GFP* in wild-type and *qko* background (**F**) under localized ammonium supply (0.8 mM N) or ammonium plus 1  $\mu\text{M}$  NPA (1-naphthylphthalamic acid) treated-roots. The pictures of second- and third-order lateral roots are representative in two different experiments ( $n=6-10$ ).

## 4.4. Discussion

### 4.4.1. A complementary role for ammonium and nitrate in lateral root development

The present study shows that not only nitrate but also ammonium is a locally sensed nitrogen form that regulates lateral root development. Under nitrogen-deficient growth conditions local ammonium supply enhanced lateral root formation in particular via a higher density of first- and higher-order lateral roots (Figures 11, 15 and table 3) and thereby provoked a highly branched phenotype in lateral root architecture (Figure 15B). This phenotype is in agreement with the bushy appearance of lateral roots of barley grown within a horizontal zone that was supplied locally with ammonium (Drew, 1975). Ammonium-triggered lateral root branching became more apparent on vertically-split than on horizontally-split agar plates (Figure 15D to 15F versus Figure 11I and 11J) and expressed in a much smaller increase in total or average lateral root length than nitrate (Figure 11C and 11D; Figure 12C and 12D), which might explain why the stimulating effect of ammonium has remained uncovered in previous studies (Zhang et al., 1999). Based on these and previous results (Zhang and Forde, 1998; Remans et al., 2006) it is proposed an opposite action of ammonium and nitrate on lateral root development. In contrast to nitrate, which mainly supports the elongation of lateral roots (Zhang et al., 1999; Remans et al., 2006), localized ammonium supply poorly stimulates lateral root elongation (Figures 11 and 15, Table 3). As is evident by a *CYCB1:GUS* reporter line, ammonium particularly increased the number of pre-emerged lateral root initials, thus primarily triggering the initiation rather than the emergence of lateral roots (Figure 14). This corroborates the recent finding that different nitrogen signals predominantly regulate lateral root establishment versus elongation (Gifford et al., 2008). With regard to the stimulation of lateral root initiation, the reduced nitrogen source glutamine could not substitute for ammonium (Figures 12, 13 and 14). Replacing part of the nitrate nutrition by ammonium strongly enhanced lateral root number and length not only beyond the level of nitrate- but also of ammonium-supplied plants (Table 3), emphasizing that ammonium and nitrate shape lateral root structure in a complementary manner. In ecological terms, this complementary regulation might reflect an adaptation of lateral root development to the different mobility of these

nitrogen forms in soils. While in most soils ammonium is highly adsorbed to negatively charged residues in the soil matrix (Miller et al., 2007), where a highly branched root system can efficiently cut diffusion distances of ammonium to the root surface, nitrate is highly mobile and may be better exploited with far-reaching lateral roots. Since ammonium is the substrate for nitrification and nitrate does not occur as an exclusive nitrogen source in soils (Miller et al., 2007), a minimum of lateral root branching is always assured even at low ammonium levels.

Several lines of evidence indicated that ammonium-triggered lateral root branching cannot be simply explained by a nutritional effect but is based on a sensing event: i) while glutamine itself poorly stimulated third-order lateral root branching, co-supply of glutamine and ammonium decreased ammonium-triggered lateral root branching, even though cumulative uptake of  $^{15}\text{N}$ -labeled ammonium was not significantly affected (Figure 13 and Figure 16); ii) millimolar ammonium supplies to the ammonium uptake-defective line *qko* could not restore wild-type levels of third-order lateral root formation (Figure 19), although cumulative ammonium uptake was sufficient to allow for third-order lateral root formation in wild-type; and iii) in transgenic lines with deregulated *AMT* gene expression third-order lateral root formation did not correlate with the cumulative uptake of  $^{15}\text{N}$ -labeled ammonium (Figures 20 and 21). Thus, ammonium appears to act as an external morphological trigger that is locally sensed by plant roots. In vertically-split agar plates, ammonium addition to the main root system (LN root fraction) suppressed third-order lateral root formation on the HN side (Figure 15E and 15F) and caused a higher N nutritional status in the LN root fraction and the shoot (Figure 15H and 15I), indicating that ammonium-mediated lateral root formation was subject to systemic repression. Likewise, glutamine supply to the main root system effectively repressed ammonium-dependent lateral root branching (Figure 17). In agreement with the study by Gifford et al. (2008) showing that glutamine/glutamate is a dominant signal repressing nitrate-responsive lateral root emergence, it is proposed that glutamine might also act as a metabolic repressor for the systemic down-regulation of ammonium-triggered lateral root initiation.

#### 4.4.2. The possible function of AMT1;3 in ammonium-triggered lateral root development

An almost complete loss of higher-order lateral root branching in *qko* (Figure 18) and the failure to restore lateral root formation by millimolar supplies of external ammonium (Figure 19) indicated that one or several of the four defective AMT transporters in Arabidopsis roots should be involved in ammonium sensing. Therefore, it was monitored third-order lateral root formation in single *amt* insertion lines and found only the *amt1;3-1* mutant had a significant decrease in lateral root density (Figure 20). This decrease was fully reversed by expression of *AMT1;3* in the *amt1;3-1* background without significantly affecting the cumulative uptake of  $^{15}\text{N}$ -labeled ammonium (Figure 21), indicating that the amount of ammonium-N accumulating via AMT1;3 in roots is not of primary relevance for the recovery of third-order lateral root formation. However, in absolute numbers the third-order lateral root density in *amt1;3-1* was not as low as in *qko* (Figure 18 and 20) suggesting that their different genetic background might account for this difference or that other AMTs might also contribute to ammonium-stimulated lateral root branching. To rule out possible effects of the different genetic background in *amt1;3-1* and *qko*, *qko* lines with reconstituted expression of *AMT1;1* or *AMT1;3* were directly compared against *qko*. Although reconstituted expression of either AMT1 yielded the same cumulative uptake of ammonium- $^{15}\text{N}$  as wild-type plants (Figure 22D), which met the observation that both reconstituted lines achieved the same short-term uptake capacity or biomass when grown on ammonium as a sole nitrogen source (Yuan et al., 2007), only *qko+13* lines but not *qko+11* lines developed third-order lateral roots with the same length and density as wild-type plants (Figure 22A and 22C; Table 4). It was therefore highly unlikely that quantitative differences in the ammonium transport capacity or in the N nutritional status of AMT1;1- or AMT1;3-reconstituted lines accounted for the stimulated lateral root branching in the presence of AMT1;3. Since average third-order lateral root length remained unchanged (Figure 22B), AMT1;3 did not promote the elongation of third-order laterals. Furthermore, differences in cell type-specific expression are not expected to account for a functional role of AMT1;3 in lateral root development as the promoter activity of both *AMT1;1* and *AMT1;3* is mainly localized in the root tips as well as in rhizodermal and cortical cells of N-deficient roots, while only *AMT1;1* shows additional expression in the stele (Loqué et al., 2006). This agreed with the observation that 35S-driven expression of *AMT1;3* in

*amt1;3-1* also conferred lateral root branching (Figure 21). Comparing mRNA levels of *AMT1;1* and *AMT1;3* in roots yielded neither for ammonium-supplied nor for N-deficient root fractions higher *AMT1;3* transcript levels than *AMT1;1* (Figure 23A and 23B). In fact, ammonium-supplemented roots even showed a transient increase only of *AMT1;1* mRNA levels, which suggests a more sensitive responsiveness of *AMT1;1* to the local availability of ammonium and is supported by previous observations of a local ammonium induction of *AMT1;1* in split-root hydroponics (Gansel et al., 2001). Taken together, all these observations pointed to a sensing function of the *AMT1;3* protein for higher-order lateral root branching that could not be fulfilled by *AMT1;1*.

Considering the inability of *nrt1;1* mutant plants to proliferate lateral root growth into nitrate-rich patches and the functional involvement of *NRT1;1* in ANR1-dependent nitrate signaling, the dual-affinity nitrate transporter *NRT1;1/CHL1* has been characterized as a nitrate sensor or as a facilitator of nitrate influx into nitrate-sensing cells (Remans et al., 2006). More recently, a nitrate sensing function of *NRT1;1* was corroborated, as substrate-induced gene expression of the high-affinity nitrate transporter *NRT2;1* was also found to depend on *NRT1;1* (Ho et al., 2009). In this case, manipulating a phosphorylation switch allowed uncoupling nitrate transport from sensing. Therefore, it was investigated whether in *AMT1;3* ammonium transport can be uncoupled from lateral root branching using a nonfunctional version of *AMT1;3* that lost ammonium transport activity due to a T471D substitution mimicking phosphorylation in the C-terminus (Figure 24A). The T471D version of *AMT1;3* did not confer third-order lateral root development, while a T471A substitution did (Figure 24B and 24C). Thus, C-terminal inactivation of ammonium transport remained coupled with the function of *AMT1;3* in stimulating lateral root branching. A tight coupling of the dual function in substrate transport and sensing has also been found for the ammonium transporter *Mep2* in yeast, where the analysis of transport-proficient/signaling-defective versus transport-defective/signaling-defective alleles indicated that transport is necessary but not sufficient to sense ammonium (Rutherford et al., 2008) thereby supporting the tight coupling between transport and sensor functions in *Mep2* (Boeckstaens et al., 2007). Since *AMT1;1* could not take over a similar function despite its comparable biochemical properties and even higher expression in the root tissue (Figure 22 and 23), it is unlikely that *AMT1;3* just acts as a facilitator for ammonium influx into ammonium-sensing root cells. In addition, the targeted mutation in the conducting pore of *AMT1;3* protein showed that ammonium is needed to be transported through the core of the channel and an active C-terminus

is insufficient to signalize for ammonium-triggered root morphology. The truncated version of AMT1;3 in the cytosolic C-terminal displayed distinguished transporter functions in yeast and in plants. While AMT1;3 Y473stop was able to transport ammonium in yeast, the same mutation yielded in an inactive protein for ammonium transport and third-order lateral root formation under ammonium supply in plants (Figure 25 and Figure 26). Thus, it is likely that when ammonium is transported through the pore, conformational changes occur in the protein which might trigger a signaling event dependent on AMT1;3 C-terminal. This assumption is in agreement with the recent observation that only external ammonium conferred C-terminal phosphorylation of AMT1;1, a process that could not be mimicked by an accumulation of ammonium inside the root (Lanquar et al., 2009). In analogy with the model proposed for AMT1;1, AMT1;3 might act as a transceptor, coupling a morphological signaling function with the physical process of ammonium transport as has been proposed for Mep2 in yeast (Lorenz and Heitman, 1998; Boeckstaens et al., 2007; Rutherford et al., 2008). In the case of nitrate-induced lateral root formation, two microRNA-dependent regulatory modules have been identified. While the miRNA167/*ARF8* module regulates the ratio between initiating and emerging lateral roots by inserting nitrogen responses at the level of auxin signaling (Gifford et al., 2008), the miRNA393/*AFB3* regulatory module confers nitrate regulation of an auxin receptor to regulate primary and lateral root growth by modifying auxin perception in roots cultured under high nitrate supplies (Vidal et al., 2010). The study presented here indicates the complementary action of ammonium and nitrate in lateral root development, and raises the question whether the sensing machinery for ammonium employs similar regulatory modules as those suggested for nitrate sensing. Furthermore, an AMT-dependent signaling might be required to a proper auxin distribution in the roots when ammonium is present (Figure 27), which suggests a transceptor mechanism is involved in ammonium-triggered root morphology.

## 5. General discussion

### 5.1. Environmental factors and responses in the root system

As nutrient availability becomes scarce, e.g. under an uneven nutrient distribution in the rooting zone or changes in soil chemistry, aeration, density, microbial activity, or the distribution of water, an adaptation of the root architecture becomes highly important for a plant's survival (Robinson, 1994). Changes in the root architecture may become apparent under particularly challenging growth conditions, such as low nutrient availability (Narang et al., 2000), but also in the case of drought stress in rice or maize, a deep and highly branched root system has been found to correlate with drought tolerance (Toorchi et al., 2002; Trachsel et al., 2009). Thus, a rapidly responding and well adapted root system represents a morphological trait that can confer an important advantage for a plant. The importance of a high morphological plasticity of the root system has been indicated in a competition experiment with different grass species, whereby one species adapted its root morphology to nitrate-enriched soil patches and efficiently acquired N, while other species grew poorly without showing a similar morphological response (Hodge et al., 2000; Robinson, 2001). Furthermore, P-efficient bean varieties, which were able to allocate the main root deeply into the soil and retain shallow roots under P-limited conditions had an elevated P efficiency (Nielsen et al., 2001). Therefore, root plasticity represents a highly important morphological mechanism for plants to adapt to environmental fluctuations.

The amount, form and type of nutrient supply are major factors that influence root plasticity. The classical work from Drew (1975) has shown that in particular lateral root growth is strongly modulated upon localized nutrient supply, leading to an intense lateral root proliferation under localized nitrate and phosphate but not under localized potassium supply in barley. On the other hand, localized ammonium supply promoted the formation of a short and dense lateral root system. More recently, *Arabidopsis* roots have been shown to respond differently to localized nitrate and phosphate supply. While nitrate had no effect on primary root growth, elevated local phosphate supplies inhibited primary root elongation (Linkohr et al., 2002). In addition, lateral root density remained constant across a broad range of phosphate concentrations, whereas an increased lateral root density was observed under nitrate

(Linkohr et al., 2002). These two studies indicated that i) the root system architecture is altered according to the type of nutrient being restricted in availability, and ii) changes in the root architecture might display at different levels of the root system, the primary root or the lateral roots, and thereby interfere with lateral root development at different developmental stages; these are lateral root initiation, emergence or elongation (Malamy, 2005). Against this background, the present thesis aimed at comparing changes in the root system architecture between localized nitrate and ammonium supply and at investigating whether localized Fe supply provokes comparable changes.

### *Primary root growth*

The primary root growth is subjected to nutrient variation in soil. Under high ammonium concentrations the primary root length is steeply affected (Cao et al., 1993; Figure 12). In chapter 4, when *Arabidopsis* seedlings were transferred to separated agar plates (SAP, Zhang et al., 1999) containing high concentrations of local ammonium supply (> 5 mM), the primary root length was inhibited, however, high nitrate concentrations did not affect primary root growth (Figure 12M and 12N). The ammonium root growth-inhibition cannot be alleviated by nitrate, but increasing potassium ( $K^+$ ) concentrations or mutations related to auxin transport (*aux1*) can rescue the primary root growth (Cao et al., 1993). Increased external potassium concentrations were shown to alleviate ammonium toxicity in plants probably due to its interference on ammonium uptake under low-affinity range (Spalding et al., 1999; Szczerba et al., 2008). Although it remains unclear, the AKT1 channel, an inward-rectifying  $K^+$  channel, is a strong candidate to be involved in low-affinity ammonium uptake (Spalding et al., 1999). Most importantly, ammonium inhibits primary root growth of *akt1* mutant seedlings by inhibiting  $K^+$  permeability, which suggest that the ammonium primary root growth-inhibition is independent of *AKT1* channel (Spalding et al., 1999).

Although under SAP growth conditions presented here and previously described in Walch-Liu and Forde (2008) could not show a nitrate effect on primary root growth, in a recent report, an increased availability of nitrate in the hydroponic growth-conditions has been shown to affect the primary root length (Vidal et al., 2010). When wild-type *Arabidopsis* roots were subjected to high concentrations of

nitrate (> 5 mM), the primary root presented a growth inhibition when compared to KCl-treated plants (Vidal et al., 2010). The underlying mechanism for nitrate-triggered primary growth inhibition was shown to be dependent on the mirRNA393, which was induced only in root tissues after 2 h of nitrate treatment (Vidal et al., 2010). According to previous publications, the mirRNA393 targets the transcripts for the auxin receptors (TIR1, ABF1, AFB2 and AFB3) and the basic-loop-helix transcript factor (bHLH77), however, only AFB3 transcripts are induced to nitrate treatment. This pattern of expression was comparable to the nitrate-reductase (NR) double mutant in *Arabidopsis*, suggesting that this mechanism is controlled by nitrate and not other reduced N forms (Vidal et al., 2010). Moreover, the fact that the overexpression of microRNA393 or *afb3-1* mutant lines displayed insensitive to the nitrate-inhibition of primary root elongation and the AFB3 is localized in the primary root tip, demonstrates that the auxin receptor AFB3 is involved in the nitrate-signaling controlling primary root growth (Vidal et al., 2010).

Apart from the two major inorganic N forms, the organic N form L-glutamate has an impact on primary root growth. *Arabidopsis* primary root is inhibited in the presence of low concentrations of L-glutamate (0.05-0.5 mM). Other amino acids such as glutamine (Gln), acid aspartate, gamma-aminobutyric acid and D-glutamate had no effect on primary root growth (Walch-Liu et al., 2006). This response was shown to be independent from N metabolism since the simultaneous supply of increased glutamine concentrations had no effect on inhibition of primary root growth by L-glutamate. Furthermore, when the remaining root system was exposed to 0.05 mM of L-glutamate (Glu) but the primary root tip was in contact with glutamate-free medium in splitted agar plates, the primary root growth was not affected (Walch-Liu et al., 2006). Therefore, L-glutamate is likely to be sensed specifically in the primary root tip (Walch-Liu et al., 2006). Interestingly, the presence of the inorganic N form nitrate seems to antagonizes the Glu inhibition effect on primary root (Walch-Liu and Forde, 2008). According to <sup>15</sup>N-Glu measurements on plates, nitrate has no effect on Glu uptake in the root tip but the additional of Gln impaired the Glu uptake (Walch-Liu and Forde, 2008). Since nitrate alleviates the primary root growth inhibition in the presence of Glu however Gln does not, it is likely that nitrate interacts with Glu-signaling rather than to affect its uptake (Walch-Liu and Forde, 2008). In agreement with that, the *nrt1;1 (chl1-5)* mutant is insensitive to nitrate rescue of primary root growth under Glu supply (Walch-Liu and Forde, 2008). Moreover, a nitrate-sensing

mechanism through NRT1;1 C-terminus was shown to be required for antagonizing the Glu signaling on primary root growth inhibition although the precise mechanism remains unclear.

In addition to N forms, Fe toxicity causes inhibition of primary root growth (Figure 1I and Ward et al., 2008). However, this root growth phenotype is caused by a lower phosphate (P) availability in the meristem zone, which leads to a meristem exhaustion (Sanchez-Calderon et al., 2005; Ward et al., 2008). Notable, the primary root growth-inhibition was only observed when Fe was supplied homogeneously but not localized under SAP plates conditions presented here (Figure 1I). Thus, Fe-toxicity causes a P-limitation in the primary root tip which turns to a lower meristem activity (Ward et al., 2008). Recently, it has been shown that the P5-type ATPase (*PDR2*) is required for maintenance of stem-cells in the meristem during Pi-limiting conditions by controlling post-transcriptionally the nuclear SCR (*SCARECROWN*) protein (Ticconi et al., 2009). The *PDR2* co-localizes with *LPR1* (*LOW PHOSPHATE ROOT1*), a multicopper oxidase gene, in the ER adjusting the meristem activity to external concentrations of P (Svistoonoff et al, 2007; Ticconi et al., 2009). The *pdr2* mutant displayed short primary root growth independently of Fe concentrations supplied (Ticconi et al., 2009). However, a chelation of an excess of Fe under P-limited medium could rescue the *pdr2* mutant phenotype which indicates that *PDR2* and *LPR1* are under regulation of P-signaling and Fe-homeostases to control the meristem activity (Ticconi et al., 2009).

### *Lateral root initiation*

Although earlier investigations could not find any lateral root response of Arabidopsis to localized ammonium supply (Zhang et al. 1999), the present investigation demonstrated that localized ammonium supply has indeed a pronounced effect on lateral root development, in particular on lateral root initiation. When 15 mm of the primary root axis were exposed to ammonium supply, the number and density of lateral roots was strongly stimulated, even to a larger extent than under localized nitrate (Figure 11I and 11J). Employing vertically-split agar plates showed that local ammonium supply also increased second- and third-order lateral root formation, whereas third-order lateral root formation was almost absent in nitrate-grown plants. Thus, the stimulatory effect of ammonium displayed at all orders

of lateral roots, indicating that ammonium generally stimulates higher-order lateral root branching (Figure 14). Notably, this ammonium effect was also apparent when plants were additionally supplied with nitrate (Table 3), showing that the ammonium-induced stimulation of lateral root branching was not dominated or even overruled by the signaling action of nitrate.

In the context of root development, an increase in lateral root density results from an enhanced initiation of lateral roots. Lateral root initiation takes place in root pericycle cells and is a process dependent on auxin signaling (Fukaki et al., 2002; Dubrovsky et al., 2008). This could be supported here by using the DR5-based auxin reporter which indicated elevated auxin levels or enhanced auxin sensitivity in second- and third-order lateral root tips that were locally treated with ammonium (Figure 27A and 27D). In this case, ammonium-triggered auxin signaling was most likely only a locally defined effect, because the auxin measurement in wild-type roots showed that ammonium did not increase auxin concentrations in the whole root system (Figure 27E). This suggested that, relative to nitrate, auxin biosynthesis is not generally enhanced in roots under local ammonium supply. On the other hand, local ammonium supply in roots of *qko* DR5::GFP reporter lines showed a greater auxin accumulation in second-order lateral roots but not in third-order laterals indicating a perturbed auxin distribution along the root (Figure 27F). In line with that, higher auxin concentrations were measured in *qko* roots grown under local ammonium supply, relative to nitrate (Figure 27E). These observations indicated that an AMT-dependent signaling process is required for a proper auxin distribution in ammonium-treated roots. The auxin distribution during lateral root initiation depends on a coordinated expression of AUX1, PIN and PGP proteins regulating the auxin flows to form a polar gradient required for the initiation of lateral roots (Titapiwatanakun and Murphy, 2009). It would now be interesting to further investigate the expression and localization of auxin-related transporters in *qko* and re-complemented *qko* lines to find out whether these auxin transporters are regulated in an AMT-dependent manner.

Among the four root-expressed AMTs tested in the present work, AMT1;3 turned out as the most promising candidate to be involved in ammonium-triggered auxin signaling (Figures 20, 21 and 22). A functional AMT1;3 was required to trigger ammonium-dependent lateral branching, since a pore mutation or C-terminal mutations in the AMT1;3 protein led to loss of functionality and, at the same time, did

not restore third-order lateral root formation. This indicates that conformational changes in the AMT1;3 protein and a functional C terminus are required to stimulate lateral root initiation (Figure 26). Whether AMT1;3 directly affects auxin signaling might be verified in transgenic lines expressing a DR5 auxin reporter in *qko+1;3* and subsequent incubation on separated agar plates with localized ammonium supply.

Plants under sulphate deficiency also show an increased number of lateral roots (Kutz et al., 2002). Although it is not yet clear whether sulfate deficiency stimulates lateral root initiation or emergence, the S deficiency-specific activation of *NIT3* (*NITRILASE3*) promoter activity suggested a direct role of auxin, since the *NIT3* gene product is directly involved in one of the auxin biosynthetic pathways (Kutz et al., 2002). In agreement with this, S-starved roots increased the conversion of indole-3-acetonitrile to indole-3-acetic acid (IAA) upon induction of *NIT3*. Considering the high IAA biosynthesis occurring in the root apex (Pettersson et al., 2009) as well the localization of *NIT3* expression in the root tip (Kutz et al., 2002), it is most likely that the increased auxin level in the primary root tip favors lateral root initiation under S-deprivation. In this regard, S deficiency most likely activate the initiation rather than the emergence of lateral roots. On the other hand, transcriptome analysis of S-depleted Arabidopsis root revealed an upregulation of the auxin-responsive IAA18 gene (Nikiforova et al., 2003). Another recent report described that IAA18 negatively regulates lateral root formation by modulating ARF7 and ARF19 activities (Uehara et al., 2008). Since ARF7 and ARF19 also participate in lateral root emergence by activation of LAX3 (Swarup et al., 2008), it is currently difficult to differentiate more precisely which auxin signaling pathway is activated under S deficiency.

Potassium (K)-starved plants displayed an arrested lateral root initiation. This root morphology was shown to be dependent on MYB77 transcription factor (TF) that interacts through the C-terminus with ARF7 controlling the lateral initiation response upon K<sup>+</sup> limitation (Shin et al., 2007). The ARF7 is a positive regulator of auxin-signaling during lateral root initiation (Fukaki et al., 2007). However, the interaction of MYB77 and ARF7 negatively modulates the lateral initiation under K<sup>+</sup> limitation (Shin et al., 2007).

Plants under Pi-deficiency present a growth inhibition in the primary root and an increase in density and length of the laterals (López-Bucio et al., 2003). The increase of lateral root formation is caused by a high auxin-sensitivity of pericycle founder cells (Perez-Torres et al., 2008). Indeed, roots grown on low-Pi availability

have a great sensitivity to exogenous auxin application which was supported by an enhanced expression of TIR1 auxin-receptor in the primary root tip and pericycle founder cells (Perez-Torres et al., 2008). The fact that, P-deficiency seedlings decreased meristem activity, thus, causing an inhibition of primary root growth could trigger the lateral initiation process was nicely tested by the authors. The mutant insensitive to the Pi-dependent primary root morphology (*lp3*) was analyzed for lateral initiation under P-deprivation. The mutant *lp3* showed a comparable increase in lateral root initiation to wild-type plants indicating that the arrested primary root growth under P-deficiency is independent of the lateral root initiation (Perez-Torres et al., 2008).

The carbon status of the root also appears to determine the extent of lateral root initiation. Using nitrate as a nitrogen source, it has been demonstrated that high C:N ratios completely inhibit lateral root initiation (Little et al., 2005). Under these conditions, *Arabidopsis* mutants were screened, and the isolated mutant *lin1* (*lateral root inhibited1*) was shown to produce lateral roots even under high sucrose:nitrogen ratios, although these were repressive in wild-type plants (Little et al., 2005). The *lin1* mutant turned out to carry a point mutation in the coding sequence of *NRT2;1* which encodes a high-affinity nitrate transporter (Little et al., 2005). Notably, even the reduced nitrate uptake of *lin1* could not explain the de-repressed lateral root initiation under high C:N ratios. This observation led the authors to conclude that *NRT2;1* behaves as a nitrate sensor. In a subsequent detailed investigation that took nitrate uptake into account, the *nrt2;1* mutant showed a reduced number of lateral root initials compared to the wild-type after transfer from high to low nitrate concentrations, which at least partially contradicted the previous report (Remans et al., 2006a). The authors argued that the high sucrose supply could have caused this contradiction and/or nitrate might have affected other stages of lateral root development (Remans et al., 2006a). Even though, the role of *NRT2;1* nitrate transporter on lateral root primordia could be confirmed (Remans et al., 2006a).

Nitrate is also able to stimulate lateral initiation/emergence in auxin-dependent signaling pathway. Roots exposed to high nitrate concentrations (> 5 mM) have an enhanced *AFB3* expression in the pericycle cells which leads to an increased lateral density (Vidal et al., 2010). The *AFB3* auxin receptor is part of SCR<sup>TIR1/AFB3</sup> ubiquitin ligase protein complex involved in Aux/IAA degradation pathway (Dharmasiri et al., 2005a and 2005b). Thus, *AFB3* has a dual function controlling nitrate-dependent root

morphology, whereby AFB3/miR393 regulatory mechanism is active during primary root growth and lateral root initiation under high nitrate availability (Vidal et al., 2010).

### *Lateral root emergence*

Effects of local nutrient supply on lateral root emergence have been insufficiently reported. Most of the previous reports described the formation of lateral roots from a developmental and genetically-determined perspective, without focussing on post-initiation phenomena (Péret et al., 2009a). The data presented in chapter 4 showed that a local Fe supply to Arabidopsis roots stimulates in particular the emergence of lateral roots. This result was brought about by assessing *CYCB1* marker lines which allowed to trace lateral root initials during their early stages of development (Malamy and Benfey, 1997). When the primary root was subjected to a wide range of Fe concentrations supplied either homogeneously or heterogeneously, lateral root number did not differ (Figure 1F). However, as soon as the primary root tip touched the Fe-deficient bottom plate segment, the number of emerging laterals increased significantly only in the middle plate segment where Fe was supplied (Figure 3B). This observation suggested the existence of an Fe sensing mechanism in the primary root tip, where Fe deficiency may release a signal to quickly develop those lateral roots that had already been initiated. This phenomenon is likely to be under control of ethylene-auxin interactions. According to a previous report, the treatment of Arabidopsis roots with the ethylene precursor 1-aminocyclopropane-1-carboxylic acid (ACC) causes an inhibition of lateral initiation, although it promotes the emergence of laterals (Ivanchenko et al., 2008). It is known that ethylene can stimulate auxin biosynthesis via *WEI2* and *WEI7* (*WEAK ETHYLENE INSENSITIVE*) genes that are involved in Trp-dependent auxin biosynthesis (Stepanova et al., 2005). A double mutant in these genes displayed lower sensitivity to a high application of ACC, thus the ethylene effect on lateral root formation required the action of auxin through the *WEI2* and *WEI7* proteins (Ivanchenko et al., 2008). Considering that Fe deficiency triggers the biosynthesis of ethylene in roots, which induces Fe deficiency-responsive genes (Romera and Alcantara, 1994), an ethylene-dependent auxin signaling might be required for lateral root emergence under localized Fe supply. This regulatory pathway certainly deserves further attention to unravel critical components in Fe-dependent changes of the root system architecture.

Another example of a nutrient affecting lateral root emergence comes from the N-repressive signaling pathway. Recently, the microRNA167a/b was found to be antagonistically regulated with *ARF8* (*AUXIN RESPONSE FACTOR8*) during lateral root emergence (Gifford et al., 2008). *ARF8* was shown to be subjected to a dual regulation. While nitrate application stimulated its expression, increasing concentrations of glutamine, as derived from nitrate reduction and assimilation, downregulated the expression of *ARF8* in pericycle cells and in the lateral root cap (Gifford et al., 2008). This case indicates that N signaling via organic N-compounds might be dominant over nitrate signaling in order to repress nitrate-responsive lateral root emergence (Gifford et al., 2008).

### *Lateral root elongation*

The most evident effect of a nutrient stimulating lateral root elongation was reported by local application of nitrate in barley roots (Drew, 1975). In addition, when *Arabidopsis* roots were grown under localized nitrate supply, emerged lateral roots elongated in a concentration-dependent manner (Zhang and Forde, 1998; Zhang et al., 1999). Most notably, the nitrate-reductase double mutant (*nia1 nia2*) showed a similar stimulatory-root response to wild-type plants which suggests that nitrate is the trigger for changing root morphology (Zhang and Forde, 1998). To date, it has not been clarified by which action nitrate promotes lateral root elongation. A simple possibility that had been discussed earlier was that nitrate uptake may increase vacuolar loading and thereby simply increase the turgor of root cells. However, Remans et al. (2006b) have shown that there is no correlation between uptake rates of <sup>15</sup>N-labeled nitrate and lateral root elongation. Since the *nrt1;1* mutant showed a reduced lateral root length compared to the wild-type after transfer to localized nitrate supply in splitted agar plates despite the comparable short-term <sup>15</sup>N-nitrate uptake in their roots, a sensing mechanism was proposed involving the NRT1;1 transporter (Remans et al., 2006b). Moreover, under the same conditions, the nitrate-inducible transcript factor *ANR1* was found to be downstream to the signaling pathway (Zhang and Forde, 1998). Transgenic lines lacking the expression of *ANR1* gene showed insensitive to the nitrate-stimulatory effect on lateral root length (Remans et al., 2006b; Zhang and Forde, 1998). Further, the involvement of auxin-signaling in the nitrate-dependent root morphology was brought by the phenotype of *axr4* auxin-

resistant, which was unable to elongate lateral roots under localized nitrate applications (Zhang et al., 1999). The *AXR4* gene codes for a  $\alpha/\beta$  hydrolase superfamily protein localized in the endoplasmic reticulum (ER) that regulates the polar localization of AUX1 transporter to the plasma membrane (Dharmasiri et al., 2006). Interestingly, the *axr4* disrupted the AUX1 trafficking in the epidermal cells but not in the lateral root cap (Dharmasiri et al., 2006). Considering that, differently from *axr4* mutant, the *aux1* mutant is still able to trigger nitrate-dependent root morphology, it can be speculated that a proper auxin distribution in the lateral root cap is essential for the nitrate-stimulatory effect on lateral root elongation. Consistent with this, the NRT1;1 and ANR1 co-localized in the lateral root tip (Remans et al., 2006b).

The lateral root length is also stimulated by Fe-dependent signaling (chapter 3). When *Arabidopsis* roots were subjected to homogenous or localized supply of 25  $\mu\text{M}$  Fe(III)-EDTA, lateral root length in wild-type plants was twofold higher under localized than under homogenous Fe supply (Figure 1E). Moreover, lateral root elongation was not only highly responsive to the mode of Fe supply but also to the supplied Fe concentration (Figure 1E). This was best observed by the strong decrease of lateral root length after supplies of higher Fe concentrations (Figure 1E). In contrast, lateral root number was stimulated by increasing Fe supply, but showed neither a repression under more elevated Fe supplies nor a consistent dependence on the mode of Fe supply (Figure 1F). Thus, only lateral root elongation but not initiation was finely tuned by localized Fe supply. Lateral root elongation in the *irt1* mutant required much higher Fe concentrations in the Fe-enriched agar patch to take place and never reached the same level as that in wild-type plants (Figure 6B). However, lateral root initiation responded in a less sensitive manner, because the number of lateral initials in *irt1* mounted up to similar levels as in wild-type plants when higher Fe concentrations were supplied (Figure 6A). Taken together, lateral root elongation clearly represented the more Fe-sensitive developmental process to be regulated by local Fe supplies in a concentration-dependent manner. The identification of the molecular target for the Fe-stimulatory effect on lateral root growth remains to be investigated.

Preliminary experiments conducted within the frame of this thesis with *DR5::GUS* reporter lines grown under localized supply of Fe(III)-EDTA indicated a strong increase of auxin accumulation in the primary root tip only after it touched the

Fe-deficient bottom segment but not when Fe was supplied homogeneously (data not shown). The pattern of auxin accumulation resembled those roots treated by ACC, which display DR5 expression in the meristematic region and in the elongation zone (Růzicka et al., 2007). Ethylene often up-regulates auxin biosynthesis and basipetal auxin transport to the elongation zone that may affect root growth (Růzicka et al., 2007). Whether ethylene-auxin interactions affect Fe-stimulated lateral root growth is still unknown. This question might be addressed experimentally by growing under different mode of Fe-supply mutants defective in polar auxin transporters, such as AUX1, PIN1 and PIN4, which are involved in ethylene-dependent changes of root morphology (Růzicka et al., 2007).

In summary, the availability of nutrients described above has an effect on post-embryonic root developmental processes. The results presented in this work (chapters 3 and 4) and others have shown the existence of nutrient-specific signal transduction pathways that sense and interpret external and internal nutrient concentrations to modulate root development. The nutrient-hormone plant signaling network that tightly controls responses of root morphology upon nutrient availability has begun to be elucidated. The future challenge will be to better understand how plants coordinate these pathways during growth in the field.

## **5.2. Systemic versus local nutrient signaling-responses controlling root morphology**

The findings that a specific nutrient affects different pathways for root development in a concentration-dependent manner demonstrate that nutrient availability in plant tissues can regulate signals responsible for changes in root system architecture (Robinson, 1994). To integrate these adaptive responses, systemic or long-distance signals are needed to rely on informations about the shoot and root nutrient conditions. In the case of systemic signals, the nutrient-signal is perceived in the shoot and subsequently converted in a signal that is mobile, through the vascular system, to the root (Liu et al., 2009). By this means, normally, the concentration of a specific nutrient or a nutrient-derived metabolite triggers a signal that coordinates root system architecture (Liu et al., 2009).

A shoot-borne long-distance signal(s) has been proposed to control an inhibition of lateral root formation in Arabidopsis roots that were exposed to high

nitrate concentrations or to high sucrose concentrations (Figure 11C; Zhang et al., 1999; Little et al., 2005). Nitrate-mediated inhibition was enhanced in a nitrate reductase mutant suggesting that the nitrate ion itself rather than downstream N metabolites regulates lateral root formation (Zhang et al., 1999). A systemic and probably, a phloem-mobile signal released by high nitrate concentrations in the shoot was postulated (Zhang et al., 1999), although the molecular identity of the signal(s) regulating root system architecture in response to (shoot) nitrate remain to be uncovered. The plant hormone abscissic acid (ABA) is a promising candidate, since exogenous ABA supply mimicked the inhibitory effect of elevated nitrate supplies on lateral root formation (Signora et al., 2001). Moreover, ABA-insensitive mutants displayed a lower although not totally abolished lateral root inhibition by nitrate, indicating that ABA-independent and ABA-dependent pathways exist for nitrate-mediated inhibition of lateral root formation (Signora et al., 2001; De Smet et al., 2003; Zhang et al., 2007). Furthermore, a genetic evidence has been obtained that inhibition by nitrate and ABA share the same signaling pathway, wherein mutants able to produce lateral roots in the presence of ABA displayed less sensitivity to high nitrate-induced inhibition of laterals (Zhang et al., 2007). The characterization of these *labi* (*lateral root ABA-insensitive*) genes will certainly provide a better understanding of lateral root inhibition in dependence of high nitrate supply (Zhang et al., 2007). The ABA-independent pathway for the nitrate-mediated inhibition of lateral formation might involve auxin. When Arabidopsis roots pre-cultured under high nitrate were transferred to a medium containing 1 mM  $\text{NO}_3^-$ , lateral root elongation remained arrested, but at the same time also the auxin content increased considerably relative to control plants on high N (Walch-Liu et al., 2006). Inversely, the auxin content in the shoot decreased. These results suggest that high nitrate concentrations in the shoot might inhibit polar auxin transport to the root and thereby repress lateral root elongation (Walch-Liu et al., 2006).

A systemic regulation of lateral root formation was also present under ammonium-grown plants. This was demonstrated on vertically-split agar plates (chapter 4), when the N status of the main root system (LN root fraction) and shoot increased due to ammonium or glutamine supply and repressed ammonium-dependent lateral root branching on the HN plate side (Figure 16 and Figure 17). Hence, the shoot-N status plays a role in controlling ammonium-triggered lateral formation. Auxin might also be a molecular player in this systemic regulation, given

that the *qko* mutant tended to show an enhanced auxin concentration in the shoot compared to wild-type plants (Figure 27E). To verify this hypothesis, more experiments are required to measure auxin concentrations in shoot tissues under different concentrations of localized ammonium supply and under an enhanced N status of the shoot. However, not only plant hormones, but also transcription factors or microRNAs might act as long-distance signals (Robert and Friml, 2009). Recently, high nitrate provision was shown to activate the *AFB3/miR393* module to control primary root growth (Vidal et al., 2010). Interestingly, reduced N forms, such as ammonium or glutamine, positively affected the expression of *miR393* in the root (Vidal et al., 2010). Thus, nitrate might represent an external while reduced N forms might represent an internal trigger that modulates root growth via auxin signaling. However, whether the *miR393* acts as a systemic or local signal remains currently unclear.

In contrast to the examples given by ammonium and nitrate, where systemic signaling had a strong impact on lateral root development, the present thesis showed that systemic signaling is not always involved in nutrient-dependent changes of the root system architecture. High concentrations of localized Fe supply inhibited the lateral elongation in *frd3-1* mutants to a similar extent as in wild-type plants, although *frd3-1* shoots suffered from Fe deficiency (Figure 8D and 8F). Notably, *frd3-1* plants accumulate Fe in roots while the shoot remains Fe deficient (Durrett et al., 2007), leading to a weaker repression of strategy I responses in roots upon Fe resupply (Figure 9; Rogers and Guerinot, 2002). Hence, Fe-mediated repression of lateral root elongation under localized Fe supply was controlled by the Fe concentration in root but not in the shoot. Thus, evidence for the involvement of a systemic, FRD3-dependent shoot signal in shaping Fe-dependent root morphology was not found.

Considering the different contribution of the shoot nutritional status under N and Fe, the dominance of systemic or local signaling in lateral root morphology appears to be a nutrient-specific event. A future challenge will be to understand why certain nutrients that generate morphological adaptations rely on systemic signals while other nutrients may favor a local signaling pathway.

### 5.3. The nutrient transceptor model for coordinating changes in root morphology

Information about the nutrient fluctuations in the environment requires a coordinated sense mechanism to trigger adaptive cell/tissue responses to support normal plant growth. This relies on two major adaptive responses: (i) improving nutrient acquisition by regulation of membrane transporters responsive to internal and external nutrient availabilities and (ii) modulation of root system development enable an efficient soil exploration by the plant (Loqué and von Wirén, 2004; Gojon et al., 2009).

Several reports showed nutrient-specific sensing functions in plants that rely on sensing events by plasma membrane transport proteins. In particular to N, the nitrate transporter NRT1;1 (CLH1) has been shown to act as a nitrate sensor by regulating expression levels of the high-affinity nitrate transporter NRT2;1 (Ho et al., 2009). Mutation analysis showed that nitrate uptake activity is not essentially required for the sensor function of NRT1;1. The current model states that when nitrate is present at low concentrations in the soil solution, nitrate binds to NRT1;1 allowing the transporter to be phosphorylated at the threonine residue T101 by the calcium-dependent protein kinase CIPK23 (Ho et al., 2009). This phosphorylation suppresses any signaling required to activate NRT2;1 expression and NRT1;1 remains active in the high-affinity range (Ho et al., 2009). In contrast, at high nitrate concentrations, nitrate binds to another site in NRT1;1, which disables the phosphorylation of T101 and leads to an up-regulation of NRT2;1 while NRT1;1 continues to be active in the low-affinity phase (Ho et al., 2009). As mentioned before, NRT1;1 and NRT2;1 also coordinate nitrate-dependent root growth. On the basis of the phenotype described for the *nrt1;1* mutant (Remans et al., 2006b; Remans et al., 2006a) the same transceptor mechanism, thus a similar interaction between these two transporters, might be required for root colonization in nitrate-rich patches, although, this remains to be elucidated.

In case of ammonium, evidence has been provided that membrane transport and ammonium sensing in roots are coupled events. Under increasing external ammonium concentrations, the cytosolic C-terminal domain of AMT1;1 interacts with other subunits in the trimer leading to an inactivation of the trimeric complex (Loqué et al., 2007). This allosteric regulation is mediated by phosphorylation of the threonine residue T460 and occurs at ammonium concentrations as low as 50  $\mu\text{M}$

(Loque et al., 2007; Lanquar et al., 2009). So far, it has not yet been clarified whether the AMT1;1 transporter itself or a neighboring receptor-like kinase is responsible for the sensing of external ammonium concentrations (Lanquar et al., 2009). In the former case, however, AMT1;1 might act as a transceptor, transporting ammonium and exerting an intracellular signal at the same time.

The results reported in chapter 4 would support a transceptor function of AMT1;3 in regulating lateral root architecture. Only AMT1;3 efficiently triggered lateral root initiation under localized ammonium supply (Figure 20 and 22), whereas AMT1;1 could not restore third-order lateral formation under the same growth conditions despite its comparable biochemical properties and even higher mRNA expression levels in the root tissue (Figure 22 and 23). Since a pore mutation and C-terminal mutations in the AMT1;3 protein not only abolished the ammonium uptake capacity but also impaired the formation of third-order lateral roots (Figure 26), ammonium-dependent lateral branching appeared to depend on a functional AMT1;3 protein (Figure 26). These observations suggested that conformational changes in the C-terminus of the AMT1;3 protein might be involved in ammonium-dependent signaling. A transceptor-based sensing mechanism has been substantiated for the N-dependent pseudohyphal growth in yeast that relies on the high-affinity ammonium transporter Mep2p (Lorenz and Heitman, 1998; Marini and André, 2000). The intracellular C-terminus of Mep2p, which is dispensable for ammonium transport, is required for filamentous growth in response to a signal induced by N starvation (Rutherford et al., 2008). Moreover, the filamentous growth is dependent on a cyclic AMP-protein kinase A (cAMP-PKA) pathway (Van Zeebroeck et al., 2008), however, Arabidopsis AMTs were not able to trigger the PKA-dependent signaling cascade. Interestingly, methylammonium (MeA) can also activate the Mep2p-PKA signaling cascade, although only ammonium, but not MeA, can cause conformational changes in the Mep2p C-terminus for filamentous growth (Van Nuland et al., 2006). Thus, ammonium binding to the carrier triggers the conformational change that initiates signaling (Van Nuland et al., 2006). This transceptor mechanism among *Meps*, *MEP-type* and *AMTs* seems to be conserved in the ammonium sensing-signaling. All together, it is possible to suggest that AMT1;3, in particular, might regulate uptake-sensing to trigger ammonium-dependent root morphology. The identification of the key components in the ammonium-sensing pathway, by transcriptome analysis using Arabidopsis re-complemented AMT1;3 and AMT1;1 in *qko* background and grown on

split agar plates with localized ammonium supply, is the next step to understand how ammonium controls adaptive root morphology in plants.

A vast number of external and internal signals govern root system architecture during plant development. In the present thesis, the influence of a localized supply of ammonium and Fe on root system architecture has been described for the first time, and in both cases the first molecular components have been identified that are involved in these morphological adaptations. Future challenges will be not only to unravel further molecular components of these nutrient-dependent signaling cascades but also to understand how these signals are integrated at the cellular and at the whole-plant level. Acquiring such knowledge from model plants, such as *Arabidopsis*, is a good starting point, although this knowledge is of particular importance for agronomically relevant plant species. The application of nutrient sensing mechanism to agricultural crops certainly carries a large potential to improve nutrient acquisition and thereby fertilizer use efficiency for more sustainable crop production (Hochholdinger et al., 2004).

## 6. References

- Andrade, S., Dickmanns, A., Ficner, R., and Einsle, O.** (2005). Crystal structure of the archaeal ammonium transporter Amt-1 from *Archaeoglobus fulgidus*. *Proc Natl Acad Sci USA* **102**, 14994-14999.
- Arnaud, N., Murgia, I., Boucherez, J., Briat, J.-F., Cellier, F., and Gaymard, F.** (2006). An iron-induced nitric oxide burst precedes ubiquitin-dependent protein degradation for *Arabidopsis* AtFer1 ferritin gene expression. *J Biol Chem* **281**, 23579-23588.
- Bauer, P., Ling, H.-Q., and Guerinot, M.L.** (2007). FIT, the FER-LIKE IRON DEFICIENCY INDUCED TRANSCRIPTION FACTOR in *Arabidopsis*. *Plant Physiol Biochem* **45**, 260-261.
- Benková, E., Michniewicz, M., Sauer, M., Teichmann, T., Seifertová, D., Jürgens, G., and Friml, J.** (2003). Local, efflux-dependent auxin gradients as a common module for plant organ formation. *Cell* **115**, 591-602.
- Bennett, M., Marchant, A., Green, H., May, S., Ward, S.P., Millner, P.A., Walker, A.R., Schulz, B., and Feldmann, K.A.** (1996). *Arabidopsis* AUX1 gene: a permease-like regulator of root gravitropism. *Science* **273**, 948-950.
- Bhalerao, R.P., Eklöf, J., Ljung, K., Marchant, A., Bennett, M., and Sandberg, G.** (2002). Shoot-derived auxin is essential for early lateral root emergence in *Arabidopsis* seedlings. *Plant J* **29**, 325-332.
- Blakeslee, J.J., Bandyopadhyay, A., Lee, O.R., Mravec, J., Titapiwatanakun, B., Sauer, M., Makam, S.N., Cheng, Y., Bouchard, R., Adamec, J., Geisler, M., Nagashima, A., Sakai, T., Martinoia, E., Friml, J., Peer, W.A., and Murphy, A.S.** (2007). Interactions among PIN-FORMED and P-glycoprotein auxin transporters in *Arabidopsis*. *Plant Cell* **19**, 131-147.
- Boeckstaens, M., André, B., and Marini, A.M.** (2007). The yeast ammonium transport protein Mep2 and its positive regulator, the Npr1 kinase, play an important role in normal and pseudohyphal growth on various nitrogen media through retrieval of excreted ammonium. *Molecular Microbiology* **64**, 534-546.
- Boerjan, W., Cervera, M., Delarue, M., Beeckman, T., Dewitte, W., Bellini, C., Caboche, M., Onckelen, H.V., Montagu, M.V., and Inze, D.** (1995). Superroot, a recessive mutation in *Arabidopsis*, confers auxin overproduction. *Plant Cell* **7**, 1405-1419.
- Brumbarova, T., and Bauer, P.** (2005). Iron-mediated control of the basic helix-loop-helix protein FER, a regulator of iron uptake in tomato. *Plant Physiol* **137**, 1018-1026.
- Cao, Y., Glass, A., and Crawford, N.** (1993). Ammonium inhibition of *Arabidopsis* root growth can be reversed by potassium and by auxin Resistance Mutations aux7, axr7, and axr2. *Plant Physiol* **102**, 983-989.
- Casimiro, I., Beeckman, T., Graham, N., Bhalerao, R., Zhang, H., Casero, P., Sandberg, G., and Bennett, M.J.** (2003). Dissecting *Arabidopsis* lateral root development. *Trends Plant Sci* **8**, 165-171.
- Casimiro, I., Marchant, A., Bhalerao, R.P., Beeckman, T., Dhooge, S., Swarup, R., Graham, N., Inzé, D., Sandberg, G., Casero, P.J., and Bennett, M.** (2001). Auxin transport promotes *Arabidopsis* lateral root initiation. *Plant Cell* **13**, 843-852.

- Castaings, L., Camargo, A., Pocholle, D., Gaudon, V., Texier, Y., Boutet-Mercey, S., Tacонат, L., Renou, J.-P., Daniel-Vedele, F., Fernandez, E., Meyer, C., and Krapp, A.** (2009). The nodule inception-like protein 7 modulates nitrate sensing and metabolism in *Arabidopsis*. *Plant J* **57**, 426-435.
- Celenza, J.L., Grisafi, P.L., and Fink, G.R.** (1995). A pathway for lateral root formation in *Arabidopsis thaliana*. *Genes Dev* **9**, 2131-2142.
- Cerezo, M., Tillard, P., Filleur, S., Muños, S., Daniel-Vedele, F., and Gojon, A.** (2001). Major alterations of the regulation of root NO<sub>3</sub><sup>-</sup> uptake are associated with the mutation of *Nrt2.1* and *Nrt2.2* genes in *Arabidopsis*. *Plant Physiol* **127**, 262-271.
- Chandler, J.W., Cole, M., Flier, A., Grewe, B., and Werr, W.** (2007). The AP2 transcription factors *DORNROSCHEN* and *DORNROSCHEN-LIKE* redundantly control *Arabidopsis* embryo patterning via interaction with *PHAVOLUTA*. *Development* **134**, 1653-1662.
- Chaney, R. L.** (1988) Plants can utilize iron from Fe-N,N9-di-(2-hydroxybenzoyl)-ethylenediamine-N,N9-diacetic acid, a ferric chelate with 106 greater formation constant than Fe-EDDHA. *J Plant Nutr* **11**, 1033-1050.
- Cheng, L., Wang, F., Shou, H., Huang, F., Zheng, L., He, F., Li, J., Zhao, F.-J., Ueno, D., Ma, J.F., and Wu, P.** (2007). Mutation in Nicotianamine Aminotransferase Stimulated the Fe(II) Acquisition System and Led to Iron Accumulation in Rice. *Plant Physiol* **145**, 1647-1657.
- Coates, J.C., Laplaze, L., and Haseloff, J.** (2006). Armadillo-related proteins promote lateral root development in *Arabidopsis*. *Proc Natl Acad Sci USA* **103**, 1621-1626.
- Colangelo, E.P., and Guerinot, M.L.** (2004). The essential basic helix-loop-helix protein *FIT1* is required for the iron deficiency response. *Plant Cell* **16**, 3400-3412.
- Cole, M., Chandler, J., Weijers, D., Jacobs, B., Comelli, P., and Werr, W.** (2009). *DORNROSCHEN* is a direct target of the auxin response factor *MONOPTEROS* in the *Arabidopsis* embryo. *Development* **136**, 1643-1651.
- Colon-Carmona, A., You, R., Haimovitch-Gal, T., Doerner, P.** (1999). Spatio-temporal analysis of mitotic activity with a labile cyclin-GUS fusion protein. *Plant J.* **20**, 503-505.
- Connolly, E.L., Fett, J.P., Guerinot, M.L.** (2002). Expression of the *IRT1* metal transporter is controlled by metals at the levels of transcript and protein accumulation. *Plant Cell* **14**, 1347-1357.
- Connolly, E.L., Campbell, N., Grotz, N., Prichard, C.L., Guerinot, M.L.** (2003) Overexpression of the *FRO2* iron reductase confers tolerance to growth on low iron and uncovers post-transcriptional control. *Plant Physiol* **133**, 1102-1110.
- Curie, C., Panaviene, Z., Loulergue, C., Dellaporta, S.L., Briat, J.-F., and Walker, E.L.** (2001). Maize yellow stripe1 encodes a membrane protein directly involved in Fe (III) uptake. *Nature* **409**, 346-349.
- Delhaize, E.** (1996) A metal-accumulator mutant of *Arabidopsis thaliana*. *Plant Physiol* **111**, 849-855.
- De Smet, I., and Jürgens, G.** (2007). Patterning the axis in plants--auxin in control. *Curr Opin Genet Dev* **17**, 337-343.

- De Smet, I., Signora, L., Beeckman, T., Inze, D., Foyer, C.H., and Zhang, H.** (2003). An abscisic acid-sensitive checkpoint in lateral root development of *Arabidopsis*. *Plant Journal* **33**, 543-555.
- De Smet, I., Tetsumura, T., De Rybel, B., Frey, N.F.D., Laplaze, L., Casimiro, I., Swarup, R., Naudts, M., Vanneste, S., Audenaert, D., Inzé, D., Bennett, M.J., and Beeckman, T.** (2007). Auxin-dependent regulation of lateral root positioning in the basal meristem of *Arabidopsis*. *Development* **134**, 681-690.
- De Smet, I., Vassileva, V., De Rybel, B., Levesque, M.P., Grunewald, W., Van Damme, D., Van Noorden, G., Naudts, M., Van Isterdael, G., De Clercq, R., Wang, J.Y., Meuli, N., Vanneste, S., Friml, J., Hilson, P., Jürgens, G., Ingram, G.C., Inzé, D., Benfey, P.N., and Beeckman, T.** (2008). Receptor-like kinase ACR4 restricts formative cell divisions in the *Arabidopsis* root. *Science* **322**, 594-597.
- Desnos, T.** (2008) Root branching responses to phosphate and nitrate. *Curr. Opin. Plant Biol.* **11**, 82–87.
- Dharmasiri, N., Dharmasiri, S., Estelle, M.** (2005a). The F-box protein TIR1 is an auxin receptor. *Nature* **435**, 441-445.
- Dharmasiri, N., Dharmasiri, S., Weijers, D., Lechner, E., Yamada, M., Hobbie, L., Ehrismann, J.S., Jürgens, G., and Estelle, M.** (2005b). Plant development is regulated by a family of auxin receptor F box proteins. *Dev Cell* **9**, 109-119.
- Dharmasiri, S., Swarup, R., Mockaitis, K., Dharmasiri, N., Singh, S.K., Kowalchuk, M., Marchant, A., Mills, S., Sandberg, G., Bennett, M.J., and Estelle, M.** (2006). AXR4 is required for localization of the auxin influx facilitator AUX1. *Science* **312**, 1218-1220.
- DiDonato, R.J., Arbuckle, E., Buker, S., Sheets, J., Tobar, J., Totong, R., Grisafi, P., Fink, G.R., and Celenza, J.L.** (2004). *Arabidopsis* ALF4 encodes a nuclear-localized protein required for lateral root formation. *Plant J* **37**, 340-353.
- Dinneny, J.R., and Benfey, P.N.** (2008). Plant stem cell niches: standing the test of time. *Cell* **132**, 553-557.
- Dinneny, J.R., Long, T.A., Wang, J.Y., Jung, J.W., Mace, D., Pointer, S., Barron, C., Brady, S.M., Schiefelbein, J., Benfey, P.N.** (2008) Cell identity mediates the response of *Arabidopsis* roots to abiotic stress. *Science* **320**, 942–320.
- Dinkelaker, B., Hengeler, C., Marschner, H.** (1995) Distribution and function of proteoid roots and other root clusters. *Bot Acta* **108**, 183–200.
- Ditengou, F.A., Teale, W.D., Kochersperger, P., Flittner, K.A., Kneuper, I., van der Graaff, E., Nziengui, H., Pinosa, F., Li, X., Nitschke, R., Laux, T., and Palme, K.** (2008). Mechanical induction of lateral root initiation in *Arabidopsis thaliana*. *Proc Natl Acad Sci USA* **105**, 18818-18823.
- Drew, M.** (1975). Comparison of the effects of a localized supply of phosphate, nitrate, ammonium and potassium on the growth of the seminal root system, and the shoot in Barley. *New Phytologist* **75**, 479-490.
- Drew, M.C., Saker, L.R.** (1975). Nutrient supply and the growth of the seminal root system in barley. II. Localized, compensatory increases in lateral root growth and rates of nitrate uptake when nitrate supply is restricted to only part of the root system. *J. Exp. Bot.* **26**, 79–90.
- Drew, M.C., Saker, L.R.** (1978). Nutrient supply and the growth of the seminal root system in barley. III. Compensatory increases in growth of lateral roots, and in the rates of

- phosphate uptake, in response to a localized supply of phosphate. *J. Exp. Bot.* **29**, 435–451.
- Dubrovsky, J.G., Doerner, P.W., Colón-Carmona, A., and Rost, T.L.** (2000). Pericycle cell proliferation and lateral root initiation in *Arabidopsis*. *Plant Physiol* **124**, 1648-1657.
- Dubrovsky, J.G., Rost, T.L., Colon-Carmona, A., and Doerner, P.** (2001) Early primordium morphogenesis during lateral root initiation in *Arabidopsis thaliana*. *Planta* **214**, 30–36.
- Dubrovsky, J.G., Sauer, M., Napsucialy-Mendivil, S., Ivanchenko, M.G., Friml, J., Shishkova, S., Celenza, J., and Benková, E.** (2008). Auxin acts as a local morphogenetic trigger to specify lateral root founder cells. *Proc Natl Acad Sci USA* **105**, 8790-8794.
- Dubrovsky, J.G., Soukup, A., Napsucialy-Mendivil, S., Jeknic, Z., and Ivanchenko, M.G.** (2009). The lateral root initiation index: an integrative measure of primordium formation. *Ann Bot* **103**, 807-817.
- Durrett, T.P., Gassmann, W., and Rogers, E.E.** (2007). The FRD3-mediated efflux of citrate into the root vasculature is necessary for efficient iron translocation. *Plant Physiol* **144**, 197-205.
- Duy, D., Wanner, G., Meda, A.R., von Wirén, N., Soll, J., and Philippar, K.** (2007). PIC1, an ancient permease in *Arabidopsis* chloroplasts, mediates iron transport. *Plant Cell* **19**, 986-1006.
- Enomoto, Y., Hodoshima, H., Shimada, H., Shoji, K., Yoshihara, T., Goto, F.** (2007) Long-distance signals positively regulate the expression of iron uptake genes in tobacco roots. *Planta* **227**, 81–89.
- Ermilova, E.V., Nikitin, M.M., Fernandez, E.** (2007). Chemotaxis to ammonium/methylammonium in *Chlamydomonas reinhardtii*: the role of transport systems for ammonium/methylammonium. *Planta* **226**, 1323-1332.
- Ettema, C.H., Wardle, D.A.** (2002) Spatial soil ecology, *Trends in Ecology and Evolution* **17**, 177–183.
- Ferreira, P.C., Hemerly, A.S., Engler, J.D., van Montagu, M., Engler, G., Inze, D.** (1994). Developmental expression of the *Arabidopsis* cyclin gene *cyc1At*. *Plant Cell* **6**, 1763-1774.
- Fraisier, V., Gojon, A., Tillard, P., and Daniel-Vedele, F.** (2000). Constitutive expression of a putative high-affinity nitrate transporter in *Nicotiana plumbaginifolia*: evidence for post-transcriptional regulation by a reduced nitrogen source. *Plant J* **23**, 489-496.
- Franco-Zorrilla, J., Martin, A., Leyva, A., and Paz-Ares, J.** (2005). Interaction between Phosphate-Starvation, Sugar, and Cytokinin Signaling in *Arabidopsis* and the Roles of Cytokinin Receptors CRE1/AHK4 and AHK3. *Plant Physiol* **138**, 847-857.
- Friml, J., Yang, X., Michniewicz, M., Weijers, D., Quint, A., Tietz, O., Benjamins, R., Ouwerkerk, P.B.F., Ljung, K., Sandberg, G., Hooykaas, P.J.J., Palme, K., and Offringa, R.** (2004). A PINOID-dependent binary switch in apical-basal PIN polar targeting directs auxin efflux. *Science* **306**, 862-865.
- Fujiwara, T., Hirai, M.Y., Chino, M., Komeda, Y., Naito, S.** (1992). Effect of sulfur nutrition on expression of soybean seed storage protein genes in transgenic petunia. *Plant Physiol* **99**, 263-268.

- Fukaki, H., Tameda, S., Masuda, H., and Tasaka, M.** (2002). Lateral root formation is blocked by a gain-of-function mutation in the SOLITARY-ROOT/IAA14 gene of Arabidopsis. *Plant J* **29**, 153-168.
- Fukaki, H., Okushima, Y., and Tasaka, M.** (2007). Auxin-mediated lateral root formation in higher plants. *International Review of Cytology* **256**, 111-137.
- Gazzarrini, S., Lejay, L., Gojon, A., Ninnemann, O., Frommer, W.B., and von Wirén, N.** (1999a). Three functional transporters for constitutive, diurnally regulated, and starvation-induced uptake of ammonium into Arabidopsis roots. *Plant Cell* **11**, 937-948.
- Gazzarrini, S., Lejay, L., Gojon, A., Ninnemann, O., Frommer, W.B., and von Wirén, N.** (1999b). Three Functional Transporters for Constitutive, Diurnally Regulated, and Starvation-Induced Uptake of Ammonium into Arabidopsis Roots. *Plant Cell* **11**, 937-948.
- Geldner, N., Richter, S., Vieten, A., Marquardt, S., Torres-Ruiz, R.A., Mayer, U., and Jürgens, G.** (2004). Partial loss-of-function alleles reveal a role for GNOM in auxin transport-related, post-embryonic development of Arabidopsis. *Development* **131**, 389-400.
- Giehl, R., Meda, A., and von Wirén, N.** (2009). Moving up, down, and everywhere: signaling of micronutrients in plants. *Curr Opin Plant Biol* **12**, 320-327.
- Gifford, M.L., Dean, A., Gutierrez, R.A., Coruzzi, G.M., and Birnbaum, K.D.** (2008). Cell-specific nitrogen responses mediate developmental plasticity. *Proc Natl Acad Sci USA* **105**, 803-808.
- Gojon, A., Nacry, P., and Davidian, J.-C.** (2009). Root uptake regulation: a central process for NPS homeostasis in plants. *Curr Opin Plant Biol* **12**, 328-338.
- Graziano, M., and Lamattina, L.** (2007). Nitric oxide accumulation is required for molecular and physiological responses to iron deficiency in tomato roots. *Plant J* **52**, 949-960.
- Green, L., Rogers, E.E.** (2004) FRD3 controls iron localization in Arabidopsis. *Plant Physiol* **136**, 2523-2531.
- Grusak, M.A., Pezeshgi, S.** (1996) Shoot-to-root signal transmission regulates root Fe(III) reductase activity in the dgl mutant of pea. *Plant Physiol* **110**, 329-334.
- Henriques, R., Jasik, J., Klein, M., Martinoia, E., Feller, U., Schell, J., Pais, M.S., Koncz, C.** (2002) Knock-out of Arabidopsis metal transporter gene IRT1 results in iron deficiency accompanied by cell differentiation defects. *Plant Mol Biol* **50**, 587-597.
- Hinsinger, P., Gobran, G.R., Gregory, P.J., Wenzel, W.W.** (2005). Rhizosphere geometry and heterogeneity arising from root-mediated physical and chemical processes *New Phytol.* **168**, 293-30.
- Hirota, A., Kato, T., Fukaki, H., Aida, M., and Tasaka, M.** (2007). The auxin-regulated AP2/EREBP gene PUCHI is required for morphogenesis in the early lateral root primordium of Arabidopsis. *Plant Cell* **19**, 2156-2168.
- Hobbie, L.** (1998). Auxin: molecular genetic approaches in Arabidopsis. *Plant Physiology et Biochemistry* **36**, 91-102.
- Ho, C.-H., Lin, S.-H., Hu, H.-C., and Tsay, Y.-F.** (2009). CHL1 functions as a nitrate sensor in plants. *Cell* **138**, 1184-1194.

- Hochholdinger, F., Park, W.J., Sauer, M., and Woll, K.** (2004). From weeds to crops: genetic analysis of root development in cereals. *Trends Plant Sci* **9**, 42-48.
- Hodge, A.** (2006). Plastic plants and patchy soils. *J Exp Bot* **57**, 401-411.
- Hu, H.-C., Wang, Y.-Y., and Tsay, Y.-F.** (2009). AtCIPK8, a CBL-interacting protein kinase, regulates the low-affinity phase of the primary nitrate response. *Plant J* **57**, 264-278.
- Ivanchenko, M.G., Muday, G.K., and Dubrovsky, J.G.** (2008). Ethylene-auxin interactions regulate lateral root initiation and emergence in *Arabidopsis thaliana*. *Plant J* **55**, 335-347.
- Jain, A., Poling, M.D., Smith, A.P., Nagarajan, V.K., Lahner, B., Meagher, R.B., Raghothama, K.G.** (2009) Variations in the composition of gelling agents affect morphophysiological and molecular responses to deficiencies of phosphate and other nutrients. *Plant Physiol* **150**, 1033–1049.
- Jakoby, M., Wang, H.Y., Reidt, W., Weisshaar, B., Bauer, P.** (2004) FRU (BHLH029) is required for induction of iron mobilization genes in *Arabidopsis thaliana*. *FEBS Lett* **577**, 528–534.
- Jiang, C., Gao, X., Liao, L., Harberd, N.P., and Fu, X.** (2007). Phosphate starvation root architecture and anthocyanin accumulation responses are modulated by the gibberellin-DELLA signaling pathway in *Arabidopsis*. *Plant Physiol* **145**, 1460-1470.
- Jung, J., Shin, R., Schachtman, D.P.** (2009). Ethylene Mediates Response and Tolerance to Potassium Deprivation in *Arabidopsis*. *Plant Cell* **21**, 607-621.
- Khademi, S., O'Connell, J., Remis, J., Robles-Colmenares, Y., Miercke, L.J.W., and Stroud, R.M.** (2004). Mechanism of ammonia transport by Amt/MEP/Rh: structure of AmtB at 1.35 Å. *Science* **305**, 1587-1594.
- Kleine-Vehn, J., Dhonukshe, P., Sauer, M., Brewer, P.B., Wiśniewska, J., Paciorek, T., Benková, E., and Friml, J.** (2008). ARF GEF-dependent transcytosis and polar delivery of PIN auxin carriers in *Arabidopsis*. *Curr Biol* **18**, 526-531.
- Koike, S., Inoue, H., Mizuno, D., Takahashi, M., Nakanishi, H., Mori, S., and Nishizawa, N.K.** (2004). OsYSL2 is a rice metal-nicotianamine transporter that is regulated by iron and expressed in the phloem. *Plant J* **39**, 415-424.
- Korshunova, Y., Eide, D., Gregg Clark, W., Guerinot, M.L., and Pakrasi, H.B.** (1999). The IRT1 protein from *Arabidopsis thaliana* is a metal transporter with a broad substrate range. *Plant Molecular Biology* **40**, 37-44.
- Krouk, G., Tillard, P., and Gojon, A.** (2006). Regulation of the high-affinity NO<sub>3</sub><sup>-</sup> uptake system by NRT1.1-mediated NO<sub>3</sub><sup>-</sup> demand signaling in *Arabidopsis*. *Plant Physiol* **142**, 1075-1086.
- Kumánovics, A., Chen, O.S., Li, L., Bagley, D., Adkins, E.M., Lin, H., Dingra, N.N., Outten, C.E., Keller, G., Winge, D., Ward, D.M., and Kaplan, J.** (2008). Identification of FRA1 and FRA2 as genes involved in regulating the yeast iron regulon in response to decreased mitochondrial iron-sulfur cluster synthesis. *J Biol Chem* **283**, 10276-10286.
- Kutz, A., Müller, A., Hennig, P., Kaiser, W.M., Piotrowski, M., and Weiler, E.W.** (2002). A role for nitrilase 3 in the regulation of root morphology in sulphur-starving *Arabidopsis thaliana*. *Plant J* **30**, 95-106.

- Lai, F., Thacker, J., Li, Y., and Doerner, P. (2007). Cell division activity determines the magnitude of phosphate starvation responses in Arabidopsis. *Plant Journal* **50**, 545-556.
- Laplaze, L., Benkova, E., Casimiro, I., Maes, L., Vanneste, S., Swarup, R., Weijers, D., Calvo, V., Parizot, B., Herrera-Rodriguez, M.B., Offringa, R., Graham, N., Dumas, P., Friml, J., Bogusz, D., Beeckman, T., and Bennett, M. (2007). Cytokinins act directly on lateral root founder cells to inhibit root initiation. *Plant Cell* **19**, 3889-3900.
- Landsberg, E.C. (1986) Function of rhizodermal transfer cells in the Fe stress response mechanism of *Capsicum annuum* L. *Plant Physiol* **82**, 511–517.
- Lanquar, V., Loqué, D., Hörmann, F., Yuan, L., Bohner, A., Engelsberger, W.R., Lalonde, S., Schulze, W.X., von Wirén, N., and Frommer, W.B. (2009). Feedback inhibition of ammonium uptake by a phospho-dependent allosteric mechanism in Arabidopsis. *Plant Cell* **21**, 3610-3622.
- Laskowski, M., Biller, S., Stanley, K., Kajstura, T., and Prusty, R. (2006). Expression profiling of auxin-treated Arabidopsis roots: toward a molecular analysis of lateral root emergence. *Plant Cell Physiol* **47**, 788-792.
- Laux, T. (2003). The stem cell concept in plants: a matter of debate. *Cell* **113**, 281-283.
- Lewis, D.R., Miller, N.D., Splitt, B.L., Wu, G., Spalding, E.P. (2007). Separating the roles of acropetal and basipetal auxin transport on gravitropism with mutations in two Arabidopsis multidrug resistance-like ABC transporter genes. *Plant Cell* **19**, 1838-1850.
- Ling, H.-Q., Bauer, P., Berczky, Z., Keller, B., and Ganai, M. (2002). The tomato fer gene encoding a bHLH protein controls iron-uptake responses in roots. *Proc Natl Acad Sci USA* **99**, 13938-13943.
- Linkohr, B., Williamson, L., Fitter, A., Leyser, O. (2002) Nitrate and phosphate availability and distribution have different effects on root system architecture of Arabidopsis. *Plant J* **29**, 751–760.
- Little, D., Rao, H., Oliva, S., Daniel-Vedele, F., Krapp, A., and Malamy, J.E. (2005). The putative high-affinity nitrate transporter NRT2.1 represses lateral root initiation in response to nutritional cues. *Proc Natl Acad Sci USA* **102**, 13693-13698.
- Liu, K.-H., and Tsay, Y.-F. (2003). Switching between the two action modes of the dual-affinity nitrate transporter CHL1 by phosphorylation. *EMBO J* **22**, 1005-1013.
- Liu, T.-Y., Chang, C.-Y., and Chiou, T.-J. (2009). The long-distance signaling of mineral macronutrients. *Curr Opin Plant Biol* **12**, 312-319.
- Ljung, K., Hull, A.K., Celenza, J., Yamada, M., Estelle, M., Normanly, J., and Sandberg, G. (2005). Sites and regulation of auxin biosynthesis in Arabidopsis roots. *Plant Cell* **17**, 1090-1104.
- Lopez-Bucio, J., Hernandez-Abreu, E., Sanchez-Calderon, L., Nieto-Jacobo, M.F., Simpson, J., and Herrera-Estrella, L. (2002). Phosphate Availability Alters Architecture and Causes Changes in Hormone Sensitivity in the Arabidopsis Root System. *Plant Physiol* **129**, 244-256.
- López-Bucio, J., Cruz-Ramírez, A., and Herrera-Estrella, L. (2003). The role of nutrient availability in regulating root architecture. *Curr Opin Plant Biol* **6**, 280-287.

- López-Bucio, J., Hernández-Abreu, E., Sánchez-Calderón, L., Pérez-Torres, A., Rampey, R.A., Bartel, B., and Herrera-Estrella, L.** (2005). An auxin transport independent pathway is involved in phosphate stress-induced root architectural alterations in *Arabidopsis*. Identification of BIG as a mediator of auxin in pericycle cell activation. *Plant Physiol* **137**, 681-691.
- Loqué, D., Yuan, L., Kojima, S., Gojon, A., Wirth, J., Gazzarrini, S., Ishiyama, K., Takahashi, H., and von Wirén, N.** (2006). Additive contribution of AMT1;1 and AMT1;3 to high-affinity ammonium uptake across the plasma membrane of nitrogen-deficient *Arabidopsis* roots. *Plant J.* **48**, 522–534.
- Loqué, D., Lalonde, S., Looger, L.L., von Wirén, N., and Frommer, W.B.** (2007). A cytosolic trans-activation domain essential for ammonium uptake. *Nature* **446**, 195–198.
- Loqué, D., and von Wirén, N.** (2004). Regulatory levels for the transport of ammonium in plant roots. *J Exp Bot* **55**, 1293-1305.
- Lorenz, M.C., and Heitman, J.** (1998). The MEP2 ammonium permease regulates pseudohyphal differentiation in *Saccharomyces cerevisiae*. *EMBO J* **17**, 1236-1247.
- Lucas, M., Guédon, Y., Jay-Allemand, C., Godin, C., and Laplace, L.** (2008). An auxin transport-based model of root branching in *Arabidopsis thaliana*. *PLoS ONE* **3**, e3673.
- Lucena, C., Waters, B., Romera, F., Garcia, M., Morales, M., Alcántara, E., and Pérez-Vicente, R.** (2006). Ethylene could influence ferric reductase, iron transporter, and H<sup>+</sup>-ATPase gene expression by affecting FER (or FER-like) gene activity. *J Exp Bot* **57**, 4145-4154.
- Malamy, J.E.** (2005). Intrinsic and environmental response pathways that regulate root system architecture. *Plant Cell Environ* **28**, 67-77.
- Malamy, J.E., and Benfey, P.N.** (1997). Organization and cell differentiation in lateral roots of *Arabidopsis thaliana*. *Development* **124**, 33-44.
- Marchant, A., Bhalerao, R., Casimiro, I., Eklöf, J., Casero, P.J., Bennett, M., and Sandberg, G.** (2002). AUX1 promotes lateral root formation by facilitating indole-3-acetic acid distribution between sink and source tissues in the *Arabidopsis* seedling. *Plant Cell* **14**, 589-597.
- Marini, A., and Andre, B.** (2000). In vivo N-glycosylation of the Mep2 high-affinity ammonium transporter of *Saccharomyces cerevisiae* reveals an extracytosolic N-terminus. *Molecular Microbiology* **38**, 552-564.
- Marini, A., Soussi-Boudekou, S., Vissers, S., and Andre, B.** (1997a). A family of ammonium transporters in *Saccharomyces cerevisiae*. *Mol Cell Biol* **17**, 4282-4293.
- Marini, A., Matassi, G., Raynal, V., André, B., Cartron, J.-P., and Chérif-Zahar, B.** (2000). The human Rhesus-associated RhAG protein and a kidney homologue promote ammonium transport in yeast. *Nature genetics* **26**, 341-344.
- Marini, A.M., Soussi-Boudekou, S., Vissers, S., and Andre, B.** (1997b). A family of ammonium transporters in *Saccharomyces cerevisiae*. *Mol Cell Biol* **17**, 4282-4293.
- Marschner, H., Römheld, V., and Kissel, M.** (1986). Different strategies in higher plants in mobilization and uptake of iron. *Journal of plant nutrition* **9**, 695-713.
- Marschner, H.** (1995) *Mineral Nutrition of Higher Plants*, Academic Press, London.

- Maruyama-Nakashita, A., Nakamura, Y., Yamaya, T., and Takahashi, H.** (2004). A novel regulatory pathway of sulfate uptake in Arabidopsis roots: implication of CRE1/WOL/AHK4-mediated cytokinin-dependent regulation. *Plant J* **38**, 779-789.
- Maruyama-Nakashita, A., Nakamura, Y., Tohge, T., Saito, K., and Takahashi, H.** (2006). Arabidopsis SLIM1 is a central transcriptional regulator of plant sulfur response. *Plant Cell* **18**, 3235-3251.
- Merrick, M., Javelle, A., Durand, A., Severi, E., Thornton, J., Avent, N., Conroy, M., and Bullough, P.** (2006). The Escherichia coli AmtB protein as a model system for understanding ammonium transport by Amt and Rh proteins. *Transfusion clinique et biologique* **13**, 97-102.
- Michniewicz, M., Zago, M.K., Abas, L., Weijers, D., Schweighofer, A., Meskiene, I., Heisler, M.G., Ohno, C., Zhang, J., Huang, F., Schwab, R., Weigel, D., Meyerowitz, E.M., Luschnig, C., Offringa, R., and Friml, J.** (2007). Antagonistic regulation of PIN phosphorylation by PP2A and PINOID directs auxin flux. *Cell* **130**, 1044-1056.
- Miller, A.J., Xiaorong, F., Orsel, M., Smith, S., Wells, D.M.** (2007). Nitrate transport and signalling. *J. Exp. Bot.* **58**, 2297-2306.
- Miller, A.J., Fan, X., Shen, Q., and Smith, S.J.** (2008). Amino acids and nitrate as signals for the regulation of nitrogen acquisition. *J Exp Bot* **59**, 111-119.
- Misson, J., Raghothama, K., Jain, A., Jouhet, J., Block, M.A., Bligny, R., Creff, A., Ortet, P., Somerville, S., Rolland, N., Doumas, P., Nacry, P., Herrera-Estrella, L., Nussaume, L., and Thibaud, M.-C.** (2005). A genome-wide transcriptional analysis using Arabidopsis thaliana Affymetrix gene chips. *Proceedings of the National Academy of Sciences* **102**, 11934-11939.
- Mravec, J., Kubes, M., Bielach, A., Gaykova, V., Petrásek, J., Skůpa, P., Chand, S., Benková, E., Zazimalová, E., and Friml, J.** (2008). Interaction of PIN and PGP transport mechanisms in auxin distribution-dependent development. *Development* **135**, 3345-3354.
- Müller, M., Schmidt, W.** (2004) Environmentally induced plasticity of root hair development in Arabidopsis. *Plant Physiol* **134**, 409-419.
- Murashige, T., Skoog, F.** (1962) A revised medium for rapid growth and bioassays with tobacco tissue culture. *Physiol Plant* **15**, 473-497.
- Nacry, Canivenc, G., Muller, B., Azmi, A., Onckelen, H.V., Rossignol, M., and Doumas, P.** (2005). A Role for Auxin Redistribution in the Responses of the Root System Architecture to Phosphate Starvation in Arabidopsis. *Plant Physiol* **138**, 2061-2074.
- Narang, R.A., Bruene, A., and Altmann, T.** (2000). Analysis of phosphate acquisition efficiency in different Arabidopsis accessions. *Plant Physiol* **124**, 1786-1799.
- Neuhäuser, B., Dynowski, M., Mayer, M., and Ludewig, U.** (2007). Regulation of NH<sub>4</sub><sup>+</sup> transport by essential cross talk between AMT monomers through the carboxyl tails. *Plant Physiol* **143**, 1651-1659.
- Neumann, G., Martinoia, E.** (2002) Cluster roots - An underground adaptation for survival in extreme environments. *Trends Plant Sci* **7**, 162-167.
- Nielsen, K., Eshel, A., and Lynch, J.** (2001). The effect of phosphorus availability on the carbon economy of contrasting common bean (*Phaseolus vulgaris* L.) genotypes. *J Exp Bot* **52**, 329-339.

- Nikiforova, V., Freitag, J., Kempa, S., Adamik, M., Hesse, H., and Hoefgen, R.** (2003). Transcriptome analysis of sulfur depletion in *Arabidopsis thaliana*: interlacing of biosynthetic pathways provides response specificity. *Plant J* **33**, 633-650.
- Norvell, W.A.** (1991) Reactions of metal chelates in soils and nutrient solutions. In: *Micronutrients in Agriculture* (Mordtvedt, J.J, Cox, F.R., Shuman, L.M., Welch, R.M., eds.), pp.187-227. Soil Sci Am Book series no.4, Madison, WI
- Ogawa, M., Kay, P., Wilson, S., and Swain, S.M.** (2009). ARABIDOPSIS DEHISCENCE ZONE POLYGALACTURONASE1 (ADPG1), ADPG2, and QUARTET2 are Polygalacturonases required for cell separation during reproductive development in *Arabidopsis*. *Plant Cell* **21**, 216-233.
- Ohkama, N., Takei, K., Sakakibara, H., Hayashi, H., Yoneyama, T., and Fujiwara, T.** (2002). Regulation of sulfur-responsive gene expression by exogenously applied cytokinins in *Arabidopsis thaliana*. *Plant Cell Physiol* **43**, 1493-1501.
- Okushima, Y., Fukaki, H., Onoda, M., Theologis, A., and Tasaka, M.** (2007). ARF7 and ARF19 regulate lateral root formation via direct activation of LBD/ASL genes in *Arabidopsis*. *Plant Cell* **19**, 118-130.
- Paciorek, T., Zazimalová, E., Ruthardt, N., Petrášek, J., Stierhof, Y.-D., Kleine-Vehn, J., Morris, D.A., Emans, N., Jürgens, G., Geldner, N., and Friml, J.** (2005). Auxin inhibits endocytosis and promotes its own efflux from cells. *Nature* **435**, 1251-1256.
- Péret, B., Larrieu, A., and Bennett, M.** (2009a). Lateral root emergence: a difficult birth. *J Exp Bot*, 1-7.
- Péret, B., De Rybel, B., Casimiro, I., Benková, E., Swarup, R., Laplace, L., Beeckman, T., Bennett, M.J.** (2009b) *Arabidopsis* lateral root development: an emerging story. *Trends Plant Sci* **14**, 399–408.
- Perez-Torres, C., Lopez-Bucio, J., Cruz-Ramirez, A., Ibarra-Laclette, E., Dharmasiri, S., Estelle, M., and Herrera-Estrella, L.** (2008). Phosphate availability alters lateral root development in *Arabidopsis* by modulating auxin Sensitivity via a Mechanism Involving the TIR1 Auxin Receptor. *Plant Cell* **20**, 3258-3272.
- Perry, P., Linke, B., Schmidt, W.** (2007) Reprogramming of root epidermal cells in response to nutrient deficiency. *Biochem Soc Trans* **35**, 161–163.
- Porra, R.J., Thompson, W.A., Kriedmann, P.A.** (1989) Determination of accurate extinction coefficients and simultaneous equations for assaying chlorophylls a and b extracted with four different solvents: verification of the concentration of chlorophyll standards by atomic absorption spectroscopy. *Biochem Biophys Acta* **975**, 384–394.
- Petersson, S.V., Johansson, A.I., Kowalczyk, M., Makoveychuk, A., Wang, J.Y., Moritz, T., Grebe, M., Benfey, P.N., Sandberg, G., and Ljung, K.** (2009). An auxin gradient and maximum in the *Arabidopsis* root apex shown by high-resolution cell-specific analysis of IAA distribution and synthesis. *Plant Cell* **21**, 1659-1668.
- Quint, M., and Gray, W.M.** (2006) Auxin signaling. *Curr Opin Plant Biol* **8**, 448-453.
- Ravet, K., Touraine, B., Boucherez, J., Briat, J.-F., Gaymard, F., and Cellier, F.** (2009). Ferritins control interaction between iron homeostasis and oxidative stress in *Arabidopsis*. *Plant J* **57**, 400-412.
- Remans, T., Nacry, P., Pervent, M., Girin, T., Tillard, P., Lepetit, M., and Gojon, A.** (2006a). A central role for the nitrate transporter NRT2.1 in the integrated

- morphological and physiological responses of the root system to nitrogen limitation in *Arabidopsis*. *Plant Physiol* **140**, 909-921.
- Remans, T., Nacry, P., Pervent, M., Filleur, S., Diatloff, E., Mounier, E., Tillard, P., Forde, B.G., and Gojon, A.** (2006b). The *Arabidopsis* NRT1.1 transporter participates in the signaling pathway triggering root colonization of nitrate-rich patches. *Proc Natl Acad Sci USA* **103**, 19206-19211.
- Robinson, D.** (1994). The responses of plants to non-uniform supplies of nutrients. *New Phytologist* **127**, 635-674.
- Robinson, D.** (2001). Root proliferation, nitrate inflow and their carbon costs during nitrogen capture by competing plants in patch soil. *Plant and Soil* **232**, 41-50.
- Robinson, N., Groom, S., and Groom, Q.** (1997). The froh gene family from *Arabidopsis thaliana*: putative iron-chelate reductases. *Plant and Soil* **196**, 245-248.
- Robinson, N., Procter, C., Connolly, E., and Guerinot, M.L.** (1999). A ferric-chelate reductase for iron uptake from soils. *Nature* **397**, 694-697.
- Rogg, L.E., Lasswell, J., and Bartel, B.** (2001). A gain-of-function mutation in IAA28 suppresses lateral root development. *Plant Cell* **13**, 465-480.
- Rogers, E.E., Guerinot, M.L.** (2002) FRD3, a member of the multidrug and toxin efflux family, controls iron deficiency responses in *Arabidopsis*. *Plant Cell* **14**, 1787-1799.
- Romera, F.J., and Alcantara, E.** (1994). Iron-Deficiency Stress Responses in Cucumber (*Cucumis sativus* L.) Roots (A Possible Role for Ethylene?). *Plant Physiol* **105**, 1133-1138.
- Römheld, V., and Marschner, H.** (1986). Evidence for a Specific Uptake System for Iron Phytosiderophores in Roots of Grasses. *Plant Physiol* **80**, 175-180.
- Römheld, R., Müller, C., Marschner, H.** (1984) Localization and capacity of proton pumps in root of intact sunflower plants. *Plant Physiol* **76**, 603-606.
- Römheld, V., and Marschner, H.** (1981). Iron deficiency stress induced morphological and physiological changes in root tips of sunflower. *Physiologia Plantarum* **53**, 354-360.
- Rosenfield, C., Reed, D., and Kent, M.** (1991). Dependency of Iron Reduction on Development of a Unique Root Morphology in *Ficus benjamina* L. *Plant Physiol* **95**, 1120-1124.
- Rutherford, J.C., Chua, G., Hughes, T., Cardenas, M.E., and Heitman, J.** (2008). A Mep2-dependent transcriptional profile links permease function to gene expression during pseudohyphal growth in *Saccharomyces cerevisiae*. *Mol Biol Cell* **19**, 3028-3039.
- Rutherford, J.C., Ojeda, L., Balk, J., Mühlhoff, U., Lill, R., and Winge, D.R.** (2005). Activation of the iron regulon by the yeast Aft1/Aft2 transcription factors depends on mitochondrial but not cytosolic iron-sulfur protein biogenesis. *J Biol Chem* **280**, 10135-10140.
- Růzicka, K., Ljung, K., Vanneste, S., Podhorská, R., Beeckman, T., Friml, J., and Benková, E.** (2007). Ethylene regulates root growth through effects on auxin biosynthesis and transport-dependent auxin distribution. *Plant Cell* **19**, 2197-2212.
- Sanchez-Calderon, L., Lopez-Bucio, J., Chacón-López, A., Cruz-Ramírez, A., Nieto-Jacobo, F., Dubrovsky, J.G., and Herrera-Estrella, L.** (2005). Phosphate starvation induces a determinate developmental program in the roots of *Arabidopsis thaliana*. *Plant and Cell Physiology* **46**, 174-184.

- Schikora, A., and Schmidt, W.** (2001). Acclimative changes in root epidermal cell fate in response to Fe and P deficiency: a specific role for auxin? *Protoplasma* **218**, 67-75.
- Schmidt, W., and Schikora, A.** (2001). Different pathways are involved in phosphate and iron stress-induced alterations of root epidermal cell development. *Plant Physiol* **125**, 2078-2084.
- Schmidt, W., Tittel, J., and Schikora, A.** (2000). Role of hormones in the induction of iron deficiency responses in Arabidopsis roots. *Plant Physiol* **122**, 1109-1118.
- Séguéla, M., Briat, J.-F., Vert, G., and Curie, C.** (2008). Cytokinins negatively regulate the root iron uptake machinery in Arabidopsis through a growth-dependent pathway. *Plant J* **55**, 289-300.
- Sena, G., Wang, X., Liu, H.-Y., Hofhuis, H., and Birnbaum, K.D.** (2009). Organ regeneration does not require a functional stem cell niche in plants. *Nature* **457**, 1150-1153.
- Shin, R., Burch, A.Y., Huppert, K.A., Tiwari, S.B., Murphy, A.S., Guilfoyle, T.J., and Schachtman, D.P.** (2007). The Arabidopsis transcription factor MYB77 modulates auxin signal transduction. *Plant Cell* **19**, 2440-2453.
- Shin, R., and Schachtman, D.P.** (2004). Hydrogen peroxide mediates plant root cell response to nutrient deprivation. *Proc Natl Acad Sci USA* **101**, 8827-8832.
- Signora, L., De Smet, I., Foyer, C.H., and Zhang, H.** (2001). ABA plays a central role in mediating the regulatory effects of nitrate on root branching in Arabidopsis. *Plant J* **28**, 655-662.
- Skoog, F., and Miller, C.O.** (1957). Chemical regulation of growth and organ formation in plant tissues cultured in vitro. *Symp Soc Exp Biol* **54**, 118-130.
- Sohlenkamp, C., Wood, C., Roeb, G., and Udvardi, M.K.** (2002). Characterization of Arabidopsis AtAMT2, a High-Affinity Ammonium Transporter of the Plasma Membrane. *Plant Physiol* **130**, 1788-1796.
- Spalding, E., Hirsch, R., Lewis, D., Qi, Z., Sussman, M.R., and Lewis, B.D.** (1999). Potassium Uptake Supporting Plant Growth in the Absence of AKT1 Channel Activity. *Journal of General Physiology* **113**, 909-918.
- Stacey, M.G., Patel, A., McClain, W.E., Mathieu, M., Remley, M., Rogers, E.E., Gassmann, W., Blevins, D.G., and Stacey, G.** (2008). The Arabidopsis AtOPT3 protein functions in metal homeostasis and movement of iron to developing seeds. *Plant Physiol* **146**, 589-601.
- Stepanova, A.N., Hoyt, J.M., Hamilton, A.A., and Alonso, J.M.** (2005). A Link between ethylene and auxin uncovered by the characterization of two root-specific ethylene-insensitive mutants in Arabidopsis. *Plant Cell* **17**, 2230-2242.
- Svistoonoff, S., Creff, A., Reymond, M., Sigoillot-Claude, C., Ricaud, L., Blanchet, A., Nussaume, a., and Desnos, T.** (2007). Root tip contact with low-phosphate media reprograms plant root architecture. *Nature genetics* **39**, 792-796.
- Swarup, K., Benková, E., Swarup, R., Casimiro, I., Péret, B., Yang, Y., Parry, G., Nielsen, E., De Smet, I., Vanneste, S., Levesque, M.P., Carrier, D., James, N., Calvo, V., Ljung, K., Kramer, E., Roberts, R., Graham, N., Marillonnet, S., Patel, K., Jones, J.D.G., Taylor, C.G., Schachtman, D.P., May, S., Sandberg, G., Benfey, P., Friml, J., Kerr, I., Beeckman, T., Laplaze, L., and Bennett, M.J.** (2008). The auxin influx carrier LAX3 promotes lateral root emergence. *Nat Cell Biol* **10**, 946-954.

- Szczerba, M.W., Britto, D.T., Balkos, K.D., and Kronzucker, H.J.** (2008). Alleviation of rapid, futile ammonium cycling at the plasma membrane by potassium reveals K<sup>+</sup>-sensitive and -insensitive components of NH<sub>4</sub><sup>+</sup> transport. *J Exp Bot* **59**, 303-313.
- Takahashi, M., Yamaguchi, H., Nakanishi, H., Shioiri, T., Nishizawa, N.K., and Mori, S.** (1999). Cloning two genes for nicotianamine aminotransferase, a critical enzyme in iron acquisition (Strategy II) in graminaceous plants. *Plant Physiol* **121**, 947-956.
- Tan, X., Calderon-Villalobos, L.I.A., Sharon, M., Zheng, C., Robinson, C.V., Estelle, M., and Zheng, N.** (2007). Mechanism of auxin perception by the TIR1 ubiquitin ligase. *Nature* **446**, 640-645
- Tatematsu, K., Kumagai, S., Muto, H., Sato, A., Watahiki, M.K., Harper, R.M., Liscum, E., and Yamamoto, K.T.** (2004). MASSUGU2 encodes Aux/IAA19, an auxin-regulated protein that functions together with the transcriptional activator NPH4/ARF7 to regulate differential growth responses of hypocotyl and formation of lateral roots in *Arabidopsis thaliana*. *Plant Cell* **16**, 379-393.
- Thevelein, J., Geladé, R., Holsbeeks, I., Lagatie, O., Popova, Y., Rolland, F., Stolz, F., Van de Velde, S., Van Dijck, P., Vandormael, P., Van Nuland, A., Van Roey, K., Van Zeebroeck, G., Yan, B.** (2005). Nutrient sensing systems for rapid activation of the protein kinase A pathway in yeast. *Biochemical Soc. Trans.* **33**, 253-6.
- Tian, Q., and Reed, J.W.** (1999). Control of auxin-regulated root development by the *Arabidopsis thaliana* SHY2/IAA3 gene. *Development* **126**, 711-721.
- Ticconi, C.A., Lucero, R.D., Sakhonwasee, S., Adamson, A.W., Creff, A., Nussaume, L., Desnos, T., and Abel, S.** (2009). ER-resident proteins PDR2 and LPR1 mediate the developmental response of root meristems to phosphate availability. *Proc Natl Acad Sci USA* **106**, 14174-14179.
- Titapiwatanakun, B., and Murphy, A.S.** (2009). Post-transcriptional regulation of auxin transport proteins: cellular trafficking, protein phosphorylation, protein maturation, ubiquitination, and membrane composition. *J Exp Bot* **60**, 1093-1107.
- Titapiwatanakun, B., Blakeslee, J.J., Bandyopadhyay, A., Yang, H., Mravec, J., Sauer, M., Cheng, Y., Adamec, J., Nagashima, A., Geisler, M., Sakai, T., Friml, J., Peer, W.A., and Murphy, A.S.** (2009). ABCB19/PGP19 stabilises PIN1 in membrane microdomains in *Arabidopsis*. *Plant J* **57**, 27-44.
- Toorchi, M., Shashidhar, H.E., Sharma, N., and Hittalmani, S.** (2002). Tagging QTLs for maximum root length in rainfed lowland rice (*Oryza sativa* L.) using molecular markers. *Cell Mol Biol Lett* **7**, 771-776.
- Trachsel, S., Messmer, R., Stamp, P., and Hund, A.** (2009). Mapping of QTLs for lateral and axile root growth of tropical maize. *Theor Appl Genet*. DOI 10.1007/s00122-009-1144-9.
- Uehara, T., Okushima, Y., Mimura, T., Tasaka, M., and Fukaki, H.** (2008). Domain II mutations in CRANE/IAA18 suppress lateral root formation and affect shoot development in *Arabidopsis thaliana*. *Plant Cell Physiol* **49**, 1025-1038.
- van der Graaff, E., Dulk-Ras, A.D., Hooykaas, P.J., and Keller, B.** (2000). Activation tagging of the LEAFY PETIOLE gene affects leaf petiole development in *Arabidopsis thaliana*. *Development* **127**, 4971-4980.
- Van Nuland, A., Vandormael, P., Donaton, M., Alenquer, M., Lourenço, A., Quintino, E., Versele, M., and Thevelein, J.M.** (2006). Ammonium permease-based sensing

- mechanism for rapid ammonium activation of the protein kinase A pathway in yeast. *Molecular Microbiology* **59**, 1485-1505.
- Van Sandt, V.S.T., Suslov, D., Verbelen, J.-P., and Vissenberg, K.** (2007). Xyloglucan endotransglucosylase activity loosens a plant cell wall. *Ann Bot* **100**, 1467-1473.
- Van Zeebroeck, G., Bonini, B., Versele, M., and Thevelein, J.M.** (2008). Transport and signaling via the amino acid binding site of the yeast Gap1 amino acid transceptor. *Nature Chem Biol* **5**, 45-52.
- Vanneste, S., De Rybel, B., Beemster, G.T.S., Ljung, K., De Smet, I., Van Isterdael, G., Naudts, M., Iida, R., Gruissem, W., Tasaka, M., Inzé, D., Fukaki, H., and Beeckman, T.** (2005). Cell cycle progression in the pericycle is not sufficient for SOLITARY ROOT/IAA14-mediated lateral root initiation in *Arabidopsis thaliana*. *Plant Cell* **17**, 3035-3050.
- Vanneste, S., Frimi, J.** (2009). Auxin: a trigger for change in plant development. *Cell* **136**, 1005-1016.
- Vert, G., Grotz, N., Dédaldéchamp, F., Gaymard, F., Guerinot, M.L., Briat, J.-F., and Curie, C.** (2002). IRT1, an *Arabidopsis* transporter essential for iron uptake from the soil and for plant growth. *Plant Cell* **14**, 1223-1233.
- Vert, G., Briat, J.F., Curie, C.** (2003) Dual regulation of the *Arabidopsis* high affinity root iron uptake system by local and long-distance signals. *Plant Physiol* **132**, 796-804.
- Vicente-Agullo, F., Rigas, S., Desbrosses, G., Dolan, L., Hatzopoulos, P., and Grabov, A.** (2004). Potassium carrier TRH1 is required for auxin transport in *Arabidopsis* roots. *Plant J* **40**, 523-535.
- Vidal, E.A., Araus, V., Lu, C., Parry, G., Green, P.J., Coruzzi, G.M., and Gutiérrez, R.A.** (2010). Nitrate-responsive miR393/AFB3 regulatory module controls root system architecture in *Arabidopsis thaliana*. *Proc Natl Acad Sci USA* **107**, 4477-4482.
- Vissenberg, K., Martinez-Vilchez, I.M., Verbelen, J.P., Miller, J.G., and Fry, S.C.** (2000). In vivo colocalization of xyloglucan endotransglycosylase activity and its donor substrate in the elongation zone of *Arabidopsis* roots. *Plant Cell* **12**, 1229-1237.
- von Wirén, N., Mori, S., Marschner, H., and Romheld, V.** (1994). Iron inefficiency in maize mutant *ys1* (*Zea mays* L. cv Yellow-Stripe) is caused by a defect in in Uptake of Iron Phytosiderophores. *Plant Physiol* **106**, 71-77.
- von Wirén, N., Lauter, F., Ninnemann, O., Gillissen, B., Engels, P.W.-L., Jost, W., and Frommer, W.B.** (2000). Differential regulation of three functional ammonium transporter genes by nitrogen in root hairs and by light in leaves of tomato. *Plant Journal* **21**, 167-175.
- von Wirén, N., and Merrick, M.** (2004). Regulation and function of ammonium carriers in bacteria, fungi, and plants. *Topic in Current Genetics* **9**, 78-120.
- von Wirén, N., Gazzarrini, S., Gojon, A., and Frommer, W.B.** (2000). The molecular physiology of ammonium uptake and retrieval. *Curr Opin Plant Biol* **3**, 254-261.
- Walch-Liu, P., and Forde, B.G.** (2008). Nitrate signalling mediated by the NRT1.1 nitrate transporter antagonises L-glutamate-induced changes in root architecture. *Plant J* **54**, 820-828.
- Walch-Liu, P., Ivanov, I.I., Filleur, S., Gan, Y., Remans, T., and Forde, B.G.** (2006). Nitrogen regulation of root branching. *Ann Bot* **97**, 875-881.

- Wang, H., Klatte, M., Jakoby, M., Bäumlein, H., Weisshaar, B., and Bauer, P. (2007). Iron deficiency-mediated stress regulation of four subgroup 1b BHLH genes in *Arabidopsis thaliana*. *Planta* **226**, 897-908.
- Ward, J.T., Lahner, B., Yakubova, E., Salt, D.E., and Raghothama, K.G. (2008). The effect of iron on the primary root elongation of *Arabidopsis* during phosphate deficiency. *Plant Physiol* **147**, 1181-1191.
- Waters, B.M., Chu, H.-H., Didonato, R.J., Roberts, L.A., Easley, R.B., Lahner, B., Salt, D.E., and Walker, E.L. (2006). Mutations in *Arabidopsis* yellow stripe-like1 and yellow stripe-like3 reveal their roles in metal ion homeostasis and loading of metal ions in seeds. *Plant Physiol* **141**, 1446-1458.
- Weigel, D., and Jürgens, G. (2002). Stem cells that make stems. *Nature* **415**, 751-754.
- Wirth, J., Chopin, F., Santoni, V., Viennois, G., Tillard, P., Krapp, A., Lejay, L., Daniel-Vedele, F., and Gojon, A. (2007). Regulation of root nitrate uptake at the NRT2.1 protein level in *Arabidopsis thaliana*. *J Biol Chem* **282**, 23541-23552.
- Wu, G., Lewis, D.R., and Spalding, E.P. (2007). Mutations in *Arabidopsis* multidrug resistance-like ABC transporters separate the roles of acropetal and basipetal auxin transport in lateral root development. *Plant Cell* **19**, 1826-1837.
- Yang, H., and Murphy, A.S. (2009). Functional expression and characterization of *Arabidopsis* ABCB, AUX 1 and PIN auxin transporters in *Schizosaccharomyces pombe*. *Plant J* **59**, 179-191.
- Yang, X., Lee, S., So, J.-H., Dharmasiri, S., Dharmasiri, N., Ge, L., Jensen, C., Hangarter, R., Hobbie, L., and Estelle, M. (2004). The IAA1 protein is encoded by AXR5 and is a substrate of SCF(TIR1). *Plant J* **40**, 772-782.
- Yuan, L., Loqué, D., Kojima, S., Rauch, S., Ishiyama, K., Inoue, E., Takahashi, H., and von Wirén, N. (2007). The organization of high-affinity ammonium uptake in *Arabidopsis* roots depends on the spatial arrangement and biochemical properties of AMT1-type transporters. *Plant Cell* **19**, 2636-2652.
- Yuan, L., Graff, L., Loqué, D., Kojima, S., Tsuchiya, Y.N., Takahashi, H., and von Wirén, N. (2009). AtAMT1;4, a pollen-specific high-affinity ammonium transporter of the plasma membrane in *Arabidopsis*. *Plant Cell Physiol.* **50**, 13–25.
- Yuan, Y., Wu, H., Wang, N., Li, J., Zhao, W., Du, J., Wang, D., and Ling, H.-Q. (2008). FIT interacts with AtbHLH38 and AtbHLH39 in regulating iron uptake gene expression for iron homeostasis in *Arabidopsis*. *Cell Res* **18**, 385-397.
- Zaid, H., El Morabet, R., Diem, H.G., and Arahou, M. (2003). Does ethylene mediate cluster root formation under iron deficiency? *Ann Bot* **92**, 673-677.
- Zhang, H., and Forde, B.G. (1998). An *Arabidopsis* MADS box gene that controls nutrient-induced changes in root architecture. *Science* **279**, 407-409.
- Zhang, H., and Forde, B.G. (2000). Regulation of *Arabidopsis* root development by nitrate availability. *J Exp Bot* **51**, 51-59.
- Zhang, H., Rong, H., and Pilbeam, D. (2007). Signalling mechanisms underlying the morphological responses of the root system to nitrogen in *Arabidopsis thaliana*. *J Exp Bot*, 1-10.
- Zhang, H., Jennings, A., Barlow, P.W., and Forde, B.G. (1999). Dual pathways for regulation of root branching by nitrate. *Proc Natl Acad Sci USA* **96**, 6529-6534.

---

## 7. Acknowledgments

First of all, I would like to thank Prof. Dr. Nicolaus von Wirén for giving me the opportunity to do my PhD thesis at this institute. Many thanks also for the corrections of my thesis and to help to develop my plant scientist side.

Thanks to the evaluators of my PhD thesis, Prof. Dr. Weber and Prof. Dr. Schaller to dedicate your time and to take part of the final examination.

Sincere thanks to Mrs. Schöllhammer for helping me in so many ways and dedicating your time so much for an ordinary Brazilian student. Also, thanks to Mrs. Berghammer to be patient and help me in several situations that I needed.

I fully dedicate my thesis to few incredible people that took care of me in many ways either in the lab. or in Germany at all. Most important to me during this period was my lovely Anne Kriegel. Anni, thanks to give me strength in several moments and to take care of me over these 4 years. You will be always important in my life. In the lab., I dedicate my thesis to Ricardo Giehl (Fião) to share so many interesting scientific discussions, to help me on iron sensing manuscript and show me good stuff from the South of Brazil. Special thanks to Anderson (Alemão) Meda to support me and push me in several difficult moments in the lab. Of course, I have to thank three special women in my life, Adriana Meda (Dli), Ana Eisermann (Aninha) and Lilia Carvalhais (Mise) to take care of me when I was alone and to give me a piece of home in several moments. Vocês sabem que não tenho palavras para descrever o que vocês são e fizeram por mim aqui na Alemanha. Felizmente, não dá' para escrever tudo que passamos juntos. Te amo Anne, e também adoro todos vocês meus amigos, Anderson, Dri, Ricardo, Ana e Lilia.

I would like to thank Alberto Laginha, Fabiano de Bonna, Lisa, Caro, Nike to help me in the lab., to make me laugh during several nice moments and to show and share with me good things in Germany.

Special thanks to Soichi Kojima, Anne Bohner, Susanne Reiner and Lucile G. to support my adaptation when I started my PhD in Germany. Anne B., thanks to be my "girl" when I was sick. Soichi and Lucile, thanks to make me laugh so much during that funny dinners and to discuss science. Susanne, thanks for the party-nights that we have enjoyed together.

I also thank the others member from S1-group: Lisa, Caro, Lilia, Silvia, Anne Bohner, Bernhard, Caro, Olga, Dmitriy, Zeynep, Susanne, Claudia, Anne Rubel, Rong-li, Mr. Singh, Nunum, Ben, Stefan, Sebastian, Enrico, Nicole and the others.

I am thankful to Mrs. Dachtler for the 15N analysis and Mrs. Ruckwied, Mrs. Margareth Braband, Mr. Bucher, Mr. Schulz, Mr. Hinrich and Fumiko for technical support.

I am indebted to Prof. Dr. Römheld, Dr. Neumann and Prof. Muller for the scientific discussions.

I thank my former supervisors Lazaro Peres, Antonio Figueira and Rodrigo Latado for giving me recommendations and support me during my PhD.

A very special thanks to all my friends from Brazil. During several moments you all kept me smiling for those incredible moments in Brazil. Muito obrigado, Eduardo, Lisa, Lilian, Maia, Deborah e outros.

I am grateful to Anne's parents, Andreas and Ines Kriegel, as well her sister, Jule and her grandparents Mr. and Mrs. Michel to led me take part in your family and for those incredible moments in your house. Vielen Dank fuer Eure Herzlichkeit.

I finally would like to express my gratefulness to my family, that even miles away from me, they were involved in my PhD thesis and giving me support to start and conclude this period of life.

I am grateful to my parents, Valter Lima and Celina Zanin, for showing their unconditional love and to give me the strength in my daily life. Amo vocês e muito obrigado, meu pai e minha mãe.

Thanks to my sister, Jenifer Laila, for being my sister and to take care of our parents while I was absent. Obrigado, gorda!



## 8. Curriculum vitae

### Joni Esrom Lima

Date of birth: October 25th, 1979

Place of birth: Piracicaba, S.P, Brazil

Address: Institut für Pflanzenernährung, Fruwirthstr. 20 D-70599, Stuttgart, Germany

Telephone: +049-0711-45924251

E-mail: jonilima@uni-hohenheim.de; limajoni@gmail.com

### Education

---

2005 - 2010

PhD in Agricultural Sciences - Molecular Plant Nutrition, Institute of Plant Nutrition, University of Hohenheim, Germany.

PhD thesis: Iron and ammonium sensing differentially modulate root plasticity in *Arabidopsis thaliana*

Supervisor: Prof. Dr. Nicolaus von Wirén

2003 - 2005:

Msc. in Biology and Agricultural Sciences in environment, Center for Nuclear Energy in Agriculture (Centro de Energia Nuclear na Agricultura-CENA), Brazil.

Master thesis: "Application of transgenic tomato plants (*Lycopersicon esculentum* cv *Micro-Tom*) harboring native *Agrobacterium rhizogenes* auxin-related genes to study *in vitro* organogenesis"

Supervisor: Prof. Dr. Lázaro E. P. Peres

1999 - 2002:

Graduation in Biology, Universidade Metodista de Piracicaba (UNIMEP), Brazil.

---

**Publications**

---

**Lima, JE;** Giehl, RFH; von Wirén, N. Local Supply of Iron Distinctly Defines Lateral Root Number and Elongation in *Arabidopsis thaliana*. *In preparation*.

**Lima, JE;** Kojima, S; Takahashi, H; von Wirén, N. Ammonium triggers lateral root branching in *Arabidopsis* in an AMT1;3-dependent manner. *Plant Cell*, *submitted*.

**Lima, JE;** Benedito, VA; Figueira, AVO; Peres, LEP (2009) Callus, shoot and hairy root formation *in vitro* as affected by the sensitivity to auxin and ethylene in tomato mutants. *Plant Cell Reports* 28: 1169-1177.

**Lima, JE;** Carvalho, RF; Tulmann Neto, A; Figueira, AVO; Peres, LEP (2004) Micro-MsK: a tomato genotype with miniature size, short life cycle and improved *in vitro* shoot regeneration. *Plant Science* 167: 753-757.

---

**Participation in Scientific conferences during the PhD study**

---

poster presentation- **Lima, JE;** Kojima, S; Takahashi, H; von Wirén, N. “Localized Ammonium Supply Increases Lateral Root Branching”. In: International Plant Molecular Biology Congress, 2009, St. Louis, USA.

poster presentation- **Lima, JE;** Kojima, S; Takahashi, H; von Wirén, N. “Localized Ammonium Supply Increases Lateral Root Branching”. In: RegioPlantScience Meeting, 2008, Tübingen, Germany.

poster presentation- **Lima, JE;** Kojima, S; Takahashi, H; von Wirén, N. “Is Ammonium a Sensed Nitrogen Form In Planta?”. In: RegioPlantScience Meeting, 2007, Tübingen, Germany.

poster presentation- **Lima, JE;** Kojima, S; Yuan, L; von Wirén, N. “Is Ammonium a Sensed Nitrogen Form In Planta?”. In: 4th International Nitrogen Conference, 2007, Lancaster, UK.

**Other activities during the PhD study and Language**

---

Organization and co-supervision of a practical course in agricultural biotechnology (Grosspraktikum Agrarbiotechnologie, 2007 - 2009).

Languages: Portuguese (mother tongue) and English (fluent).

Stuttgart- Hohenheim, September 2010.

Joni Esrom Lima

---

### **Declaration of autonomy**

I declare that the submitted work has been completed by me, the undersigned, and that I have not used any other than permitted reference sources or materials nor engaged any plagiarism. All the references and the other sources used in the presented work have been appropriately acknowledged in the work. I further declare that the work has not been previously submitted for the purpose of academic examination, either in its original or similar form, anywhere else.

### **Selbständigkeitserklärung**

Ich versichere, dass ich diese Arbeit selbständig verfasst und keine anderen als die angegebenen Quellen und Hilfsmittel verwendet habe. Die den benutzten Hilfsmitteln wörtlich oder inhaltlich entnommenen Stellen habe ich unter Quellenangaben kenntlich gemacht. Die vorliegende Arbeit wurde in gleicher oder ähnlicher Form noch keiner anderen Institution oder Prüfungsbehörde vorgelegt.

Name: Joni Esrom Lima

Stuttgart, 11th of June, 2010.



---

---